

Numerical Model of Phosphate Esters in the Chattahoochee River

by

Samuel Fraad Haffey

Sc.B. Computer Science, A.B. Anthropology
Brown University, 1996

SUBMITTED TO THE DEPARTMENT OF CIVIL AND ENVIRONMENTAL
ENGINEERING IN PARTIAL FULFILLMENT OF THE REQUIREMENTS FOR THE
DEGREE OF

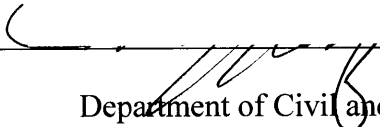
MASTER OF ENGINEERING IN CIVIL AND ENVIRONMENTAL ENGINEERING
AT THE
MASSACHUSETTS INSTITUTE OF TECHNOLOGY

JUNE 2004

© 2004 Samuel Fraad Haffey. All rights reserved.

The author hereby grants to MIT permission to reproduce
and to distribute publicly paper and electronic
copies of this thesis document in whole or in part.

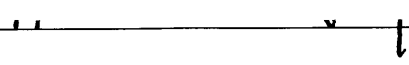
Signature of Author: _____

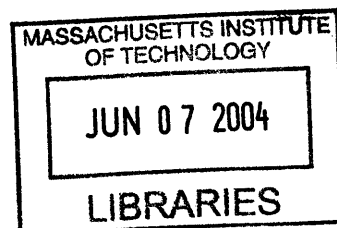

Samuel Fraad Haffey
Department of Civil and Environmental Engineering
May 7, 2004

Certified by: _____


Peter Shanahan
Lecturer of Civil and Environmental Engineering
Thesis Supervisor

Accepted by: _____


Heidi Nepf
Chairman, Committee for Graduate Students



BARKER

Numerical Model of Phosphate Esters in the Chattahoochee River

by

Samuel Fraad Haffey

Submitted to the Department of Civil and Environmental Engineering
on May 7, 2004 in Partial Fulfillment of the
Requirements for the Degree of Master of Engineering in
Civil and Environmental Engineering

ABSTRACT

A numerical model was constructed to assess the magnitude of organophosphoric acid triester sinks in the Chattahoochee River and to identify concentration patterns downstream of point source discharges. The model was built using WASP5 and supporting software packages. The model simulated mass transport of tri-butyl phosphate, tri (2-butoxyethyl) phosphate, and tri (2-chloroethyl) phosphate within a reach of the river bounded by Buford Dam and Northern Atlanta. Several potential mechanisms for the removal of the phosphate esters from the water column were considered. These were biodegradation, sorption to settling solids, volatilization, and oxidation by free radicals.

Of the three phosphate esters considered by the model, tri (2-chloroethyl) phosphate was predicted to be the most resistant to degradation by natural attenuation processes. Tri (2-butoxyethyl) phosphate showed the most potential for degradation in surface waters. Biodegradation and sorption to settling solids were predicted to be the most effective processes for the removal of tri (2-butoxyethyl) phosphate. Concentration patterns at several locations downstream of point source discharges were predicted for the three compounds. Concentration patterns were found to be affected by the diurnal flow variation caused by the operation of two hydroelectric dams within the modeled reach.

Thesis Supervisor: Peter Shanahan

Title: Lecturer of Civil and Environmental Engineering

*To My Meema
Rita Fraad*

May 11, 1915-May 9, 2004

Table of Contents

1	Introduction.....	7
1.1	Scope.....	7
1.2	Motivation.....	7
1.3	Methods and Materials.....	8
1.4	Model Time Frame	8
2	Physical Setting.....	9
2.1	Location	9
2.1.1	Geographic Location.....	9
2.1.2	Terrain.....	10
2.1.3	Climate.....	10
2.2	Land Use	11
2.2.1	Land Use Upstream of Buford Dam.....	11
2.2.2	Land Use In Modeled Reach.....	11
2.3	Hydroelectric Plants and Flow Regulation	11
2.4	Municipal Water Use	13
3	WASP Model.....	15
3.1	Overview of WASP	15
3.1.1	Basic Water Quality Model	15
3.1.2	Mass Balance Equation.....	16
3.2	Flow Routing Model.....	17
3.2.1	Overview of Problem.....	17
3.2.2	Data Requirements.....	19
3.2.3	HEC-RAS Model.....	21
3.2.3.1	Overview of HEC-RAS	21
3.2.3.2	Steady State Flow Simulation.....	21
3.2.3.3	Description of HEC RAS Model Results.....	22
3.2.4	Muskingum Routing	22
3.2.4.1	Description of Muskingum Method.....	22
3.2.4.2	Muskingum Routing Applied to Chattahoochee River.....	24
3.2.4.3	Calibration of Muskingum Coefficients	25
3.2.4.4	Muskingum Routing Results vs. Observation	27
3.2.4.4.1	Buford Dam to Morgan Falls.....	28
3.2.4.4.2	Morgan Falls Dam to GA 280 Crossing	30
3.2.4.4.3	Discussion of Inaccuracies.....	32
3.2.5	Estimation of Tributary Inflow	33
3.2.5.1	Identification of Tributaries.....	33
3.2.5.2	Identification of Significant Tributaries.....	33
3.2.5.3	Estimation of Combined Tributary Inflow	36
3.3	Tanks in Series Model	36
3.3.1	Overview and Design Goals	36
3.3.2	Modeling Dispersion.....	37
3.3.2.1	Overview of Dispersion.....	37
3.3.2.2	Dispersion in the Tanks in Series Model	38
3.3.2.3	Dispersion Model.....	42

3.3.3 Determination of Tank Boundaries.....	42
3.3.4 Determination of Discharge Coefficients	43
3.3.4.1 Discharge Coefficients and WASP	44
3.3.4.2 Estimation of Discharge Coefficients	45
3.3.4.3 Discharge Coefficient Results.....	47
3.4 Suspended Solids Model.....	56
3.4.1 Suspended Solids Overview	56
3.4.2 Suspended Solids in WASP	56
3.4.3 Data Requirements.....	56
3.4.4 Model Implementation.....	58
3.4.4.1 Suspended Solids Distribution.....	59
3.4.4.2 Settling	60
3.4.4.3 Fraction of Organic Carbon	61
3.4.5 Results.....	62
3.4.5.1 Comparisons with Field Observation.....	65
3.5 Phosphate Esters Model.....	68
3.5.1 Phosphate Esters	68
3.5.1.1 TBP	69
3.5.1.2 TBEP.....	69
3.5.1.3 TCEP.....	70
3.5.2 Estimate of Loads	71
3.5.2.1 Point Source Loads	72
3.5.2.1.1 Estimation of Daily Discharge.....	72
3.5.2.1.2 Determination of Time Variable Discharge.....	73
3.5.2.1.3 Determination of Point Source Discharge Concentration.....	73
3.5.2.1.4 Determination of Mass Loadings.....	74
3.5.2.2 Estimate of Boundary Condition Concentrations	74
3.5.2.2.1 Upstream Boundary at Buford Dam	75
3.5.2.2.2 Boundary Concentration at Suwanee Creek	75
3.5.2.2.3 Boundary Condition at Big Creek.....	76
3.5.2.3 Comparisons of Load Magnitude.....	79
3.5.3 Generation of Initial Conditions	80
3.5.4 Physical Processes Model.....	81
3.5.5 Sorption.....	81
3.5.5.1 Overview of Sorption.....	81
3.5.5.2 WASP Implementation of Sorption.....	82
3.5.5.2.1 Determining K_{oc}	83
3.5.5.3 Sorption Constants Used For Phosphate Esters	84
3.5.6 Biodegradation.....	84
3.5.6.1 Overview of Biodegradation.....	84
3.5.6.2 WASP Implementation of Biodegradation	84
3.5.6.3 Biodegradation First Order Rates	84
3.5.7 Volatilization.....	85
3.5.7.1 Overview of Volatilization	85
3.5.7.2 WASP Implementation of Volatilization.....	86
3.5.7.3 Volatilization Constants Used.....	87

3.5.8 Oxidation.....	88
3.5.8.1 Overview of Oxidation	88
3.5.8.2 WASP Implementation of Oxidation.....	88
3.5.8.3 Oxidation Model.....	88
3.5.9 Neglected Reactions.....	89
3.5.9.1.1 Hydrolysis.....	89
3.5.9.2 Photolysis.....	89
4 Model Results	91
4.1 Flow Pattern vs. Concentration.....	91
4.1.1 Initial Conditions Model Results	91
4.1.1.1 Five Day Simulation and Initial Conditions Model.....	92
4.1.2 Concentration Patterns above Morgan Falls	93
4.1.2.1 Above Suwanee Creek.....	93
4.1.2.2 Suwanee Creek to Crooked Creek	94
4.1.2.3 Crooked Creek to the Mouth of The Big Creek.....	95
4.1.2.4 Mouth of Big Creek to Bull Sluice Lake	96
4.1.3 Concentration in Bull Sluice Lake.....	97
4.1.4 Concentration Downstream of Morgan Falls.....	99
4.1.4.1 Concentration between Morgan Falls Dam and Atlanta.....	99
4.1.4.2 Downstream of the Atlanta Treatment Plants.....	100
4.1.5 Longitudinal Concentration Distribution.....	102
4.2 Sorption Model Results.....	102
4.3 Biodegradation Model Results.....	104
4.4 Volatilization Model Results	107
4.5 Oxidation Model Results	109
4.6 Comparison to Field Studies.....	110
5 Model Sensitivity	113
5.1 Suspended Solids Sensitivity	113
5.2 Phosphate Load Sensitivity.....	116
5.3 Biodegradation Sensitivity.....	119
6 Conclusions.....	121
6.1 General Conclusions	121
6.2 Suggestions for Further Study	122
6.2.1 Free Radical Distribution.....	123
6.2.2 Suspended Solids and Organic Carbon Content	123
6.2.3 Biodegradation Rates.....	123
6.2.4 Varying Loads.....	123

1 Introduction

In 2000 the Centers for Disease Control and the United States Geological Survey published results of a study that detected three phosphate esters in samples of treated sewage effluent and municipal drinking water in the greater Atlanta area (Frick and Zaugg, 2003).

We constructed a numerical water quality model of the Chattahoochee River, which is main the receptacle of treated municipal sewage and the main source of drinking water for the greater Atlanta area. The water quality model focused on the fate and transport of the three phosphate esters.

The aim of the water quality model is to identify potential phosphate ester sinks within the Chattahoochee River and to a greater extent in surface waters in general. The phosphate esters are used in similar applications and identifying the natural sinks will determine which esters are more likely to remain intact in the environment and therefore become a growing hazard. In addition the numerical model can identify periods during which concentrations may be elevated. These predictions could be used to schedule drinking water withdrawals or when to apply extra treatment measures.

1.1 Scope

This thesis has been prepared in accordance with the requirements of the Masters of Engineering degree in Civil and Environmental Engineering at the Massachusetts Institute of Technology. It was done as part of an integrated project performed by a team of Master of Engineering students.. The project studied phosphate ester pollutants in the Chattahoochee River.

1.2 Motivation

In 2000 the Centers for Disease Control along with the United States Geological Survey conducted a survey of treated wastewater effluent discharged to the Chattahoochee and raw and treated drinking water drawn from the Chattahoochee (Frick and Zaugg, 2003). Four municipal wastewater treatment plants (WWTP) and three municipal drinking water treatment plants (DWTP) were tested.

The survey screened for a wide array of compounds that were classified as either pharmaceuticals or personal care products. In all, forty-six compounds were detected in at least some of the samples and nine had 100% detection rates in treated wastewater. Most troubling was that fourteen of the compounds were detected in samples of finished drinking water.

Out of the fourteen, three were phosphate esters that have similar usages. These are tri-butyl phosphate, tri (2-butoxyethyl) phosphate, and tri (2-chloroethyl) phosphate. The phosphate esters represent an emerging environmental hazard that deserves increased study.

1.3 Methods and Materials

A numerical modeling approach was used to make predictions of phosphate ester concentrations and to identify potential sinks within the environment. To this end a water quality model was using the Waster Quality Analysis Simulation Program (Ambrose et al., 1993) and supported by two additional software packages. Hydrologic Engineering Center – River Analysis System (Brunner, 2002) was used to estimate the characteristics of the river flow in the modeled reach. ArcGIS (ArcGIS, 2003) was used to identify the locations of point sources, tributary inflows, drinking water intakes and other important features of the river reach. ArcGIS also aided in the estimation of ungauged tributary flow.

1.4 Model Time Frame

In-stream concentration data for the modeled reach was collected during the period January 12, 2004 – January 14, 2004 (Andrews et al., 2004). The model time frame was selected so as to simulate the river conditions during the sampling period. The data collected during that study was used in constructing and assessing the accuracy of the numerical model.

2 Physical Setting

2.1 Location

2.1.1 Geographic Location

The Chattahoochee River's headwaters are in north-central Georgia approximately 100 kilometers northeast of Atlanta (Frick et al., 1998). From its origin, the mainstream and several tributaries flow into Lake Sydney Lanier, the impoundment formed by Buford Dam (Willey and Huff, 1978). It continues southwest past Atlanta, forming part of the Alabama-Georgia border and eventually the Georgia-Florida border. Here it joins the Flint River and forms the Apalachicola River. Finally after traveling approximately 650 kilometers from the headwaters it discharges to Apalachicola Bay on the Gulf of Mexico (Frick et al., 1998).

The reach being modeled consists of the 80 kilometers between Buford Dam and the crossing of Highway GA 280 in Northwest Atlanta. Figure 2-1 shows a map of the modeled reach.

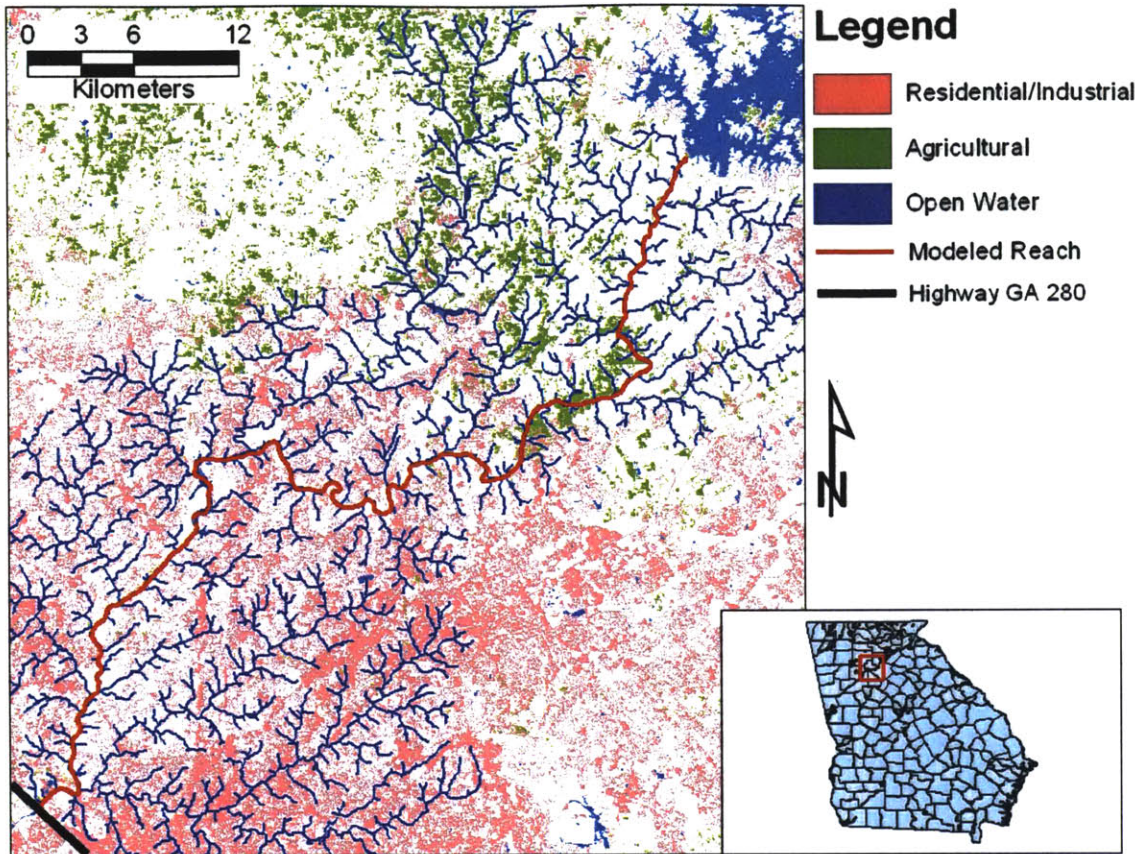


Figure 2-1 Map Showing Modeled Reach and Location in Georgia (Land Cover Data USGS, 1992)

2.1.2 Terrain

The modeled reach is in the piedmont terrain region of Georgia that is marked by its hilly landscape. Elevations in the modeled reach range from approximately 275 meters above sea level at Buford Dam (the upstream boundary) down to 225 meters above sea level at the GA 280 crossing (downstream boundary) (Olson, 2004) .

2.1.3 Climate

Monthly averages range from 34 °C in the mid to late summer to winter lows of 0°C. Average yearly rainfall is 140 cm with peak monthly precipitation between 10 and 15 cm occurring in February or March. (NSTATE, 2004).

2.2 Land Use

The area drained by the modeled reach can be divided into two sections: the area drained above Buford Dam and the area contributing to drainage within the modeled reach.

2.2.1 Land Use Upstream of Buford Dam

The area drained above Buford Dam is 80% forestland. The second largest land use category, at 16%, is agriculture, which is dominated by poultry production (Frick et al., 1998). Poultry production activities are concentrated in the stream valleys of the headwaters (Cherry et al., 1980) with the result that litter and waste discharges from the poultry production comprise the major water quality issue in the headwaters region of the Chattahoochee (Frick et al., 1998).

Residential areas are clustered around Lake Sydney Lanier. Gainesville is the largest urban center in this region (Cherry et al., 1980). Five municipal wastewater treatment plants of less than 4,000 m³/day discharge into the watershed drained at Buford Dam. In addition Gainesville has two (11,000 m³/day) wastewater plants that discharge into Lake Sydney Lanier (GNR, 1997)

2.2.2 Land Use In Modeled Reach

The area downstream of Buford Dam is still predominantly forestland however becomes increasingly residential as the river approaches Atlanta. Tributary watersheds draining the areas nearest Buford Dam are 80% forestland, 13% agriculture (poultry production), and 3% residential. These ratios change in favor of residential land in the downstream direction. The Peachtree Creek watershed, the last to join the Chattahoochee in the modeled reach, is 55% residential and 40% forest (USGS, 1992).

2.3 Hydroelectric Plants and Flow Regulation

One of the main uses of the modeled reach is electrical power generation. The upstream boundary of the modeled reach, Buford Dam, is a hydroelectric dam that generates power from scheduled releases of water impounded at Lake Sydney Lanier. Forty-eight kilometers downstream of Buford Dam there is another hydroelectric dam, Morgan Falls. This dam creates a much smaller impoundment called Bull Sluice Lake. Morgan Falls

Dam is a run-of-the-river dam and generates power from the high flows generated by the Buford Dam releases (Cherry et al., 1980). Figure 2-2 shows the locations of Buford Dam, Morgan Falls Dam, and Lake Sydney Lanier. Lake Sydney Lanier is the large body of water directly upstream of Buford Dam that is plainly visible on Figure 2-2. Bull Sluice Lake is not wide enough (0.5 km) to be visibly different from the river in Figure 2-2. It extends for about 2 kilometers upstream of Morgan Falls Dam (USGS, 1997).

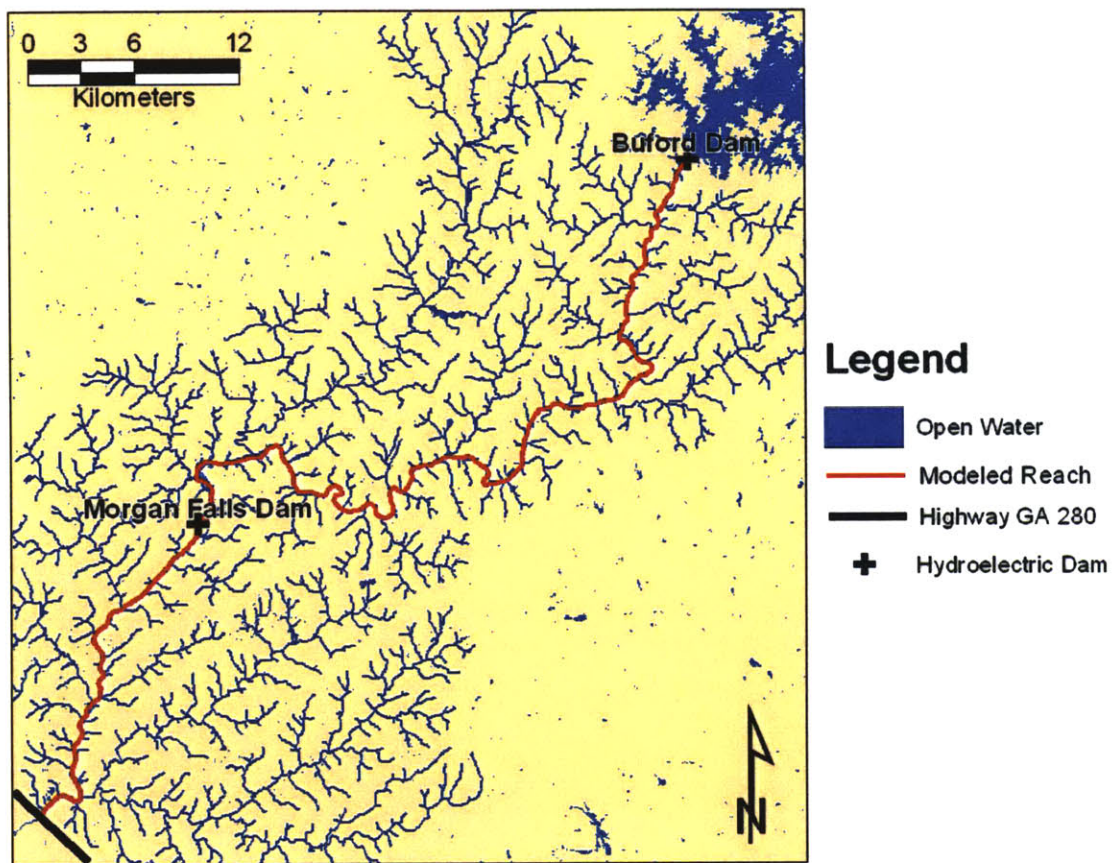
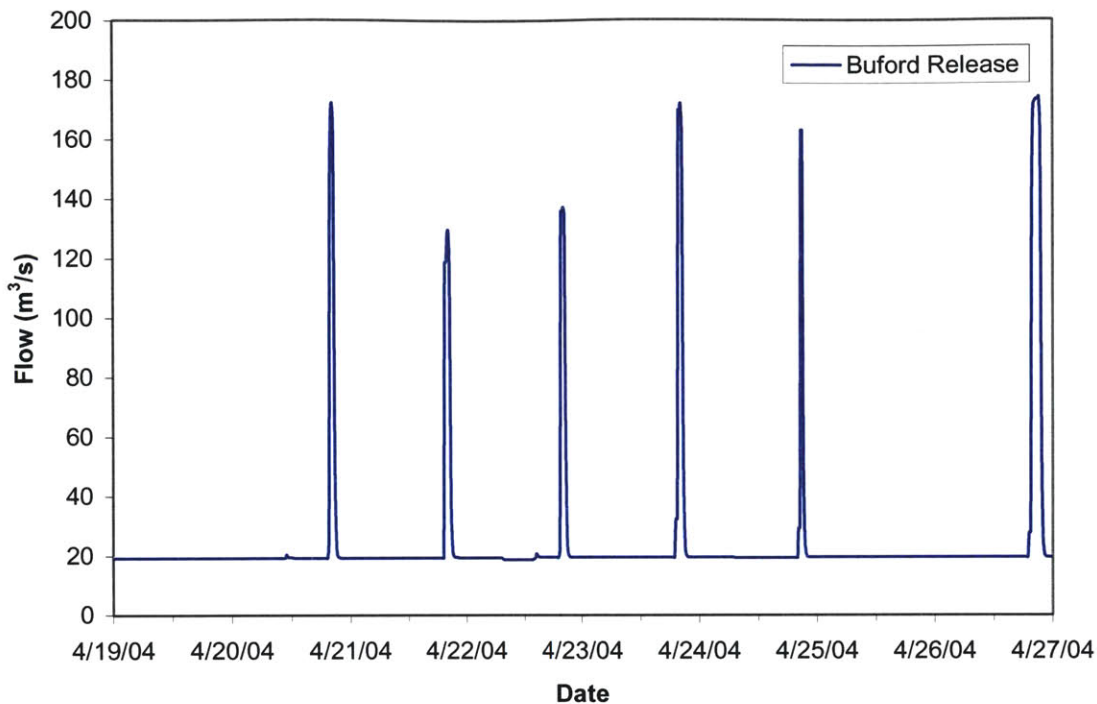


Figure 2-2 Map Showing Locations of Buford Dam and Morgan Falls Dam

The Buford Dam is a peak-power generating facility (Cherry et al., 1980) which generates power for peak demand on a five-day schedule and then does not generate for two days. Figure 2-3 shows the typical seven-day release schedule, the frequency of the releases on power generation days can be as high as two per day (Stamey, 2004).



**Figure 2-3 Typical Release Pattern from Buford Dam (USGS, 2004)
(April 19, 2004 – April 26, 2004)**

The five-day power generation cycle generates a diurnal variation in flow throughout the reach bounded by Buford Dam and Morgan Falls Dam. The off days are characterized by relatively low constant flows.

The Morgan Falls Dam generates power from the flood waves released by Buford Dam. Although its operation alters the propagation of the flood wave downstream, it does not release a flood wave in the same manner as Buford Dam. A more detailed discussion of the hydrology can be found in Section 3.2.

2.4 Municipal Water Use

In addition to being a source of hydroelectric power for the region, the Chattahoochee is the main source of municipal water for the over two million people of greater Atlanta (Frick and Zaugg, 2003). Two municipal drinking water treatment plants (DWTP), Cobb County and Atlanta Water Works, draw raw drinking water from the modeled reach.

The river also accepts treated effluent from municipal wastewater treatment plants (WWTP). Five WWTPs discharge directly into the modeled reach and two discharge into tributaries that join the modeled reach above Morgan Falls Dam (GNR, 1997). It is these WWTPs that are hypothesized to be the main source of phosphate ester loads to the modeled reach. From Figure 2-4 it is apparent that the DWTPs in the reach are downstream from the majority of wastewater treatment plants.

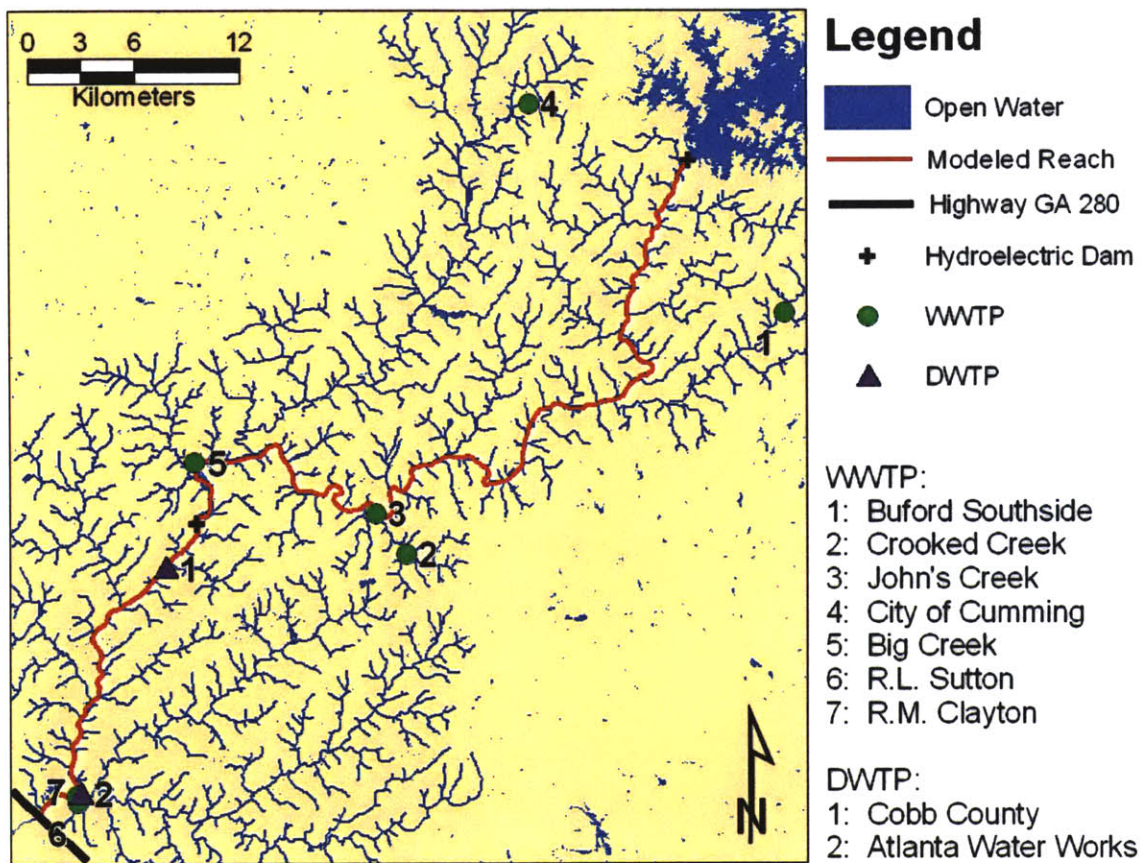


Figure 2-4 Location of Municipal DWTPs and WWTPs in Modeled Reach (EPA, 2003 & Frick and Zaugg, 2003)

3 WASP Model

3.1 Overview of WASP

The Water Quality Analysis Simulation Program, or WASP, is a numerical surface water quality model distributed by the U.S. Environmental Protection Agency. The WASP5 version of WASP was used for this analysis. WASP5 can be run in two modes: EUTRO5 or TOXI5. EUTRO5 is used to model traditional surface water quality constituents such as dissolved oxygen and phosphorus (Ambrose et al., 1993). TOXI5 is used to model toxic pollutants and was the mode used in this study to model the fate and transport of the three phosphate esters.

The following is a brief description of the WASP model. For a more in-depth description the reader is referred to Ambrose et al. (1993).

3.1.1 Basic Water Quality Model

WASP is a tanks-in-series model that allows the user to structure surface water models in one, two or three dimensions (Ambrose et al., 1993). The user divides the surface water body into a series of tanks that represents the characteristics of the water body important to the model. Individual WASP tanks can be used to model surface water, deep-water regions and the underlying benthos. Exchange flows can occur vertically, laterally, or longitudinally between tanks (Ambrose et al., 1993).

The user specifies time-variable advective and diffusive transport across tank boundaries. This establishes the exchange of mass between tanks and across the model boundaries. Time-variable boundary conditions for each water-quality constituent are required at each boundary that the advective and diffusive transport functions identify as exchanging mass with outside the model. Initial concentrations of all modeled constituents are required in each model tank. Time-variable point and diffuse source waste loads for each water quality constituent can be specified. Figure 3-1 illustrates the segmentation of a water body into model tanks and the exchange flows between tanks.

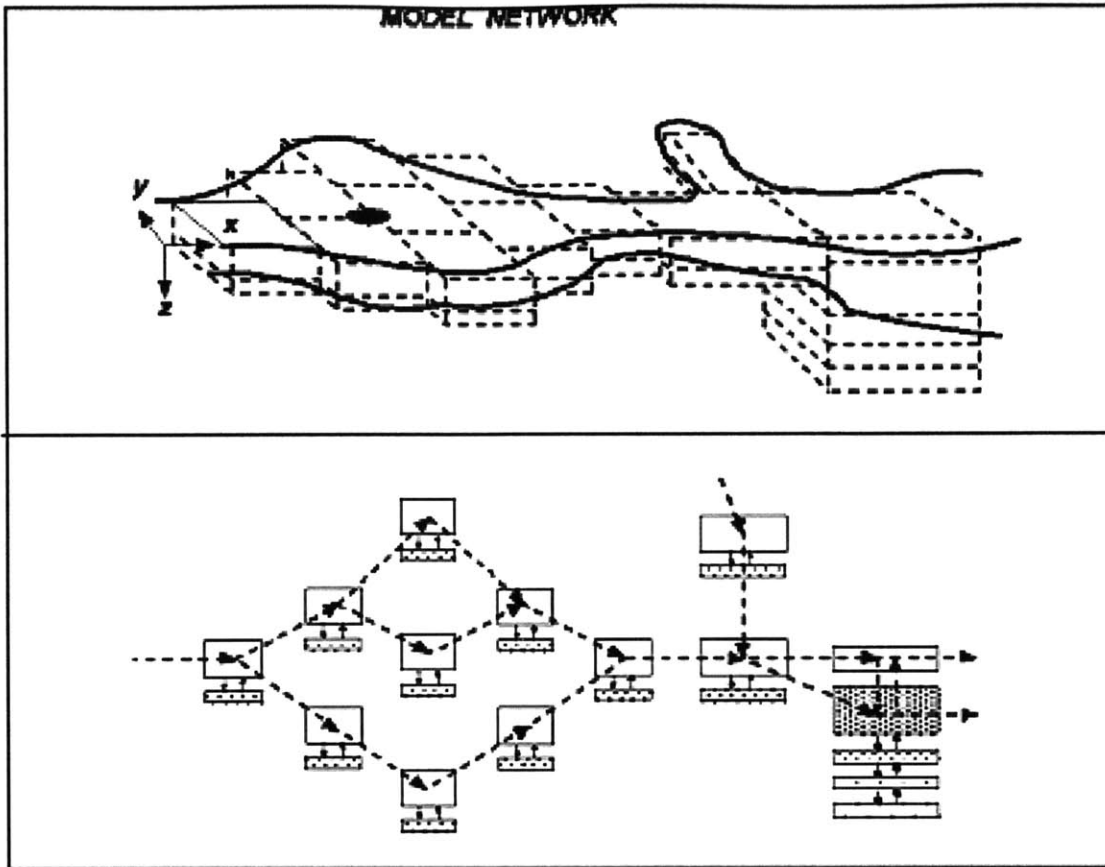


Figure 3-1 Illustration of tanks in series model (Ambrose et al., 1993)

The user specifies the kinetics of the reactions that the modeled water quality constituents undergo. There is a great deal of flexibility in the amount of detail that can be used to encode these reactions. The level of detail chosen for this specific model will be indicated when discussing the individual reactions modeled.

3.1.2 Mass Balance Equation

WASP uses a mass balance approach to compute the constituent concentration at each time step in model tanks. Each tank in the model defines a control volume in which WASP performs a mass balance to determine the water quality constituent concentration within the tank. For each time step, fluxes across each tank boundary are summed and the changes in mass storage as well as fluxes across tank interfaces are determined.

Given a three-dimensional coordinate system x, y, z the concentration at any point in the model is given by the general mass transport equation in three dimensions.

$$\begin{aligned} \frac{\partial C}{\partial t} = & -\frac{\partial}{\partial x}(U_x C) - \frac{\partial}{\partial y}(U_y C) - \frac{\partial}{\partial z}(U_z C) \\ & + \frac{\partial}{\partial x}\left(E_x \frac{\partial C}{\partial x}\right) + \frac{\partial}{\partial y}\left(E_y \frac{\partial C}{\partial y}\right) + \frac{\partial}{\partial z}\left(E_z \frac{\partial C}{\partial z}\right) \\ & + S_L + S_B + S_K \end{aligned}$$

Equation 3-1

Where:

- C = concentration of the water quality constituent [M/L³]
- t = time [T]
- U_x, U_y, U_z = longitudinal, lateral and vertical advection [L/T]
- E_x, E_y, E_z = longitudinal, lateral and vertical diffusion coefficients [L²/T]
- S_L = direct and diffuse loadings [M/L³/T]
- S_B = loadings entering the model across boundaries [M/L³/T]
- S_K = total kinetic transformation rate [M/L³/T]

WASP uses the user specifications to approximate Equation 3-1 at each tank and time step with a finite difference approximation (Ambrose et al., 1993).

3.2 Flow Routing Model

3.2.1 Overview of Problem

As discussed in Section 2.3, two hydroelectric dams regulate flow in the modeled reach of the Chattahoochee River. Buford Dam, the upstream boundary of the model, generates power during diurnal flow releases from Lake Sydney Lanier during weekdays. The flood waves induced by these releases have the effect of increasing Chattahoochee flow by an order of magnitude. Flow may shift by an order of magnitude as many as four times per day at downstream locations. As the flood wave travels down stream it diffuses, decreasing its peak flow rate while increasing its longitudinal width. This attenuation decreases the magnitude of diurnal variation further down stream; still, locations as far as 47 kilometers downstream of Buford Dam experience variations on the order of a factor of two and can be as high as an order of magnitude.

The second dam, Morgan Falls, situated approximately 48 kilometers downstream of Buford, is a run-of-the-river-dam, generating power off of the Buford Dam releases (Cherry et al., 1980). The process of generating power from the flood wave changes the width and amplitude of the wave so that the flood wave past Morgan Falls Dam is more of a function of the power generation schedule at Morgan Falls than at Buford Dam. The magnitude of diurnal variation between Morgan Falls Dam and GA 280 is between factors of two and four.

Natural channels are not uniform in cross section and different portions of a river will respond differently to variations in flow. Changes in flow are compensated for with a combination of velocity, depth and surface width changes at a cross section. The amount of variability in these variables with respect to flow can be understood through an analysis of the river flow with respect to its hydraulic geometry.

Variations in flow and hydraulic geometry can have a considerable effect on the fate and transport of water quality constituents. Increased flow dilutes concentration; low flow may be favorable for some reactions while others may be favored at high flow. Therefore an accurate flow routing model that represents the flows and the effect of hydraulic geometry of the Chattahoochee River reach of interest is important to represent the water quality conditions.

As mentioned in Section 3.1.1, flow functions are entered to WASP directly by the user. During execution, WASP only solves the mass balance equation and does not solve the hydrodynamics or hydrology of the system (Ambrose et al., 1993). Therefore errors in the flow function can cause tank volumes to grow indefinitely or to drop below zero. In order for the WASP model to accurately represent the variation of concentrations and reaction rates of the phosphate esters, a routing of the flood wave through the reaches defined by Buford Dam, Morgan Falls and GA 280 was preformed. This computation estimated inflows and outflows at each model tank during the simulation period.

3.2.2 Data Requirements

Development of the flow routing model required the acquisition of river channel cross section surveys, observed time series flow data for the days being simulated, digital topographic data for the watershed, and land usage data for the watershed. These data elements are described below.

River channel cross-sections were obtained through Robert Olson who has been assisting Dr. Roy Burke at the Georgia Department of Natural Resources. Dr. Burke and Mr. Olson have been working on hydrodynamic and water quality models of the Chattahoochee River since 1994. Each cross section is identified by a longitudinal position along the channel. The cross section is described by a series of station number and elevation pairs. The station number indicates the position of the elevation reading along the later dimension of the channel (HEC, 1990). One hundred and eighty four of these cross sections were used in the development of the flow routing model.

Observed flow data was obtained from the United States Geological Survey (Stamey, 2004). The USGS maintains several gauges throughout the watershed. Observations of flow and gauge height at fifteen minute intervals over the simulated period were acquired. The locations of the gauges that collected the data used in the flow routing model are displayed in Figure 3-2.

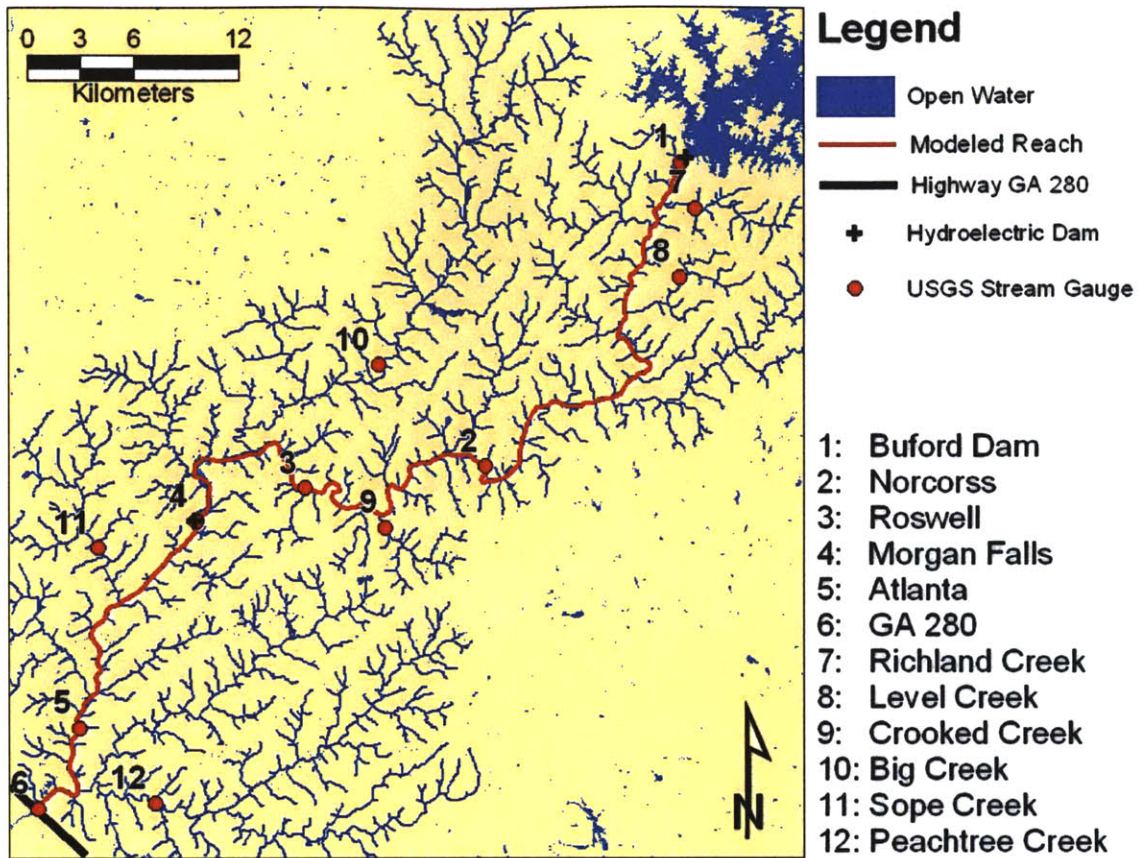


Figure 3-2 Locations of USGS Gauges used in the Flow Routing Model (USGS, 2004)

Digital elevation data for the area containing the modeled reach was obtained from the National Elevation Dataset (NED) administered by the USGS (USGS, 2002). NED data contain elevation observations with resolution of a thirty-by-thirty meter grid. The elevation stored in the grid cell is taken to be at the center of the cell..

Land cover data was obtained from the USGS National Land Cover Dataset (NLCD) (USGS, 1992). These are digital files also on a thirty-by-thirty-meter grid. Each grid cell contains an Anderson level II classification code indicating the land cover occupying the cell. The data was compiled using satellite data supported by census, topography, agricultural statistics and soil characteristic data.

3.2.3 HEC-RAS Model

3.2.3.1 Overview of HEC-RAS

Hydrologic Engineering Center's River Analysis System, HEC-RAS, is a hydraulic modeling system available from the United States Army Corps of Engineers (Brunner, 2002). HEC-RAS allows the user to perform one-dimensional steady flow analysis on a network of channels. Channel geometry is specified by entering a series of channel cross sections. Steady-state flows at the upstream boundary and water surface elevation at both the upstream and downstream boundaries are required.

The energy equation gives the total energy at a given channel cross section (Evetts and Liu, 1987):

$$H = \frac{v^2}{2g} + d + z$$

Equation 3-2

Where:

- H = total energy head in units of length [L]
- v = velocity of the fluid [L/T]
- g = acceleration of gravity [L/T²]
- d = depth of the fluid [L]
- z = elevation of the channel bed above a reference elevation [L]

The basic computation performed by HEC-RAS is a solution of the energy equation between cross sections to determine water surface profiles along the channel. The effects of obstructions such as culverts and bridges are considered by the computation provided they are input in the cross section specification (Brunner, 2002).

3.2.3.2 Steady State Flow Simulation

HEC-RAS was used to obtain approximations of width, depth, velocity and cross-sectional area along the channel of the modeled reach. The cross sections discussed in Section 3.2.2 were imported into HEC-RAS. A steady state model was run with three different profiles simulating low, medium and high flow conditions. The data for each of

the profiles was taken from 15-minute USGS gauge and stage height data recorded over January 14, 2004 – January 16, 2004. In order to determine the specification for the low, medium and high profiles the maximum, average and minimum flows were taken from each of the gauge stations. Profile stage height at the models upstream and downstream boundaries was computed in the same way. The specific gauges and values that were used are listed in Table 3-1.

**Table 3-1 Gauge Flow and Stage used in HEC-RAS Model
(Stamey, 2004)**

Station Name	Profile Boundary Conditions					
	Low		Medium		High	
	Stage (m)	Flow (m ³ /s)	Stage (m)	Flow (m ³ /s)	Stage (m)	Flow (m ³ /s)
Buford Dam	277.70	10.00	278.37	89.19	279.02	176.78
Above Morgan Falls	259.73		259.97		260.17	
Below Morgan Falls	251.38	54.17	251.81	110.79	252.43	196.64
GA 280	226.36		226.90		227.33	

*Stage given in meters above NGVD29

Due to the regulation of flow at Morgan Falls, the HEC-RAS model was divided into two sub models with Morgan Falls Dam as the dividing point. The model of the reach above Morgan Falls was run with the stage data from directly above Morgan Falls as the downstream boundary condition, and flow and stage from just downstream of Buford Dam as the upstream boundary condition. Boundary conditions for the model of the lower reach were taken from stage and flow data from directly below Morgan Falls and stage data at the GA 280 highway, the downstream boundary of the model.

3.2.3.3 Description of HEC RAS Model Results

The runs of each model generated high, medium and low flow profiles. Predictions of velocity, water surface elevation, energy slope, water surface width, and cross sectional areas were made at each cross section..

3.2.4 Muskingum Routing

3.2.4.1 Description of Muskingum Method

The Muskingum Method of hydrologic river routing is based on the equation of continuity (Viessman and Lewis, 2003):

$$I - O = \frac{dS}{dt}$$

Equation 3-3

Where:

- I = inflow rate to river reach [L^3/T]
- O = outflow rate to river reach [L^3/T]
- $\frac{dS}{dt}$ = change of storage within the reach [L^3/T]

The Muskingum Method divides the river being modeled into a series of discrete reaches and time into a number of discrete intervals. The storage in a reach at any time interval, Δt , can be calculated as a function of inflow and outflow to the reach (Viessman and Lewis, 2003):

$$S = \frac{b}{a} [XI^{m/n} + (1 - X)O^{m/n}]$$

Equation 3-4

Where:

- S = storage in the reach [L^3/T]
- a, n = constants reflecting the relationship between stage and discharge at the up and down stream faces of the reach [dimensionless]
- b, m = constants reflecting the relationship between volume and stage within the reach [dimensionless]
- X = constant reflecting the relative weights of inflow and outflow to determining the storage [dimensionless]

The Muskingum Method assumes that $\frac{m}{n}$ is equal to one and that $\frac{b}{a}$ is equal to the constant K . K is usually taken to be the travel time through the reach and X is a value between 0.0 and 0.5 that describes the amount of attenuation of the flood wave within the reach (0.5 being pure translation) (Viessman and Lewis, 2003).

The Muskingum Method proceeds by determining the change in storage in the reach during each Δt . A finite-difference approximation is used to calculate this derivative so that given the mean inflow and outflow over the time step n , storage can be calculated (Viessman and Lewis, 2003):

$$\frac{I_{n-1} + I_n}{2} + \frac{O_{n-1} + O_n}{2} = \frac{S_{n-1} - S_n}{\Delta t}$$

Equation 3-5

Given a hydrograph at the upstream boundary, I_{n-1} and I_n are known for all n time steps on the hydrograph. The routing is completed by successively calculating O_n at every time step using Equation 3-5 and S_n using Equation 3-4.

3.2.4.2 Muskingum Routing Applied to Chattahoochee River

Muskingum Routing was applied to the modeled reach in two different sections. The first section started at Buford Dam and terminated at the impoundment behind Morgan Falls Dam (Bull Sluice Lake). Initial conditions were supplied from the Buford Dam gauge flow data described in Section 3.2.2. The second began at the out flow from Morgan Falls Dam and ended at the crossing of highway GA 280. The hydrograph observed directly below Morgan Falls Dam was used for the initial inflow conditions. Both models routed a five-day flow record from January 12, 2004 to January 16, 2004.

Average velocities at each cross section were taken from the results of the HEC-RAS model described in Section 3.2.3.2. Each of the two river sections being routed was subdivided into reaches, the extents of which were determined by coalescing consecutive cross sections with similar average velocities. The boundary between two reaches was determined to be half way between the last cross section in the upstream reach and the first cross section in the downstream reach.

The values of X were taken from the water quality analysis of the Chattahoochee River conducted in 1978 by the US Army Corps of Engineers Hydrologic Engineering Center (Willey and Huff, 1978). This study examined a much larger reach of the river,

encompassing the reach being modeled here and extending 100 kilometers further downstream. In cases where an exact match between the Corps of Engineers study and the current reaches could not be made X values from a single reach were applied over several current reaches. Values of K were taken to be the travel time through the reach calculated using the average velocity through the reach and the reach length.

The time step, Δt , was selected using the following guidelines for theoretical stability of the model: $2KX \geq \Delta t \geq 2K(1 - X)$ (Viessman and Lewis, 2003).

Tributary inflow was neglected in conducting the Muskingum routing. Flow in gauged tributaries stayed relatively constant through out the five-day period being modeled, the largest of which is about 10% of the Chattahoochee low flow. The constant flow is considered to have minimal effect on the propagation of the flood wave. The water quality model represents tributaries as a constant flow. Representation of tributary flow in the WASP model is discussed in Section 3.2.5.

3.2.4.3 Calibration of Muskingum Coefficients

When the flows generated from the routing described above were first used in the WASP5 model, a discontinuity between the two reaches was exposed. As mentioned above, Morgan Falls is a run of the river hydroelectric plant and generates power from the flood waves released at Buford. The observed hydrograph directly below Morgan Falls is used for the outflow of the tank directly preceding Morgan Falls Dam as well as the inflow to the tank directly following it. If the flood wave routed from Buford Dam does not arrive at Bull Sluice Lake at approximately the same time as the corresponding release from Morgan Falls, the tank preceding the dam will experience a two-order-of-magnitude decrease in volume.

The decrease in volume calculated by the model did not seem realistic based on the fact that the observed water surface of Bull Sluice Lake fell by less than half a meter during the period from January 12, 2004 to January 16, 2004.

Comparison of the routed flood wave arriving at Bull Sluice Lake with the observed hydrograph below Morgan Falls revealed that the arriving flood was out of phase with the

release at Morgan Falls by about half a day. The period of one half day between the first release from Morgan Falls and the first arriving flood from Buford Dam resulted in the decrease in volume described above.

In order to ameliorate the discontinuity the values of K for each reach were adjusted in an attempt to bring the arriving flood wave back into phase with the release at Morgan Falls. The limit to the amount of adjustment was based on the preservation of the inequality, $2KX \geq \Delta t \geq 2K(1 - X)$ discussed in the previous section.

Calibrating the K value in this way decreased the precision of the Muskingum Method approximation further upstream. The accuracy of the model will be discussed further in Section 3.2.4.4

The results of bringing the arriving flood wave into phase with the Morgan Falls release are displayed in Figure 3-3. The predicted flood wave shown in Figure 3-3 balances the observed output also shown. Adjustment of the K constants in the reaches up stream resulted in a phase shift of 0.5 days.

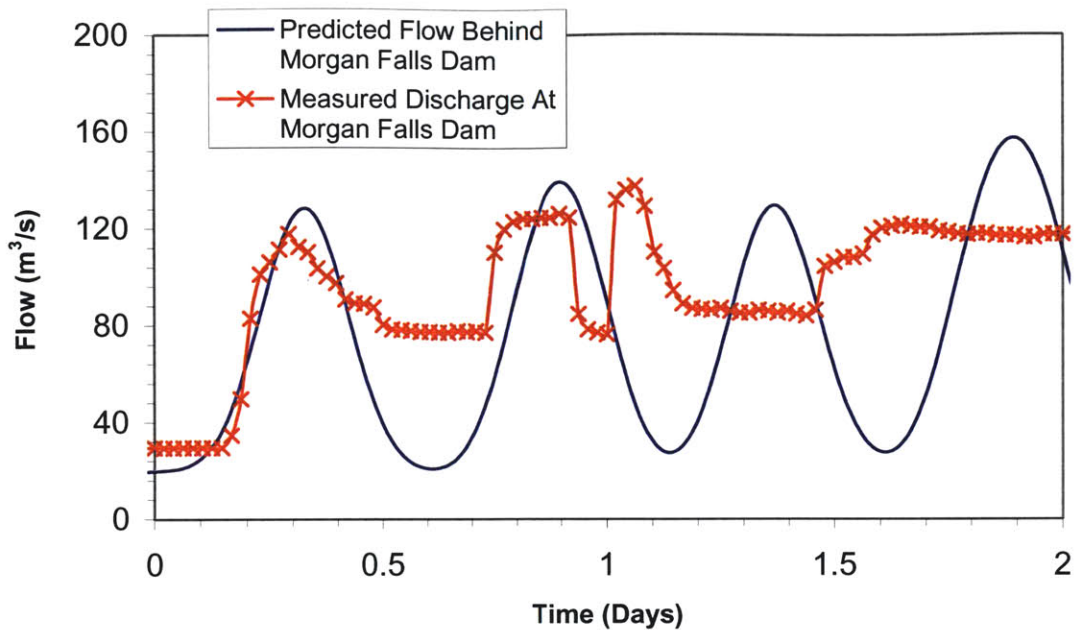


**Figure 3-3 Final Result of Calibrating Muskingum K Values
(Zero on the time axis corresponds to midnight January 13, 2004)
(Observed Data Stamey, 2004)**

3.2.4.4 Muskingum Routing Results vs. Observation

To evaluate their accuracy, the results of the Muskingum routing were compared to observed hydrographs at USGS gauge stations within the routed reaches. Observations during the time period January 14, 2004 – January 16, 2004 were used for the comparison. Table 3-2 lists the gauges that were used for this purpose and their distance downstream from the upstream boundary of the reach. Figure 3-2 can be used to locate gauge positions.

Table 3-2 USGS Gauge Stations Used in Evaluation of Muskingum Routing

Gauge Station Name	Distance Downstream From Buford Dam (km)
Norcross	29
Roswell	46
Morgan Falls	58
GA 280	79

3.2.4.4.1 Buford Dam to Morgan Falls

Figure 3-4 shows the hydrograph observed just downstream of Buford Dam from January 13, 2004 – January 15, 2004. The flood wave peak indicated on the figure by the triangle will be traced downstream and serve as a marker to compare the modeled and the observed hydrographs.

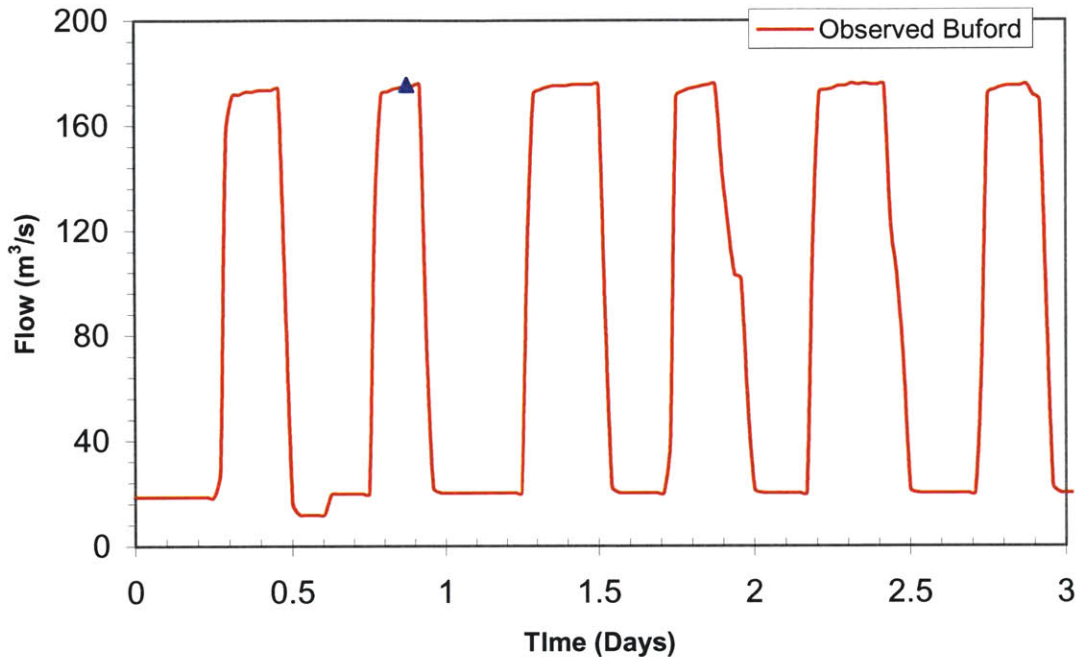


Figure 3-4 Observed Hydrograph Downstream of Buford Dam (01/13/2004-01/15/2004) (Stamey, 2004)

The blue triangle is a time marker as discussed in the text.

Figure 3-5 displays the modeled and observed hydrograph at Norcross, twenty-nine kilometers downstream. Data for Norcross was only available for the dates January 14, 2004 – January 16, 2004 therefore the time axis crosses the origin at Day 1. The marked peak arrives at 1.60 days, 0.7 days after release at Buford Dam. The same peak arrives on the observed flood wave at 1.62 days moving only 2% faster than the modeled flood wave. However looking at the graph one can see obvious discrepancies between the modeled and observed flood wave. The marked peak arrives with a flow of 175 m³/s while the same wave on the observed hydrograph has amplitude of 138 m³/s. In this case

the modeled flow is 27% greater than the observed. The flow inaccuracies between model and observation can be as high as 60% of observed flow in some cases.

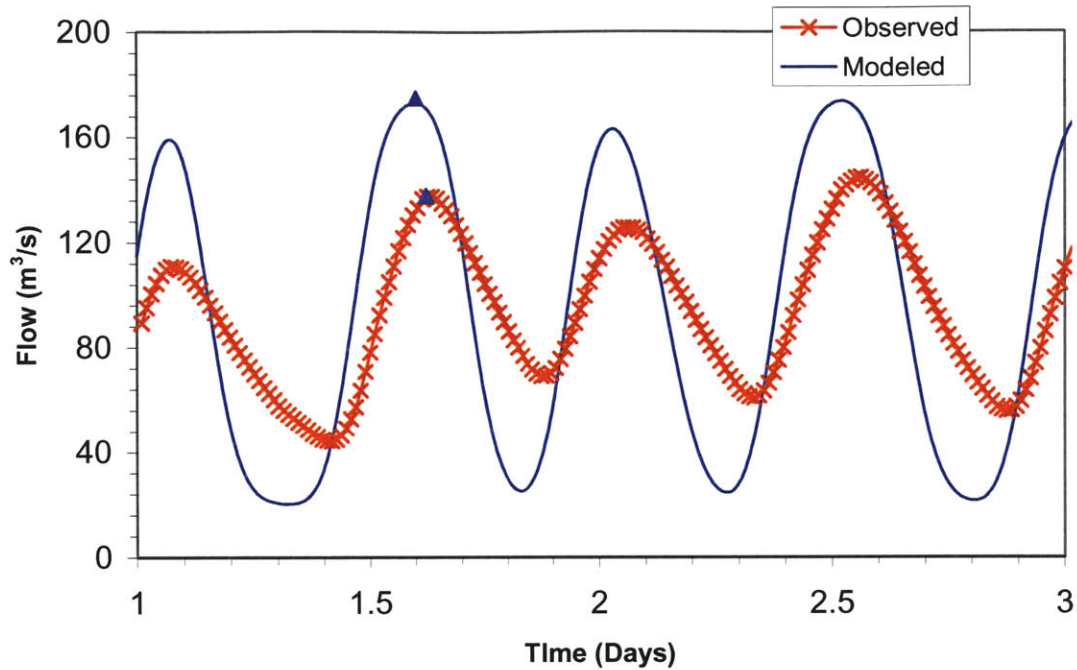


Figure 3-5 Observed and Modeled Hydrographs at Norcross (01/14/2004-01/15/2004) (Observed Data Stamey, 2004)
The blue triangle is a time marker as discussed in the text.

The modeled and observed hydrographs at the Roswell station are shown in Figure 3-6. The marked peak has now traveled another 18 kilometers below Norcross and a total of 46 kilometers since being released at Buford. The modeled and observed peaks arrive within 28 minutes of one another, 7% of the total travel time of the observed wave. Discrepancies were still significant at the Roswell station, varying by 27% of observed flow at the marked peak and as much as 50% at some points.

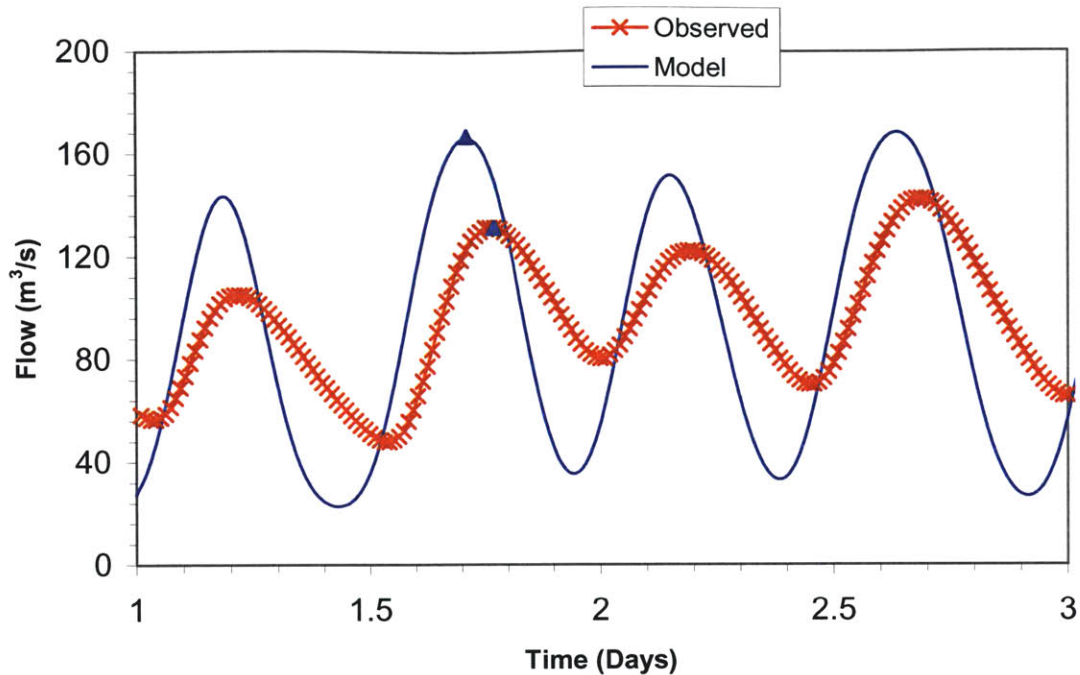


Figure 3-6 Modeled and Observed Hydrographs at Roswell (01/14/2004-01/15/2004) (Observed Data Stamey, 2004)
The blue triangle is a time marker as discussed in the text.

Routing of flood waves through the upstream reaches between Buford Dam and Morgan Falls was accurate with respect to travel time. Modeled travel time to Bull Sluice Lake is approximately one day and given the above results should be accurate to within 10%. The routing was inaccurate with respect to the evolution of flood wave shape. Calibration of the Muskingum constants was attempted however the flow discontinuity at Bull Sluice Lake (Section 3.2.4.3) dictated the value of the K constants. Values of X taken from the US Army Corps of Engineers Study were on the order of 0.01 and were close enough to zero that decreasing them had little effect. The effects of this inaccuracy on the water quality model are discussed in Chapter 4.

3.2.4.4.2 Morgan Falls Dam to GA 280 Crossing

Figure 3-7 shows the hydrograph observed just downstream of the Morgan Falls Dam from January 14, 2004 – January 15, 2004. As in the previous discussion, we will use a triangle to trace a flood peak down stream and assist in evaluating the accuracy of the Muskingum routing of this reach.

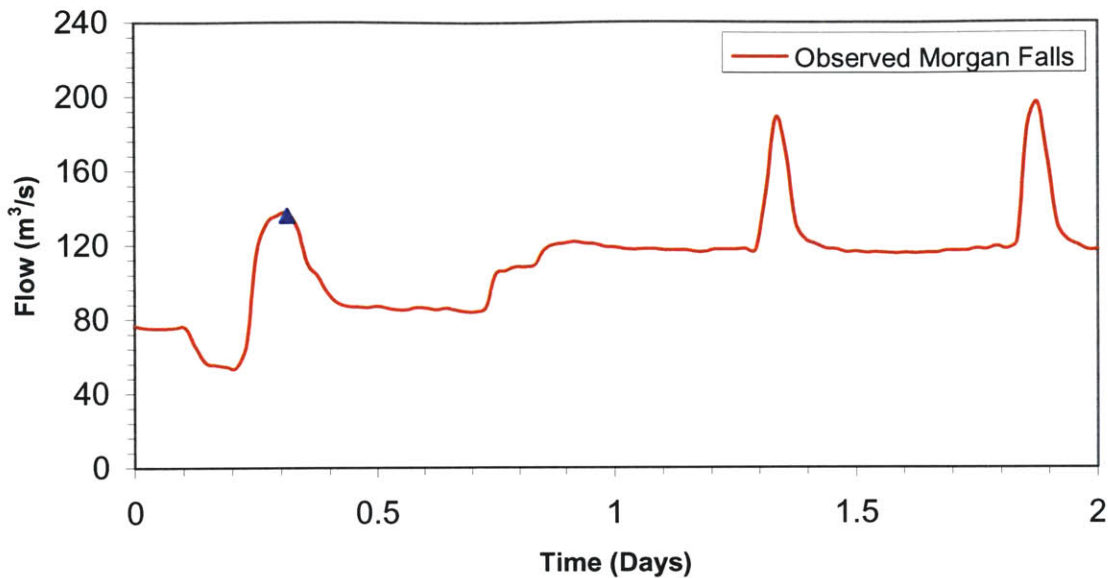


Figure 3-7 Observed Hydrograph Downstream of Morgan Falls Dam (01/14/2004-01/15/2004) (Stamey, 2004)

The blue triangle is a time marker as discussed in the text.

Figure 3-8 displays the modeled and observed hydrograph at the GA 280 crossing, twenty-one kilometers downstream of Morgan Falls Dam. The modeled flood peak arrives at 0.66 days, 0.35 days after release at Morgan Falls Dam. The same peak arrives on the observed flood wave at 0.51 days showing that the observed wave is moving 29% faster than the modeled flood wave. Accuracy of flow is better in this reach with discrepancies between the marked peaks at 4% of the observed flow. The differences in flow between model and observation go no higher than 10% of observed flow at this station.

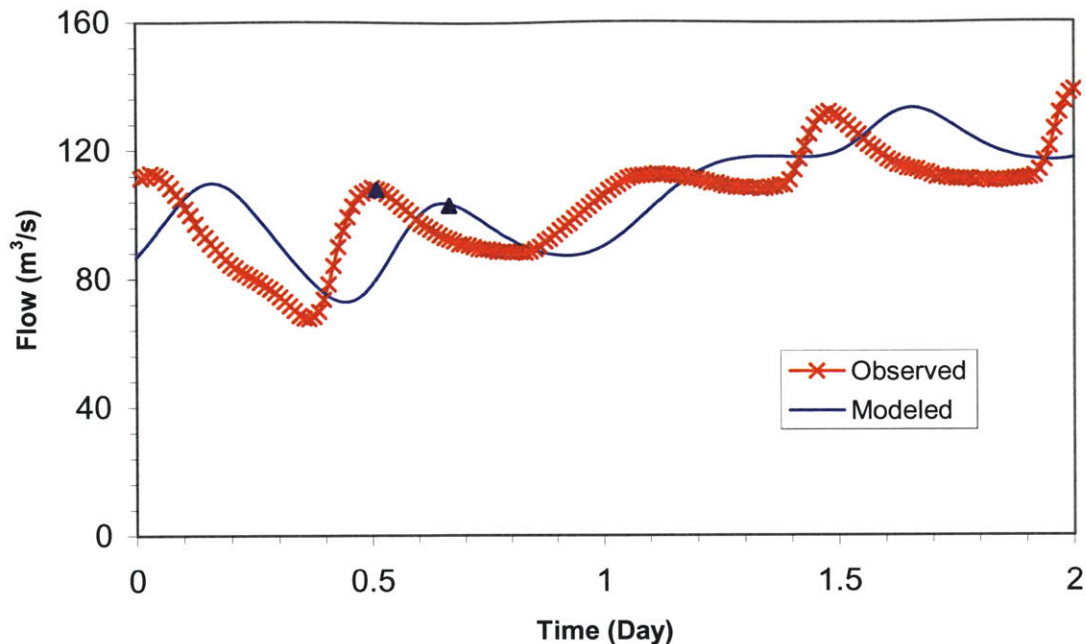


Figure 3-8 Modeled and Observed Hydrographs at GA 280 Crossing (01/14/2004-01/15/2004) (Observed Data Stamey, 2004)
The blue triangle is a time marker as discussed in the text.

The routing of this reach was less accurate with respect to travel time. Modeled fluid leaves the model through the downstream boundary an average of 25% earlier than observed fluid released at the same time. The significance of this inaccuracy is diminished by the fact that the reach is only twenty-one kilometers long. Travel times are small enough that the discrepancy in travel time accounts for a difference less than 3.75 hours. Differences in modeled and observed flow were smaller in this reach and modeled results were about 10% off. The absence of the continuity constraint at the downstream boundary of the reach allowed for more manipulation of Muskingum constants and therefore the ability to sacrifice accuracies in time for accuracies in flow.

3.2.4.4.3 Discussion of Inaccuracies

The results suggest that higher order terms in the energy equation affect the flood wave. More sophisticated routers that account for such effects have been developed and would likely improve the flow predictions, but were impractical within the time and resources

available for this study. Nonetheless, as mentioned above, the flow predictions are sufficiently accurate for the purposes of this study.

3.2.5 Estimation of Tributary Inflow

3.2.5.1 Identification of Tributaries

Tributaries were identified using ArcMap and a NED file describing the elevation in the area around the modeled reach (NED files are described in Section 3.2.2). Given a NED file, ARC Map can calculate the direction of drainage from any grid cell through the comparison of its elevation to that of the surrounding cells. Each cell can have zero to eight cells draining directly into it. If $n_{i,j}$ is the total number of cells draining directly into the cell in row i and column j then the total number of cells, $d_{i,j}$, draining into cell i,j is given by:

$$d_{i,j} = \sum_{k=-1}^1 \sum_{l=-1}^1 n_{i+k,j+l}$$

Equation 3-6

ArcMap determines if a cell is part of a stream channel by evaluating the inequality $d_{i,j} < T$ where T is a threshold value set by the user. If the inequality is false then the cell is determined to be part of a stream channel. The value of the threshold used in this study was 400. It is the value most commonly used to determine the location of stream channels in humid regions (Sheehan, 2003). Once the stream channels were identified on the map the area being drained by each tributary could be calculated.

3.2.5.2 Identification of Significant Tributaries

The approach to modeling tributary inflow was to explicitly handle tributaries that were as large as 2.5% of low flow in the Chattahoochee. Handling of the combined flow of smaller tributaries is discussed in Section 3.2.5.3.

Several of the tributaries are gauged at some point in the channel. Table 3-3 lists the USGS gauging stations on tributaries to the modeled reach. The area drained by the tributary above the gauge is listed along with the average flow observed at the gauge.

Table 3-3 Gauged Tributary Drainage Area and Flow

Station Name	Area Drained (km ²)	Average Flow (m ³ /s)
Richland Creek	27.5	0.31
Level Creek	14.8	0.13
Crooked Creek	26.6	0.15
Big Creek	214	2.07
Sope Creek	86	0.69
Peachtree Creek	251	0.98

The land cover of the watersheds was determined by intersecting the drainage basin of the watershed with the NLCD file (for a description of NLCD data see Section 3.2.2).

Table 3.4 lists the major land cover percentages of the gauged tributary watersheds.

Table 3-4 Gauged Tributary Land Cover

Station Name	Land Cover			
	Residential	Agriculture	Forest	Bareground
Richland Creek	9%	4%	82%	5%
Level Creek	8%	9%	80%	3%
Crooked Creek	46%	2%	49%	2%
Big Creek	6%	22%	69%	1%
Sope Creek	38%	5%	56%	0%
Peachtree Creek	60%	3%	37%	0%

The figures contained in the tables were used as a metric to estimate the flow of the ungauged tributaries. The land cover of the ungauged tributary watershed was compared to the data in Table 3-4, and the gauged watershed with the most similar land cover distribution was identified. The ungauged tributary inflow was estimated using Equation 3-7.

$$Q_U = Q_G * \frac{A_U}{A_G}$$

Equation 3-7

Where:

- Q_U = ungauged tributary flow [L^3/T]
- Q_G = gauged tributary flow [L^3/T]
- A_U = area drained by ungauged tributary [L^2]
- A_G = area drained by gauged tributary [L^2]

The tributaries that were estimated to have a flow greater than 2.5% of low flow in the Chattahoochee are identified in Figure 3-9.

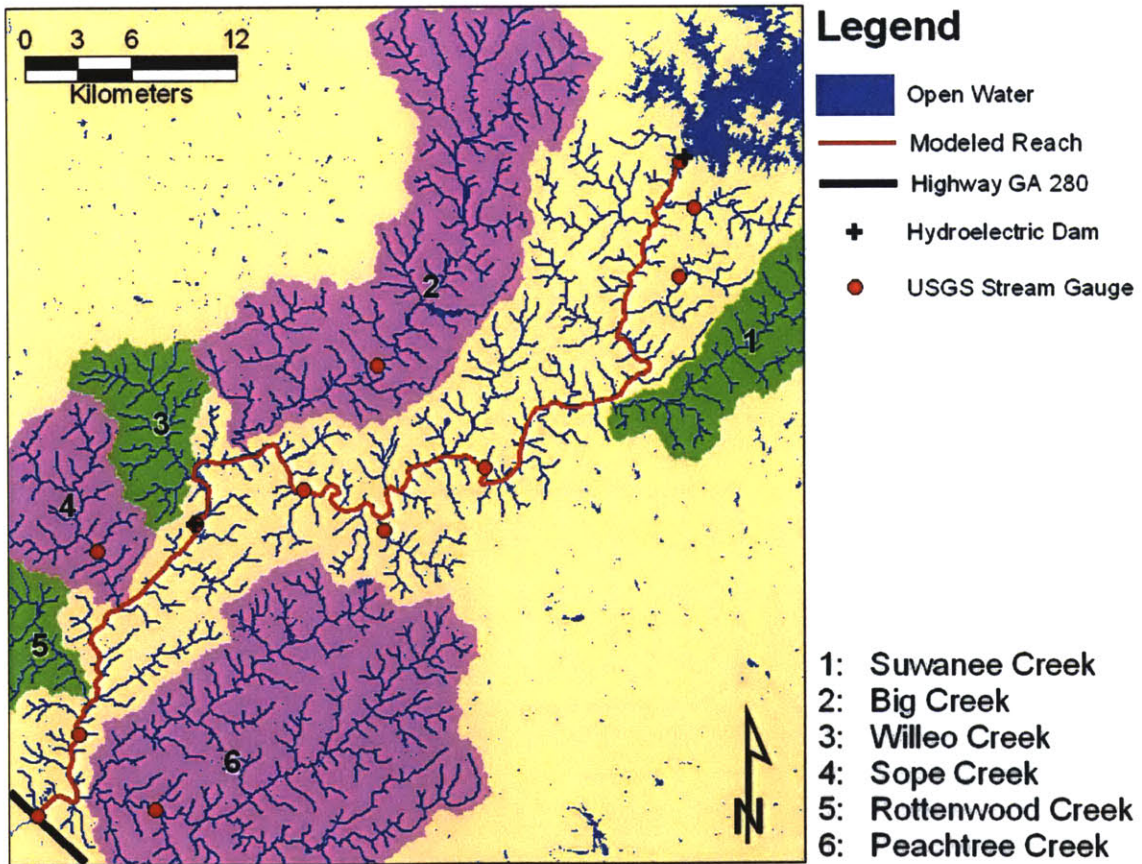


Figure 3-9 Significant Tributary Watersheds

3.2.5.3 Estimation of Combined Tributary Inflow

The combined inflow of the additional tributaries was estimated by comparing the low flow release through Morgan Falls Dam with the estimated flow entering Bull Sluice Lake under the same conditions. Over the weekend of January 11, 2004 power was not generated at Buford Dam and flows remained relatively constant at about 20 m³/s. Assuming that Bull Sluice Lake was not decreasing or increasing in storage during this time there should be an equal flow entering the lake as leaving it over Morgan Falls Dam. This flow should be the observed outflow at Buford Dam plus any inflow within the reach.

$$Q_x = Q_{MF} - Q_B - Q_T$$

Equation 3-8

Where:

- Q_x = unknown inflow [L³/T]
- Q_{MF} = flow over Morgan Falls Dam [L³/T]
- Q_B = low flow at Buford Dam [L³/T]
- Q_T = estimated tributary inflow [L³/T]

The unknown inflow, Q_x , was then distributed linearly throughout the reach between Buford Dam and Morgan Falls. The only tributary inflow accounted for in the lower reach was the tributary inflow determined as described in section 3.2.5.2.

3.3 Tanks in Series Model

3.3.1 Overview and Design Goals

As discussed in section 3.1.1, WASP requires that the user represent the modeled water body as a series of discrete tanks. Each tank can be thought of as being fully mixed, i.e. any contaminant mass that enters the tank at the upstream end instantly mixes across the entire volume of the tank. This is not the way things occur naturally and care must be taken when designing the model so that the natural mixing processes are accurately represented by the model abstraction.

For the purposes of the current study a one-dimensional approach was taken, modeling the Chattahoochee as a single line of surface water tanks. The one-dimensional model neglects concentration gradients in the lateral and vertical. Inaccuracies due to this assumption will be discussed in Chapter 4. The boundaries of the tanks were determined with the following criteria:

1. Point sources are at the upstream edge of a tank
2. Sampling stations are at the center of a tank (Ambrose et al., 1993)
3. The series of fully mixed tanks should be a good approximation of natural mixing processes in the river.
4. The tanks should be a good approximation of river geometry

Locations of sample stations and point sources were known and therefore tank boundaries could be positioned to accommodate them. Fulfilling the third and fourth criteria required further consideration.

3.3.2 Modeling Dispersion

3.3.2.1 Overview of Dispersion

Flow within a river channel is not uniform. Friction at the channel bed and sides causes the fluid at these boundaries to move slower than the fluid in the channel center. Contaminants that enter the river will be advected downstream at different velocities depending on their lateral and vertical position within the channel. This process, called dispersion mixes the contaminant mass longitudinally. Turbulent eddies mix fluid laterally and vertically across the channel abolishing the concentration gradients caused by the differential flow. The relationship between how quickly turbulence destroys the concentration gradients and how quickly the differential flow creates them is embodied in a dispersion coefficient.

The shear velocity, u^* , characterizes the friction causing the retardation of fluid flow at the channel bed (Hemond and Fechner-Levy, 1994). Shear velocity is given by:

$$u^* = \sqrt{gdS}$$

Equation 3-9

Where:

- g = acceleration of gravity [L/T²]
- d = channel depth [L]
- S = slope of water surface [L/L]

A dispersion coefficient, E_L , is a constant that characterizes the magnitude of the dispersive process in a fluid system. The dispersion coefficient for a river can be approximated with Fischer's formula (Shanahan & Gaudet, 2000):

$$E_L = \frac{.011U^2\overline{W}^2}{du^*}$$

Equation 3-10

Where:

- U = mean stream velocity [L/T]
- \overline{W} = mean channel width [L]
- d = mean depth [L]
- u^* = shear velocity given by Equation 3-9 [L/T]

Consider a pulse injection of a conservative tracer into a river at point x . The center of mass is advected downstream by the mean current and dispersed longitudinally within the channel through dispersion. The strategy for accurately approximating these processes in the current model is discussed below.

3.3.2.2 Dispersion in the Tanks in Series Model

As discussed in Section 3.2.1, the contaminant mass is assumed to instantly mix across the entire volume of the tank upon introduction across a tank boundary. When a conservative concentration pulse of c_0 is introduced at the upstream boundary of a fully mixed tank with mean residence time t^* , the output concentration, $c(t)$, is observed at the tank outlet according to (Adams, 2004):

$$c(t) = c_0 e^{-(t/t^*)}$$

Equation 3-11

The concentration response curve at the outlet of the fully mixed tank is shown in Figure 3-10.

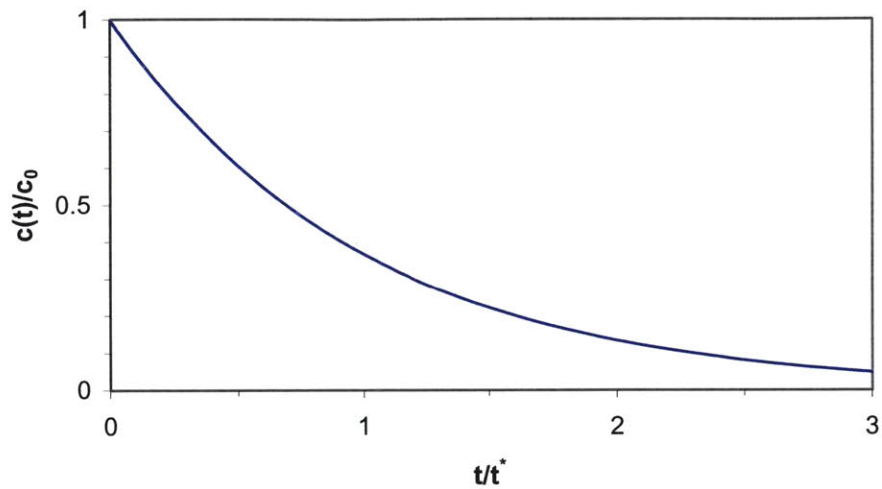


Figure 3-10 Concentration Response Curve in Fully Mixed Tank

A plug flow tank is one in which no mixing occurs and the mass introduced at the upstream boundary is observed to exit the tank in its entirety at t^* . The concentration response curve at the outlet of the plug flow tank is displayed in Figure 3-11.

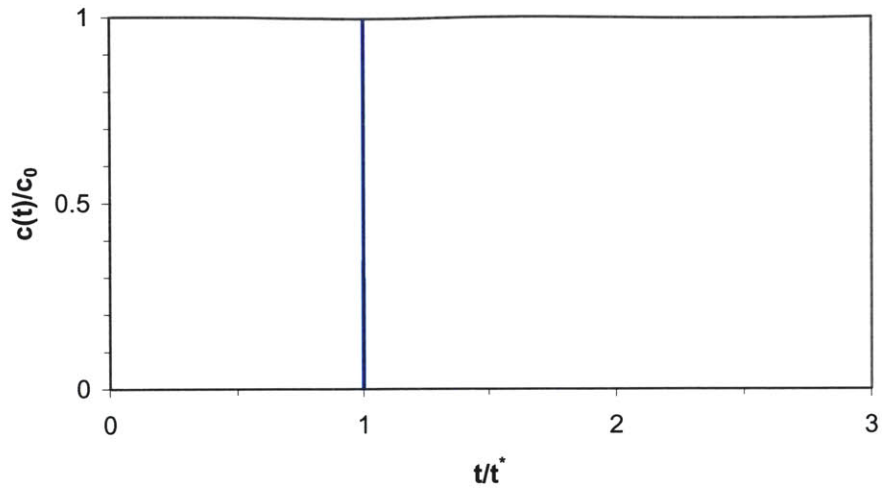


Figure 3-11 Concentration Response Curve in Plug Flow Tank

Through the serial combination of n well mixed tanks a combination of the well mixed and plug flow models can be achieved. The concentration response at the outlet of the final tank is given in the following equation (Shanahan & Harleman, 1984):

$$c(t) = c_0 \frac{n^n}{(n-1)!} \left(\frac{t}{t^*}\right)^{n-1} e^{-n\frac{t}{t^*}}$$

Equation 3-12

Concentration response curves at the outlet of a series of tanks with n equal to two, four, eight, sixteen and thirty-two are displayed in Figure 3-12.

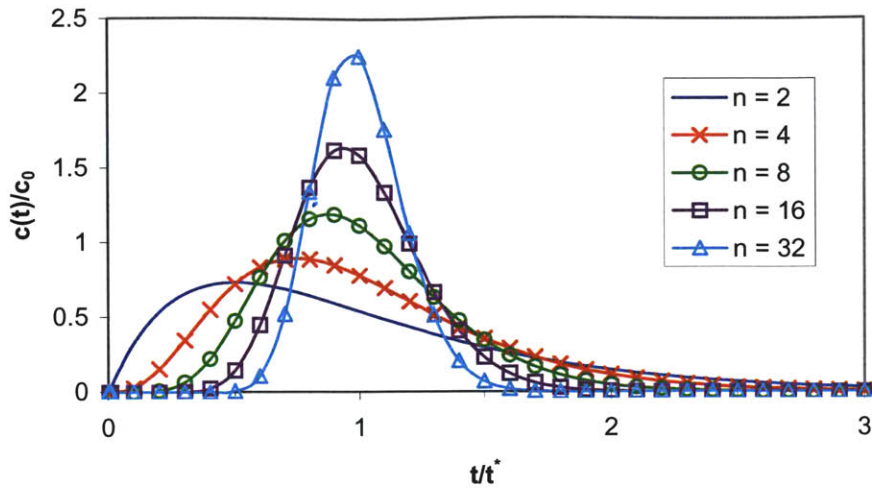


Figure 3-12 Concentration Response Curve in Series of Fully Mixed Tanks

Inspection of Figure 3-12 reveals that as the number of fully mixed tanks in series grows the system approaches plug flow behavior, which is achieved in the limit $n \rightarrow \infty$.

Due to the combined affect of advective and dispersive processes, river systems do not behave as either fully mixed or plug flow but as some combination of the two. The Peclet number is a non-dimensional number that describes the effects of advection relative to dispersion within the system:

$$Pe = \frac{UL}{E_L}$$

Equation 3-13

Where:

- U = mean velocity in the river reach [L/T]
- L = length of river reach [L]
- E_L = the dispersion coefficient for the river reach [L^2/T]

In order to accurately represent these mixing processes with the tanks in series model, the number of tanks must be such that they approximate the Peclet number of the system being modeled.

Shanhan and Harleman (1984) state that the Peclet number of a system can be used to determine the number of fully mixed tanks in series required to reasonably approximate the dispersion in a river.

$$Pe = 2n - 1$$

Equation 3-14

3.3.2.3 Dispersion Model

In the current study dispersion in the Chattahoochee was modeled using the only the dispersion encompassed in the series of fully mixed tanks. As discussed in the previous section it first necessary to calculate a Peclet number to determine the number of tanks in series required to accurately describe the longitudinal mixing processes in the river.

Using Equation 3-9 and Equation 3-10 on the pertinent output from the HEC RAS model (Section 3.2.3), three dispersion coefficients were calculated for each cross section in the HEC-RAS model; one for each profile. These values were averaged to estimate a mean dispersion coefficient for the modeled reach. Taking the average velocity in the river to be the mean of each profile velocity at each cross section a Peclet number was calculated for the modeled reach using Equation 3-13. The velocity, length and dispersion coefficient used in the Peclet number are listed in Table 3-5.

Table 3-5 Figures Used to Calculate Peclet Number

Mean Velocity	0.75 m/s
Length of Reach	80,000m
Mean Dispersion Coefficient	290 m ² /s
Pe	207

Using Equation 3-14 the number of tanks in the current model was set at 103.

3.3.3 Determination of Tank Boundaries

The tank boundaries were determined by identifying consecutive cross sections with similar characteristics. The characteristics being compared were taken from the output of the HEC-RAS model (Section 3.2.3). Utilizing every cross-section, we obtained 103 mutually exclusive sets of consecutive cross sections, each representing a tank in the

model. The boundaries between tanks were determined either by the modeling criteria 1 and 2 (Section 3.2.1) or to be half way between the cross sections at the up and downstream ends of consecutive tanks.

3.3.4 Determination of Discharge Coefficients

The equation of continuity of flow states that at a given cross section flow is a direct function of velocity and area:

$$Q = AV$$

Equation 3-15

Where:

- Q = flow [L^3/T]
- A = area [L^2]
- V = velocity [L/T]

According to Equation 3-15 a river will change cross-sectional area and velocity in response to changes in flow. Natural channels tend to vary area while keeping velocity relatively constant, in regions where the river has been altered, such as with culverts, the river may be constrained and be forced to vary velocity in response to flow variability. Many chemical reactions that are important in a water quality model are affected by changes in fluid velocity and cross-sectional area. It is therefore important to understand how the water body responds to changes in flow in order to accurately model these reactions.

3.3.4.1 Discharge Coefficients and WASP

At any given tank in the model the velocity, depth, and width are functions of river flow (Ambrose et al., 1993) so that:

$$V = aQ^b$$

Equation 3-16

$$D = cQ^d$$

Equation 3-17

$$W = eQ^f$$

Equation 3-18

Where:

- V = mean velocity in the tank [L/T]
- D = mean depth in the tank [L]
- W = mean width in the tank [L]
- Q = flow through the tank [L^3/T]
- a, b, c, d, e & f are empirical coefficients and exponents [dimensionless]

The cross sectional area of a tank is approximately the average width multiplied by average depth. Therefore by continuity (Ambrose et al., 1993)

$$Q = VDW$$

Equation 3-19

By substituting Equation 3-16, Equation 3-17 and Equation 3-18 into Equation 3-19 it is shown that (Ambrose et al., 1993)

$$ace = 1$$

Equation 3-20

$$b + d + f = 1$$

Equation 3-21

Given that reaction rates can depend strongly on fluid velocity, channel depth and channel width it is important that there be an accurate approximation of the discharge coefficients for each tank. WASP5 requires that the discharge coefficients for velocity and depth be entered for each tank.

3.3.4.2 Estimation of Discharge Coefficients

Using the tank definition described in Section 3.3.3 an average high, medium and low flow velocity, depth, and width was calculated for each tank. These averages were calculated using the output of the HEC-RAS model so that the average high flow velocity for a tank was an average of the high flow velocity of the cross sections comprising the tank. The other averages were computed in the same way.

The discharge coefficients for a particular tank were estimated using a least squares fit through the computed averages using the equation $y = ax^b$ (Microsoft Excel, 1999). As an example of this process consider the velocity in tank eighty-eight. The low, medium and high flow conditions in the tank are listed in Table 3-6.

Table 3-6 High, Medium & Low Profile Averages for Tank 88

Profile	Flow (m ³ /s)	Velocity (m/s)	Depth (m)	Width (m)
High	198	0.9	4.0	67
Medium	111	0.7	3.5	63
Low	54	0.4	2.8	59

The least-squares-fit was used to approximate the functions for velocity, depth, and width. Figure 3-13, Figure 3-14, and Figure 3-15 display the least squares fit to each of the power functions. In each tank the two fits with the highest R² value were used to calculate the WASP5 discharge coefficients for velocity and depth using equations 3.17a and b.

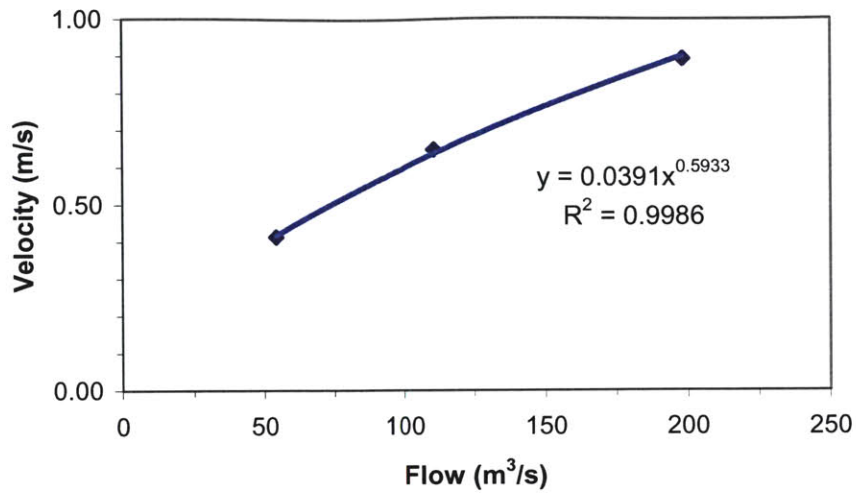


Figure 3-13 Power Function Fit to Velocity vs. Flow Data

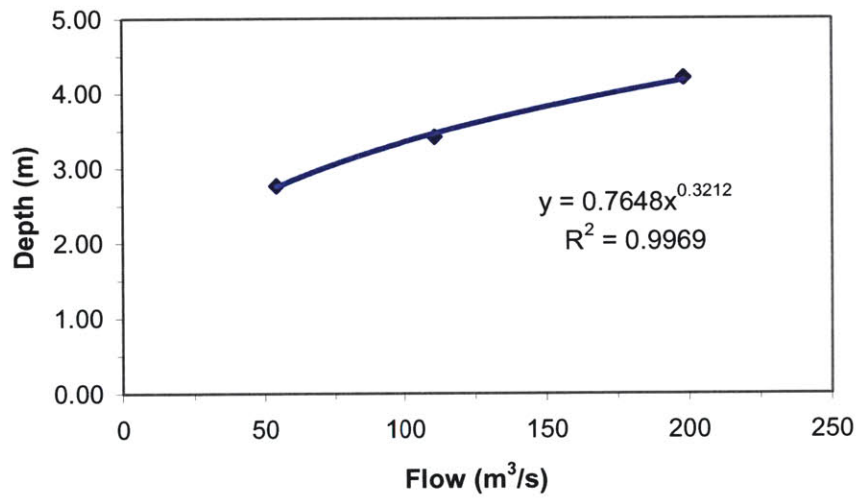


Figure 3-14 Power Function Fit to Depth vs. Flow Data

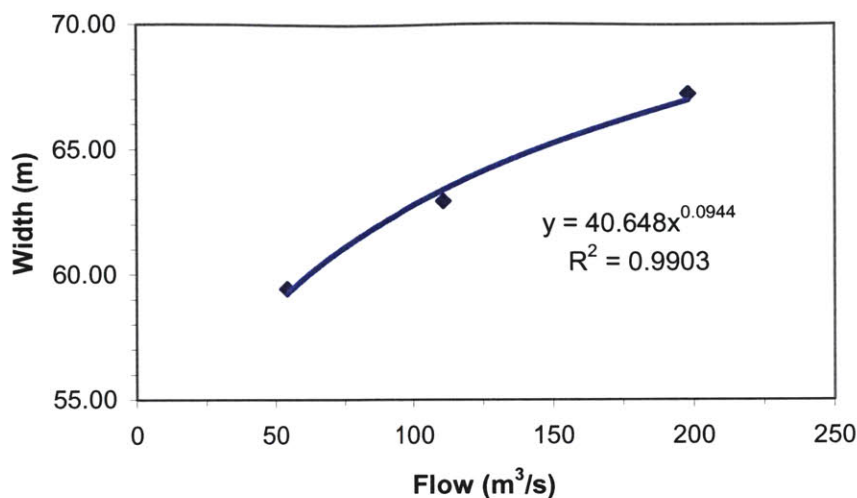


Figure 3-15 Power Function Fit to Width vs. Flow Data

3.3.4.3 Discharge Coefficient Results

The accuracy of the method used to estimate the discharge coefficients can be evaluated by comparing tank depth in the model to observed stage changes at the USGS gauge stations. The discussion here will be considered when evaluating the results of the water quality model.

Five USGS gauge stations recorded stage height in the reach between Buford Dam and Morgan Falls. Data was available for these gauges for the period January 14, 2004 – January 16, 2004. The stage height was converted to depth using the available cross section closest to the gauge. The gauges and the model tanks to which they are being compared are listed in Table 3-7. The gauge locations can be found on Figure 3-2.

Table 3-7 USGS Gauge Stations and Model Tanks Used to Compare Accuracy of Discharge Coefficients

Station Name	Model Tank
Norcross	19
Roswell	33
Bull Sluice Lake	55
Atlanta	90
GA 280	103

Figure 3-16 shows observed and modeled depth at the Norcross gauge station. It should

be kept in mind that the observed hydrograph displays depth at a single cross section in the river while the model is displaying the average depth at a model tank representing the portion of the channel encompassing the gauged cross-section. Tank 19 in particular is 1.2 kilometers long. In light of this, the maximum difference in depth of a half meter is a fairly good match. The range between maximum and minimum depths is greater in the model. This and the phase shift of the modeled wave can be accounted for by the inaccuracies in the flood routing discussed in section 3.2.4.4.

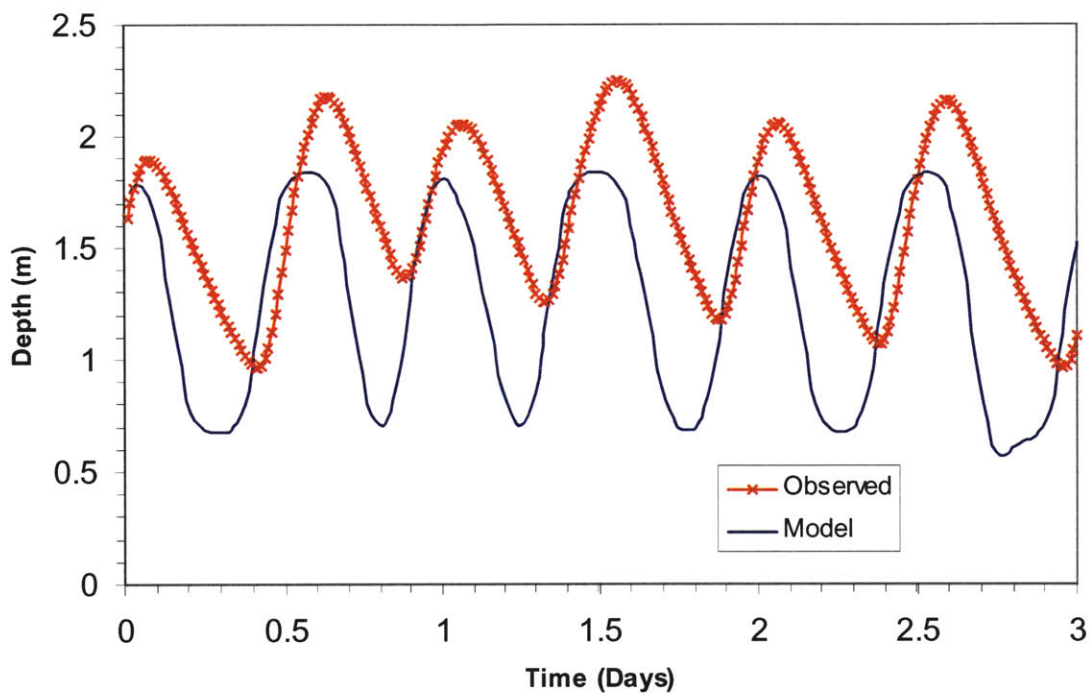


Figure 3-16 Modeled and Observed Depth at Norcross (01/14/2004-01/16/2004) (Observed Data Stamey, 2004)

The modeled and observed depth at Roswell during the same period is shown in Figure 3-17. In this case the modeled depth does not match the observed at any time and on average the modeled depth is about 0.7 meters less than observed. However the range of both modeled and observed curves is approximately 0.5 meters, which supports the values assigned to d in Equation 3-17. The Roswell gauge is at the upstream end of tank 33, which extends downstream 610 meters from the gauge; thus, the gauge location is unlikely to coincide with the center of the tank where depth is calculated.

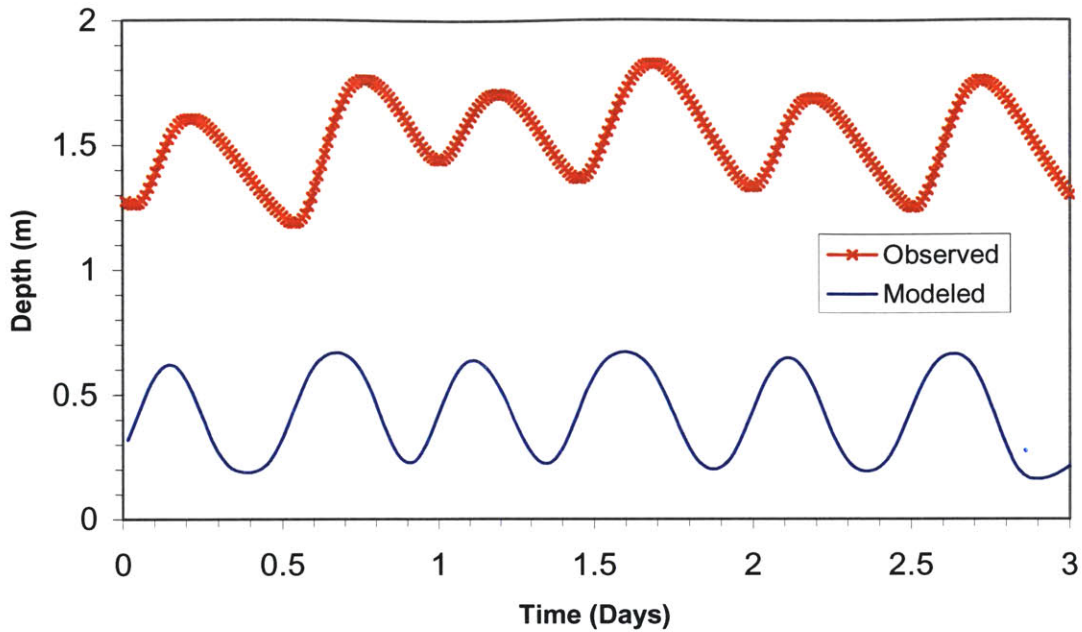


Figure 3-17 Molded and Observed Depth at Roswell (01/14/2004-01/16/2004) (Observed Data Stamey USGS, 2004)

Further insight is gained by looking at the depth rate of change in the observed data and model results. This indicates if the modeled discharge coefficients are correctly approximating the response to flow in terms of change in volume in this reach of the Chattahoochee. Figure 3-18 shows the derivative with respect to time of observed and modeled depth at the Roswell gauge. The model wave has a larger and steeper derivative at local minimums that can be explained as stemming from the imprecision in the flood routing model (Figure 3-6). Taking this into account the modeled curve is a fairly good approximation of the observed and supports the estimated discharge coefficients.

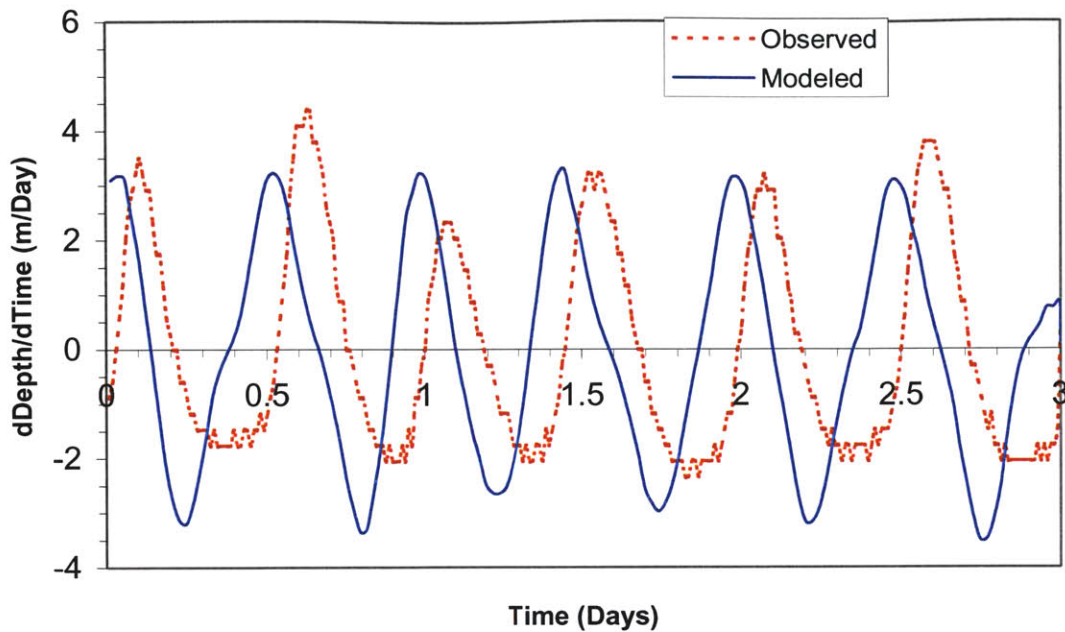


Figure 3-18 Modeled and Observed Change in Depth with Time at Roswell (01/14/2004-01/16/2004) (Observed Data Stamey, 2004)

Bull Sluice Lake is deeper, wider, and slower flowing than the rest of the modeled reach and it is worthwhile to look at the results from this area to evaluate the performance of the discharge coefficients under these conditions. The USGS gauge above Morgan Falls records stage only and was therefore only available for comparison to depth data. Figure 3-19 shows depth while Figure 3-20 shows the derivative of depth with respect to time for both model and observed in Bull Sluice Lake. The gauge is directly above the dam and therefore probably in the deepest part of the impoundment, suggesting that the difference of over a meter in depth at some points could be due to the placement of the gauge. The range between depth maxima and minima in the model is comparable to observation. As in the other examples the modeled wave is not as smooth as the observed which is an artifact of inaccuracies in the flood routing (Section 3.2.4).

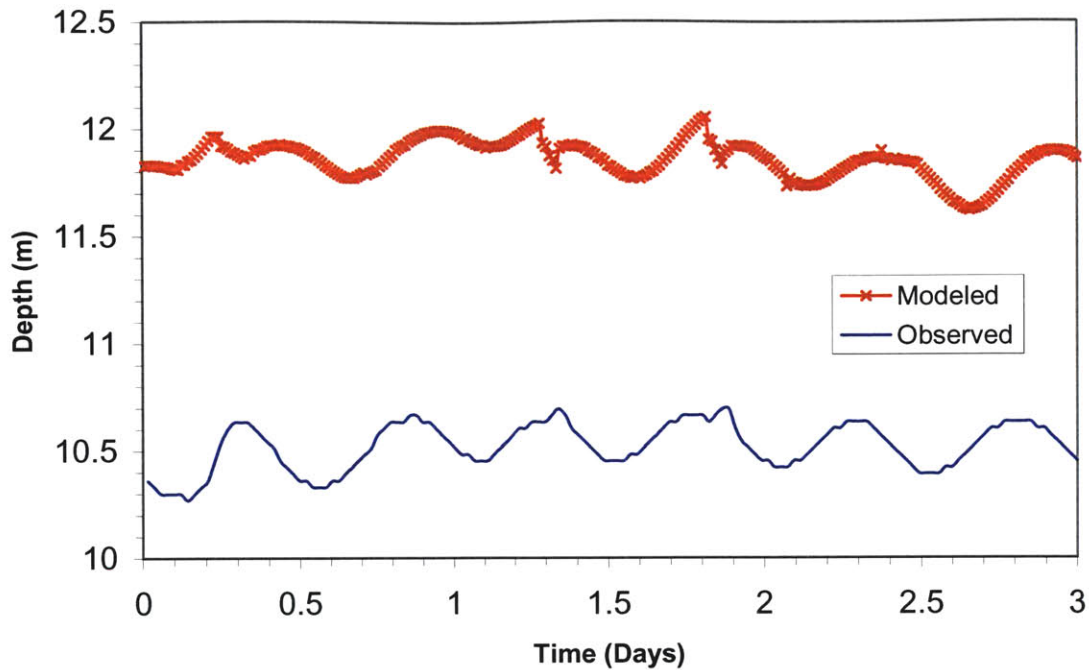


Figure 3-19 Modeled and Observed Depth at Bull Sluice Lake (01/14/2004-01/16/2004) (Observed Data Stamey, 2004)

One interesting feature to note is the sharp changes in the observed wave at 1.30 and 1.85 days. This is more clearly seen in Figure 3-20 where a sudden shift in the derivative occurs at both these points. This is possibly caused by dam operation and may be a result of rapid changes in flow

Although the modeled wave appears to have some irregularity in the crest of the wave at around 1.7 days, the model does not account for the effects of the dam operation. The noticeable effects are probably not extremely significant in terms of the water quality model, as they seem to occur only very close to the dam and are not sustained for long periods.

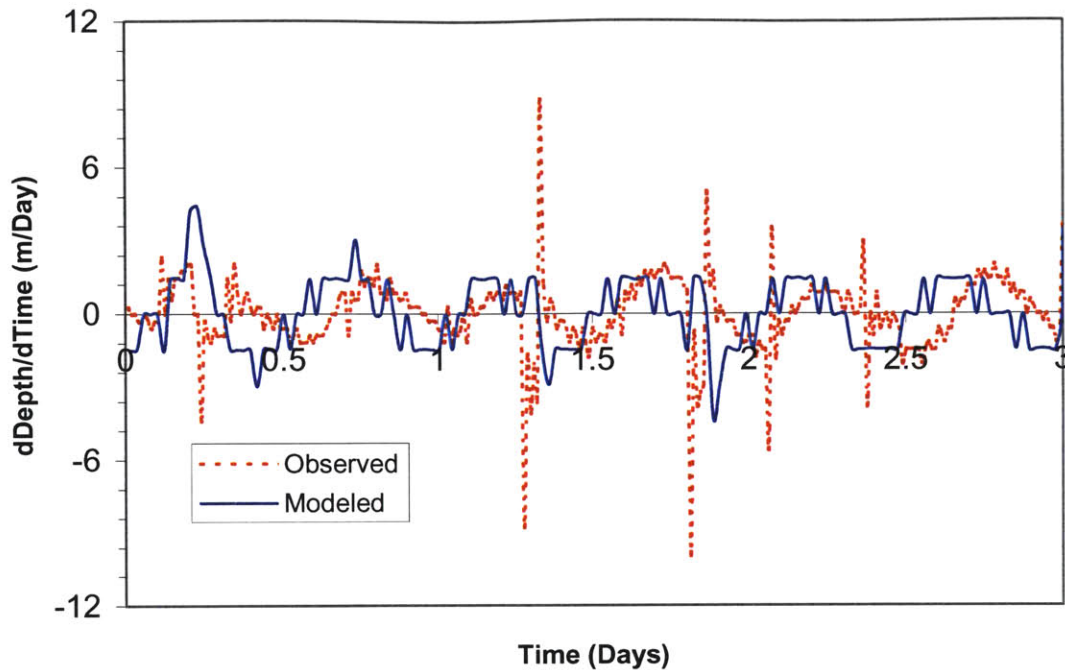


Figure 3-20 Modeled and Observed Change in Depth at Bull Sluice Lake (01/14/2004-01/16/2004) (Observed Data Stamey, 2004)

Inspection of Figure 3-20 shows that the modeled derivative, aside from the observed sudden maxima and minima, fluctuates more rapidly and irregularly. This is an effect of the difficulty in aligning perfectly the arrival of the flood wave from Buford Dam and the release at Morgan Falls. The sudden increases are due to the flood wave arriving before the Morgan Falls Release and the decreases are due to the continuation of the Morgan Falls release during the low flow between flood waves.

Two stage observation stations are available downstream of Morgan Falls for gauging the accuracy of the discharge coefficients in this reach. The modeled and observed depth at the Atlanta station is displayed in Figure 3-21. The modeled depth is in general 0.2 meters greater than observed and the two peaks occurring at about 1.5 and 2.2 days do not perfectly match the observed. Still tank 90 appears to be the sample point where the approximation of depth made by the model most accurately represents reality.

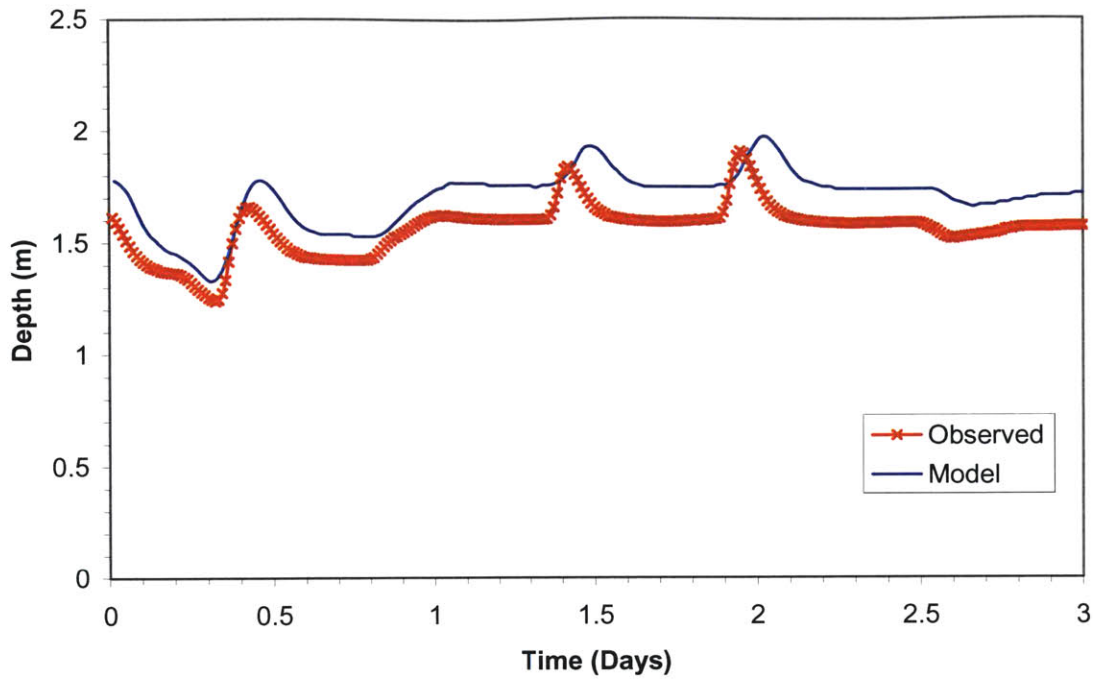


Figure 3-21 Modeled and Observed Depth at Atlanta (01/14/2004-01/16/2004) (Observed Data Stamey, 2004)

The final comparison will be made between the final tank in the model and the GA 280 USGS gauge station. Modeled depth is greater than observed and it should be noted that tank 103 measures 1.46 kilometers and the GA 280 gauge station may not be representative of average depth conditions in the reach. Both curves appear to be in phase.

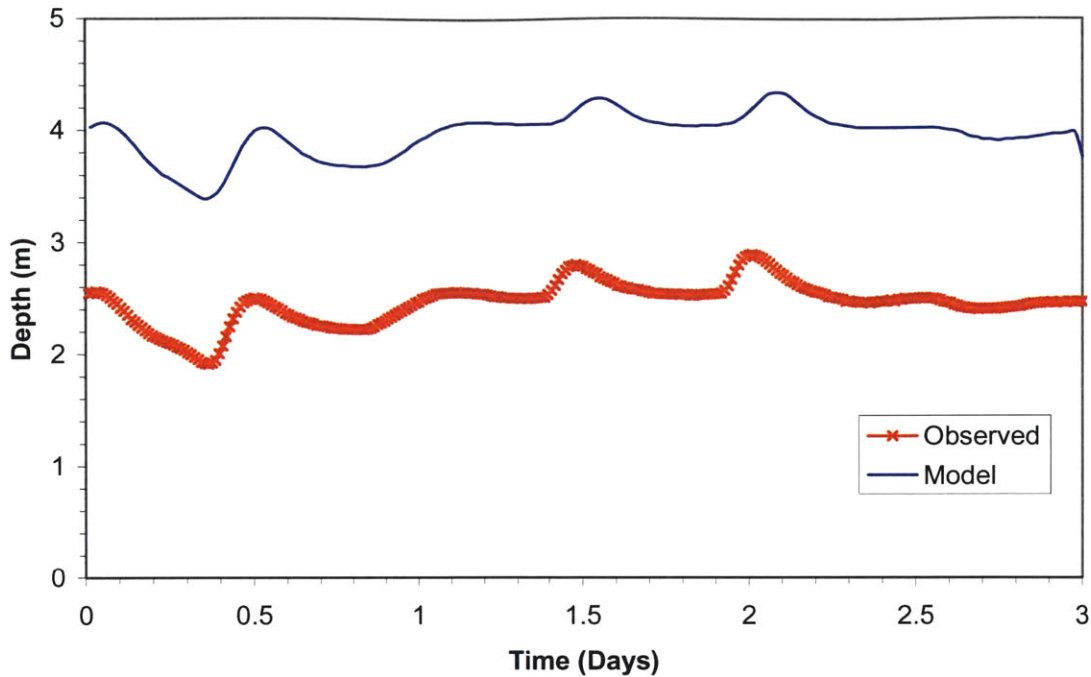


Figure 3-22 Modeled and Observed Depth at the GA 280 Crossing (01/14/2004-01/16/2004) (Observed Data Stamey, 2004)

Since there was some discrepancy in depth between modeled and observed at the GA 280 crossing we will consider the graph of the derivative of depth with respect to time as a final check on the discharge coefficient approximation. Observing the plots in Figure 3-23 one can see that the model rate of depth change is a good approximation of the observed rate of change. At 1.5 and 2 days the observed derivative is higher but these are the only places where significant differences exist. Closer inspection of these two peaks reveals that they are in the same spot as the irregularities observed in Figure 3-20 however the peaks are reversed. At the GA 280 crossing the sharp increase in depth is followed by a decrease, above Morgan Falls the increase follows the decrease. This lends support to the presumption that this is due to rapid increases in flow observed at the two peak flows visible in Figure 3-21 and Figure 3-22 at 1.5 and 2 days.

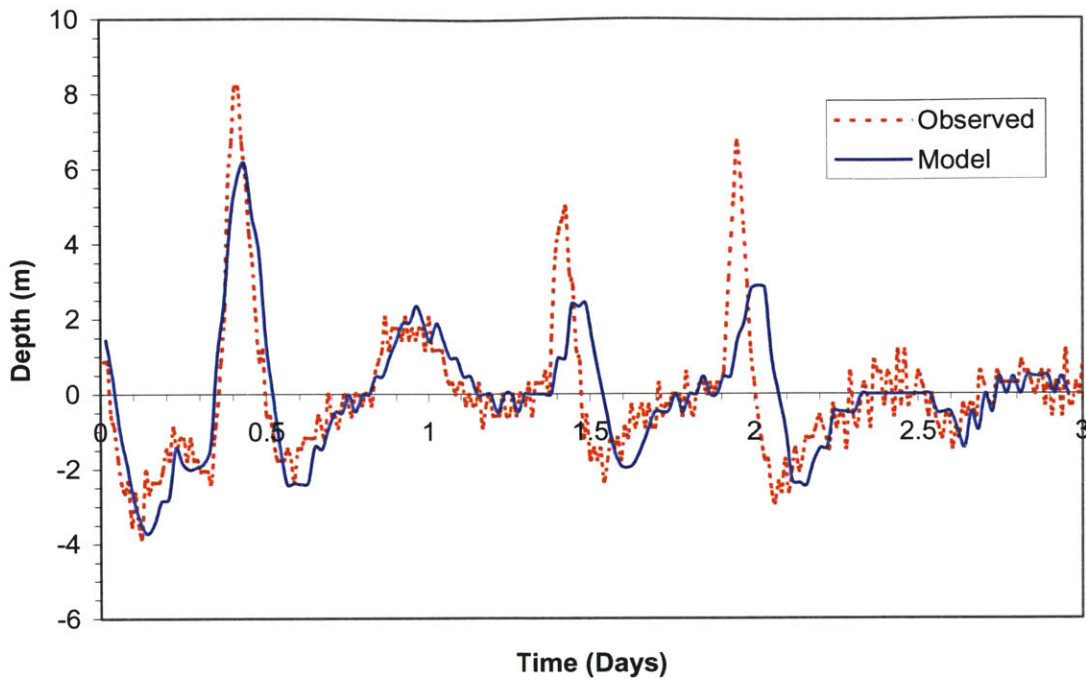


Figure 3-23 Modeled and Observed Change in Depth with Time at the GA 280 Crossing (01/14/2004-01/16/2004) (Observed Data Stamey, 2004)

In summary the plots show that the accuracy of the depth approximation is much better in the reach below Morgan Falls Dam than above it. As described in Section 3.3.4.2 the method for approximating these coefficients was the same for both reaches and there is no reason to believe that characteristics of the Chattahoochee above Morgan Falls would interfere with the approximations. Therefore it is logical that the inaccuracies observed above Morgan Falls are due to the difficulties with the flood routing model in this reach (Section 3.2.4.3).

Observations of river velocity and width were not available at any point within the modeled reach and we were unfortunately unable to compare the results of all the modeled discharge coefficients.

3.4 Suspended Solids Model

3.4.1 Suspended Solids Overview

Rivers transport suspended solid material. Watersheds draining into the Chattahoochee River have been estimated to carry up to 300 tons per square kilometer drained per year (Cherry et al., 1980). Among the sources of suspended solids are bank erosion, urban runoff, and wastewater discharges. Reactions with the solid phase particles in the water column may substantially affect the fate and transport of water quality constituents. Therefore modeling of the suspended solid load within the Chattahoochee is important.

3.4.2 Suspended Solids in WASP

WASP has the capability to simultaneously model up to three different types of solids (Ambrose et al., 1993). The user defines settling and erosion rates and organic carbon content for each solid type modeled. The mass balance discussed in Section 3.1.2 is applied to solids and used to determine the solids concentration at each model tank as well as sediment fluxes across boundaries. Solids enter the system in the same way as other water quality constituents, either through a concentration boundary condition or through mass loadings within tanks.

In addition solids can enter and leave the system through settling and scouring. As mentioned above the user defines the settling and scouring velocities of the solids. The user enters the settling velocities across tank boundaries and a constant surface area for each tank. WASP computes the product of the settling velocity and tank surface area to determine the downward flow of settling particles. Water quality constituents sorbed to particles are transported with them (Section 3.5.5).

3.4.3 Data Requirements

Detailed information regarding the character of suspended solids in the Chattahoochee was not available. Estimates based on generalizations from other river systems were made to fill gaps in the information. The data that was available dealt with general suspended solids concentrations and provided insight into how suspended solids were distributed through out the modeled reach.

Observations of turbidity were made at four locations along the modeled reach during the period January 15, 2004 – January 16, 2004. The location of the sample sites can be viewed in Figure 3-24. Turbidity was converted to an estimate of total suspended solids (TSS) using the conversion of 1 NTU equal to 1 mg/L (State of New Mexico Environment Department, 2002). The turbidity data used in this conversion is listed in Table 3-8.

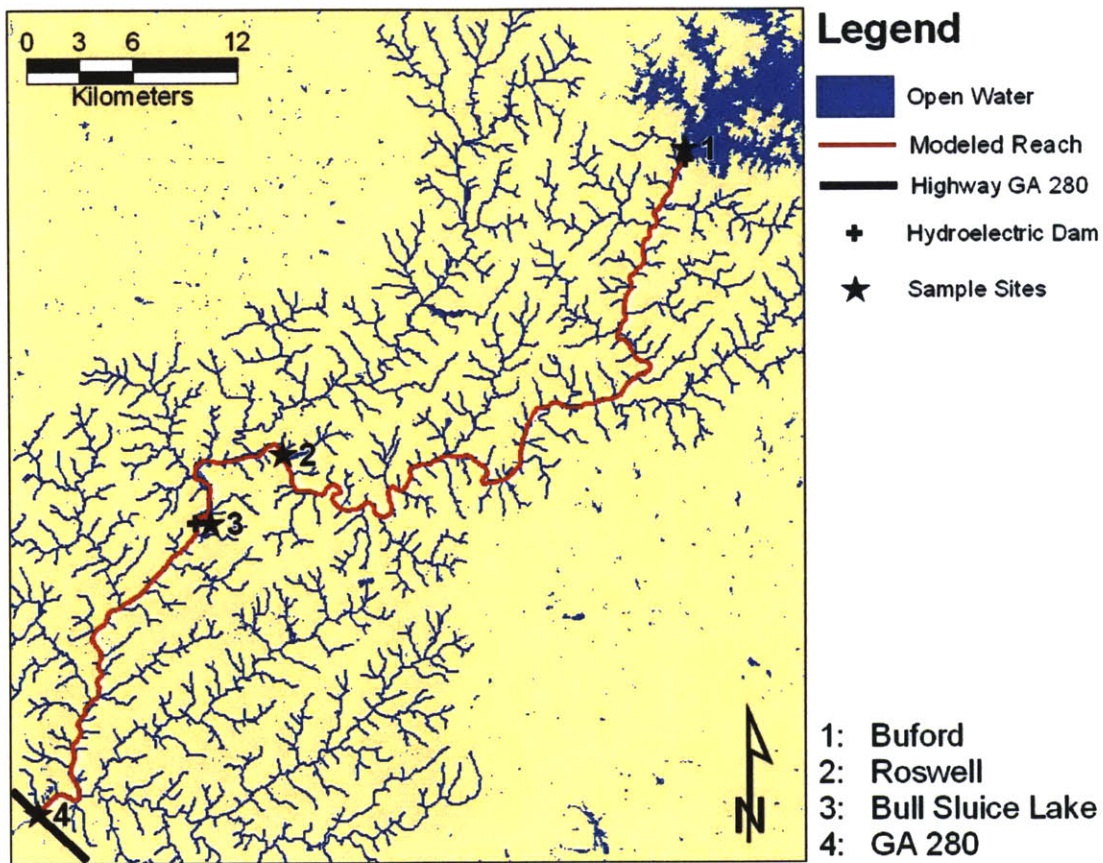


**Figure 3-24 Location of Turbidity Measurements
(01/15/2004-01/16/2004)**

**Table 3-8 Turbidity Observations in the Chattahoochee River
(01/15/2004-01/16/2004) (Andrews et al., 2004)**

Site	Date	Time	Turbidity (NTU)
Atlanta	1/15/2004	10:50	11.2
Roswell	1/15/2004	14:48	5.19
		15:31	6.98
Bull Sluice Lake	1/16/2004	14:04	5.04
Buford	1/16/2004	10:42	2.82
		11:14	3.13

Turbidity Measurements are +/- 0.5

The turbidity at the Atlanta sampling site agrees with average values observed at the Atlanta Water Works Drinking Water Treatment Plant, located towards the end of the modeled reach (Figure 2-4). Averages at the plant intake were reported at 15 NTU (Kopanski, 2004). There is also evidence of occasional turbidity observations two-orders-of-magnitude higher than those reported above. Technicians at the Atlanta Water Works Drinking Water Treatment Plant reported that turbidity measurements as high as 2000 NTU were observed during storm events. Support is given to these observations in a USGS circular from 1998 that states that over 60% of all suspended sediment transport in the Chattahoochee River occurs during storms (Frick et al., 1998). As the observations listed above were made in dry weather there is a strong possibility that concentrations of suspended solids can be at least an order of magnitude larger under storm conditions.

3.4.4 Model Implementation

Given the lack of information regarding the range of suspended solids within the modeled reach a single solid type was used to model total suspended solids in the river. The turbidity reading sample points were located within the model and using the conversion discussed in Section 3.4.3 the turbidity measurements were converted into units of milligrams per liter. The sample sites are listed along with the corresponding model tank in Table 3-9. The converted turbidity data was then plotted against model tank location. It was assumed that suspended solids concentrations increased exponentially downstream according to an exponential fit of the observed data.

Table 3-9 Sample Site Locations Within Model

Site Name	Model Tank
Atlanta	103
Bull Sluice Lake	55
Roswell	38
Buford	Upstream BC

3.4.4.1 Suspended Solids Distribution

A total suspended solids distribution was estimated based on the field data and the hypothesis that solids concentration increases downstream as in Figure 3-25. A series of solids loads were arbitrarily positioned through out the model in order to approximate this distribution. Modeled sediment loads at the most upstream tanks were 2500 kilograms per day and those at the downstream end were 8750 kilograms per day.

Typically a river will carry relatively less sediment load during low flow periods (Hemond and Fechner-Levy, 1994). In an attempt to mimic this behavior all loads were reduced by a factor of two during the low flow period that occurs during the first day of the simulation, January 12, 2004.

Running the water quality model for a 42-day simulation generated initial conditions for each tank. During this simulation solids loads were the same as those described above and flows were kept steady at 77.5 m³/s for five days followed by two days of low flow at 20 m³/s. This was intended to represent the weekly flow pattern of diurnal fluctuations on weekdays and steady low flow on the weekends.

In all cases the average of the suspended solids concentrations observed at the Buford sample site on January 16, 2004 was used as the upstream boundary condition. Boundary conditions at tributaries were assigned so as to not dilute the modeled concentration at the tank they enter.

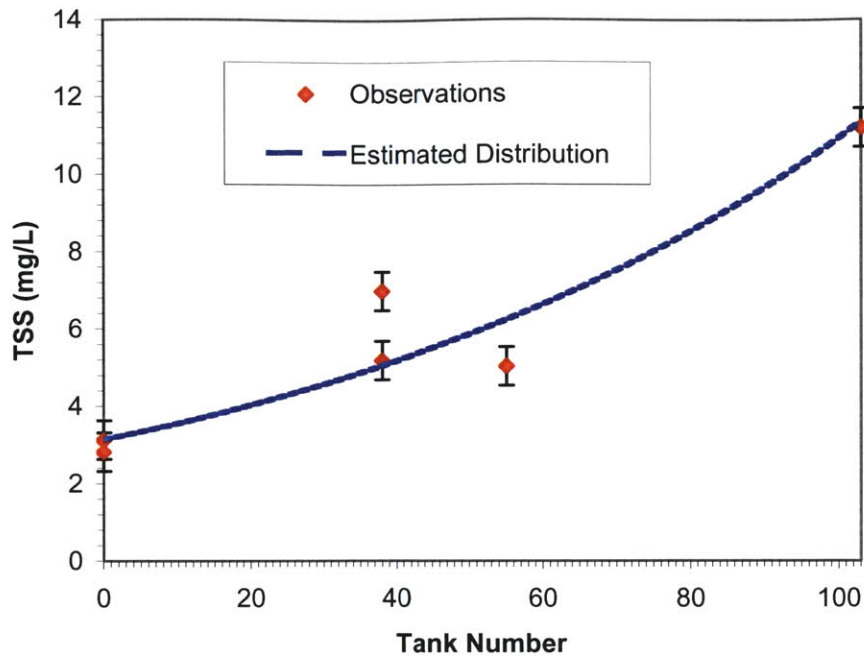


**Figure 3-25 Observed and Estimated TSS Distribution
(Observed Data Andrews et al., 2004)**

Increasing the magnitude of the solids loads changes the distribution of suspended solids. The response to an increase in the load is a proportional increase in total suspended solids concentration. Adjustments such as these were made during the model sensitivity testing discussed in Chapter 5.

3.4.4.2 Settling

Information on particle size and density were not available and estimates had to be made based on generalizations made from other rivers and from intuition based on observation of the river during the modeled period. Suspended solids were assumed to be mostly silt based solely on observation of the particles within water samples taken during the period January 15, 2004 – January 16, 2004. Solid density and settling velocities were taken off the chart of general values in the EPA WASP manual reproduced here in Table 3-10.

**Table 3-10 Particle Settling Velocities (m/day) for Typical Particles
(Ambose et al., 1993)**

Particle Diameter (mm)		Particle Density (g/cm ³)			
		1.80	2.00	2.50	2.70
Fine Sand	0.3	300.00	400.00	710.00	800.00
	0.05	94.00	120.00	180.00	200.00
Silt	0.05	94.00	120.00	180.00	200.00
	0.02	15.00	19.00	28.00	32.00
	0.01	3.80	4.70	7.10	8.00
	0.005	0.94	1.20	1.80	2.00
	0.002	0.15	0.19	0.28	0.32
Clay	0.002	0.15	1.90	0.28	0.32
	0.001	0.04	0.05	0.07	0.08

The density of mineral particles is often approximated as 2.6 g/cm³, while suspended organic matter is only slightly denser than water (Hemond and Fechner-Levy, 1994). Since no information regarding the composition of the solid particle population was available we assumed a mixture of mineral and organic solid material and assigned an average particle density of 1.80 g/cm³. Estimating a range of particle sizes we chose a diameter of 0.01 mm, the median value of silt particle diameters listed in Table 3-10, to be representative of the average particle size. The subsequent table lookup results in a settling velocity of 3.80 m/day.

Cross sectional surface areas for each tank were estimated by multiplying the average surface width by the length of the tank. Average surface width was taken to be the average surface width at medium flow determined as in Section 3.3.4.2. Surface widths do not remain constant and as has been discussed (Section 3.3.4) may change considerably. Therefore assigning constant surface widths is somewhat unrealistic and is a limitation of the WASP model.

3.4.4.3 Fraction of Organic Carbon

No information was available regarding the amount of organic carbon contained in the suspended solids and an estimate was based on typical values observed in the environment. The EPA WASP manual states that typical values for suspended solid fraction of organic carbon (f_{oc}) is in the range from 0.5% to 50% (Ambrose et al., 1993).

Given the above numbers we set the f_{oc} in the base case to 1%. Sensitivity analysis discussed in Chapter 5 varies this parameter between 1% and 10%.

3.4.5 Results

The results of the suspended solids model will be studied briefly here to understand the patterns of solid particle transport within the modeled reach. Comparison of the modeled results to the observations during January 15, 2004 and January 16, 2004 will also be made.

By looking at the modeled suspended solids distribution at different time snapshots we can understand how the solid transport varies with flow. Figure 3-26 shows the total suspended solids (TSS) distribution at an early model time step. Flow is low and relatively constant coming out of the weekend of January 10, 2004. Suspended solid concentrations increase downstream as would be expected and range from 2 mg/L to between 12 and 11 mg/L at the downstream end. The erratic pattern displayed by the TSS concentrations is due to the fact that at low flow solids settle quickly and therefore leave the system in between source loadings. This has the effect of decreasing the TSS in between solid point sources, the most dramatic decreases occurring in the slowest moving reaches.

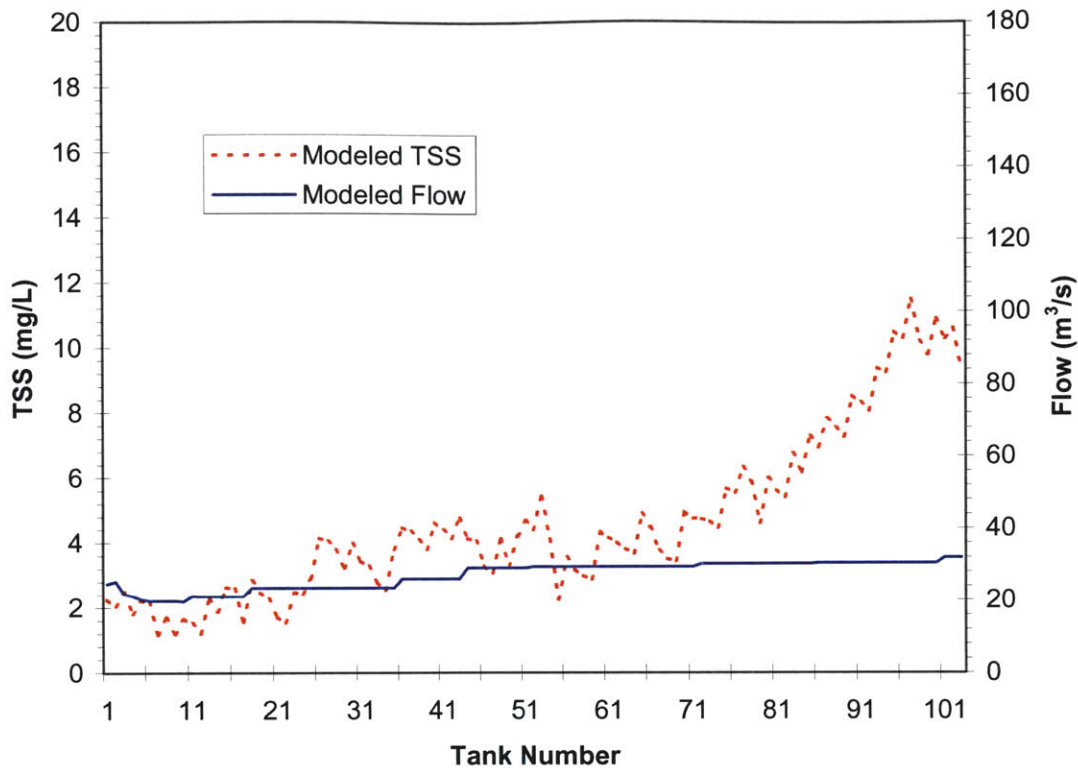


Figure 3-26 Modeled TSS and Flow Distribution at Model Time Step 0.2 Days

By the beginning of the third day of the simulation several flood waves from the dam releases have passed through the reach and a snapshot of the TSS distribution shows typical total suspended solids concentrations in the reach during a weekday. Figure 3-27 shows the flow and TSS distribution at time step 2.0 days. Solids concentrations have now increased throughout the modeled reach showing the most dramatic increase between tank 36 and tank 54. As can be seen these tanks are experiencing a low flow between flood waves. The high concentrations are a result of the high sediment loads being discharged into the low flow conditions in this reach. The pattern of TSS concentrations in this region is erratic and this can be explained as above due to the increased flux of solids out of the model in slow flowing reaches. The most dramatic settling can be seen in tank 55. It is this tank that represents Bull Sluice Lake, the slowest flowing tank in the model, and it is here that we predict the maximum sediment sink exists.

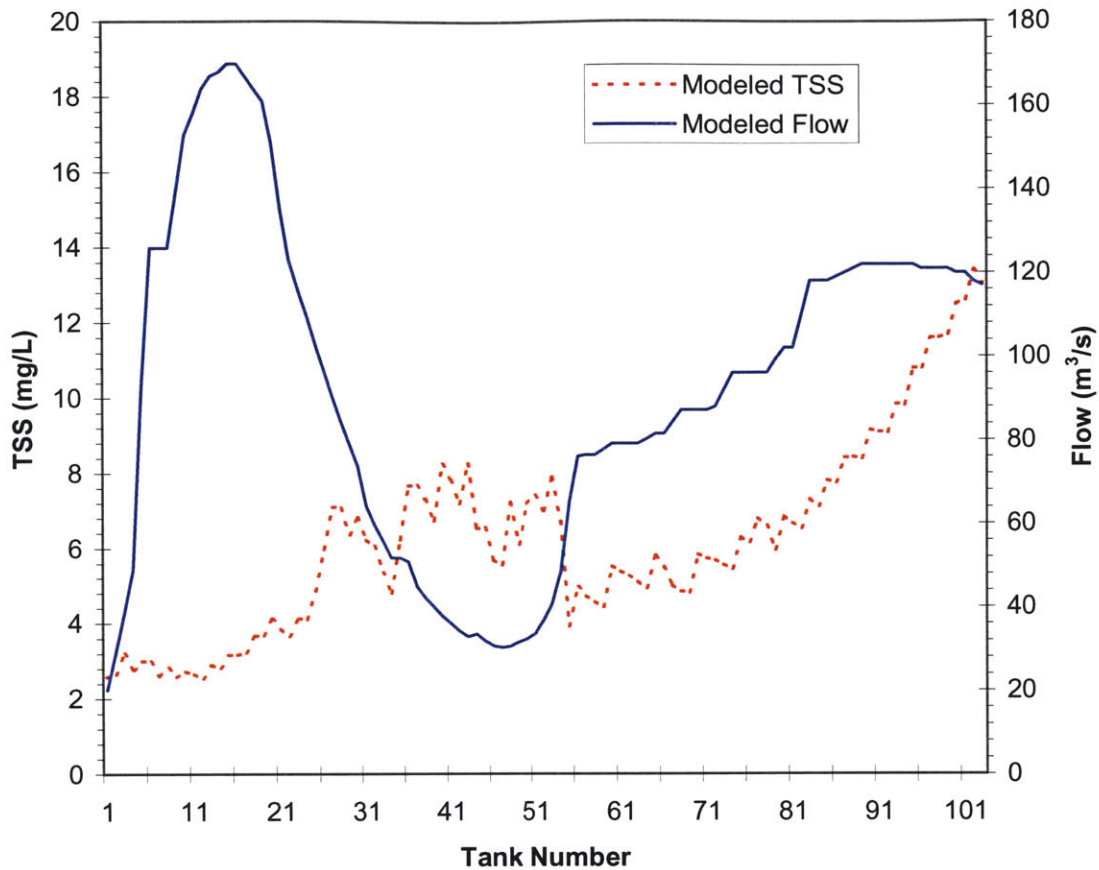


Figure 3-27 Modeled TSS and Flow Distribution at Model Time Step 2.0 Days

Figure 3-28 shows a snapshot taken 0.7 days later. The flood wave now has traveled into Bull Sluice Lake. Concentrations in the upstream end of the modeled reach are now relatively higher and display the erratic pattern between tanks that is typical of the model in between flood waves. It is important to observe that the dramatic drop in TSS still exists at tank 55 and therefore the large flux of solids out of the model in this tank is still a feature during high flows. Also note that the flood wave from Morgan Falls Dam has now left the model and higher as well as more erratic concentrations can now be observed in this reach.

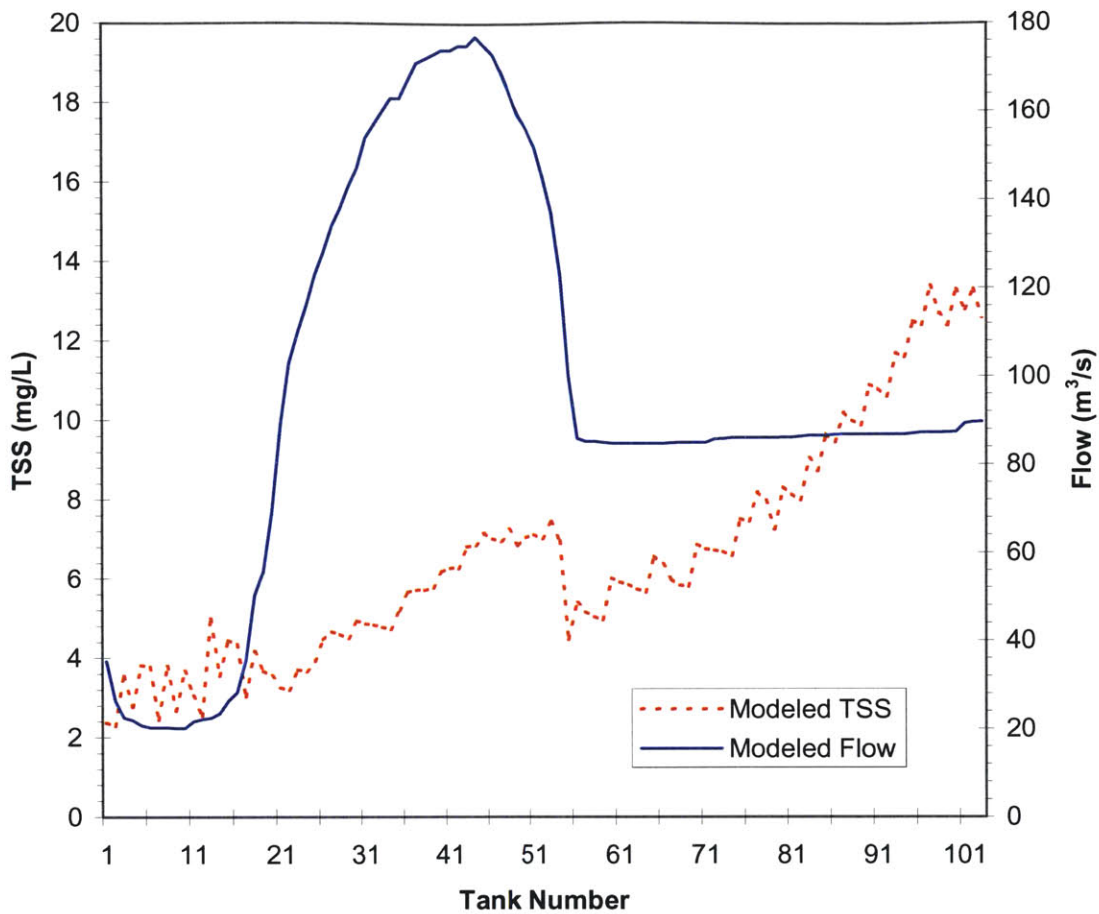
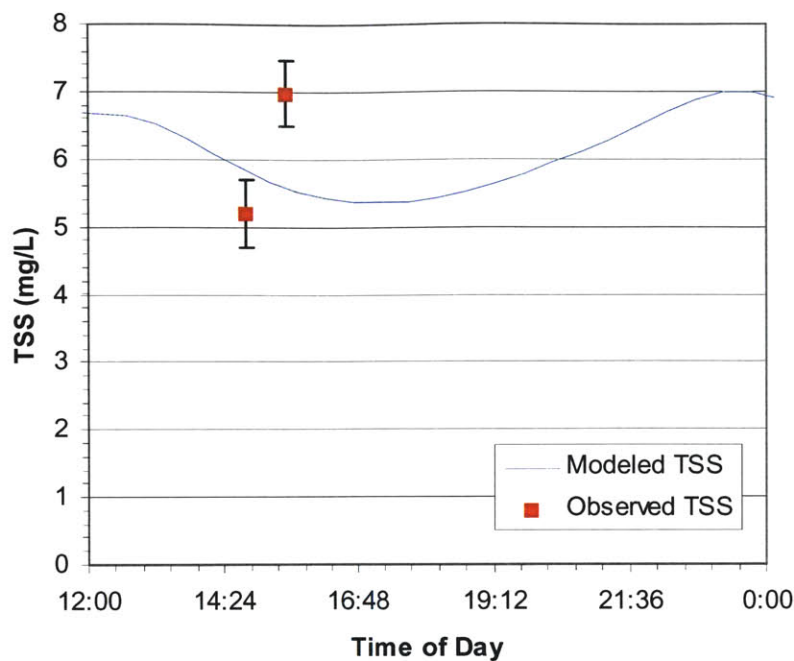


Figure 3-28 Modeled TSS and Flow Distribution at Model Time Step 2.7 Days

The results of the solids transport model indicate that fluxes of solid particles out of the model can be expected at model tanks experiencing low flows. Regardless of flow, tank 55 appears to be a significant sink of suspended solids as was expected of the relatively slow moving waters in Bull Sluice Lake.

3.4.5.1 Comparisons with Field Observation

To evaluate how well the solids transport model approximates reality we compared the results of the model with the observations made in field and listed in Table 3-8.



**Figure 3-29 Modeled and Observed TSS at Roswell (Tank 38)
(January 15, 2004 Noon-Midnight) (Observed Data Andrews et al., 2004)**

Figure 3-29 displays the modeled and observed suspended solids concentration at the Roswell sampling site. The modeled wave agrees with the observed data and it is possible that with a slight shift of the concentration wave the observed concentrations would match the model almost exactly. Figure 3-30 shows that the comparison to the model at Bull Sluice Lake is a good one. Figure 3-31 shows the comparison at the final tank in the model. The modeled TSS is higher and stays constant at about 1 mg/L above observed. The average concentrations in this tank were 12 mg/L during the run of the model, which was considered to be accurate for the purposes of the model.

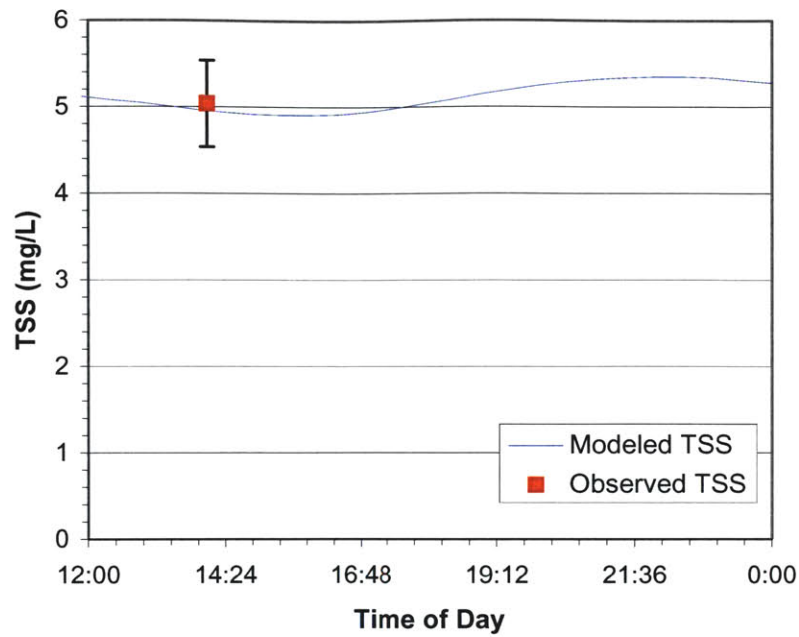


Figure 3-30 Modeled and Observed TSS at Bull Sluice Lake (Tank 55) (January 16, 2004 Noon–Midnight) (Observed Data Andrews et al., 2004)

The comparison of modeled to observed suspended solids concentrations show that the solids transport model reaches its goal of approximating conditions observed during the modeled period.

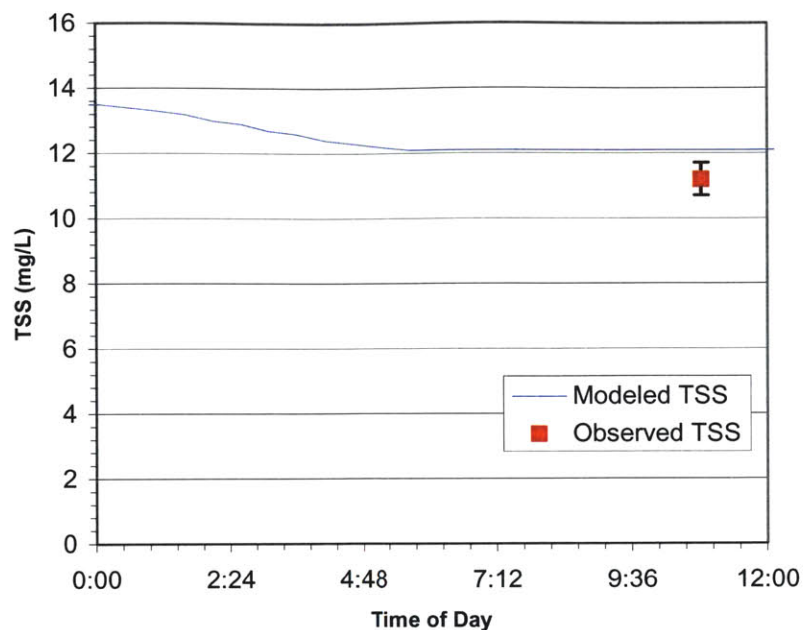


Figure 3-31 Modeled and Observed TSS at the GA 280 (Tank 103) (January 15, 2004 Midnight-Noon) (Observed Data Andrews et al. 2004)

3.5 Phosphate Esters Model

Up to this point Chapter 3 has dealt with the portions of the model that describe the river system and in effect the transport processes. In fact many other organic chemicals could be analyzed using the same hydrologic and solids transport model. The following section deals with the model of the phosphate esters themselves. The section will first describe how the loadings were estimated and then describe how the reactions governing their fate were modeled

3.5.1 Phosphate Esters

The three phosphate esters considered by this study are tri-butyl phosphate (TBP), tri-(2-butoxyethyl) phosphate (TBEP), and tri-(2-chloroethyl) phosphate (TCEP). They were selected out of a suite of organic compounds that were detected by the USGS and CDC in treated wastewater entering the Chattahoochee through municipal sewage treatment plants (for more information on this study see Chapter 1). The same study detected the three compounds in raw and treated municipal drinking water drawn from the

Chattahoochee downstream of the wastewater discharges (Frick and Zaugg, 2003). Their presence in the Chattahoochee River was confirmed in January (Andrews, 2004).

The phosphate esters being modeled here are briefly described below.

3.5.1.1 TBP

The chemical structure of tri-butyl phosphate ($C_{12}H_{27}O_4P$) is displayed in Figure 3-32. At room temperatures it is a colorless, odorless liquid (Nakamura, 1991). TBP is used in plastics, floor finishes and fire resistant hydraulic fluids. It is used for its dual role as a plasticizer and fire retardant. The CDC detected TBP in wastewater effluent entering the Chattahoochee in every location sampled in the 1999 survey. As mentioned previously it was also detected in raw and finished drinking water being drawn downstream of the discharges (Frick and Zaugg, 2003). The sampling conducted January 15 and 16, 2004 confirmed its presence in the Chattahoochee River (Andrews, 2004). Not much is known concerning the long-term health effects of chronic exposure to concentrations at the levels found in these studies (ng/L), but its consistent presence is a potential concern.

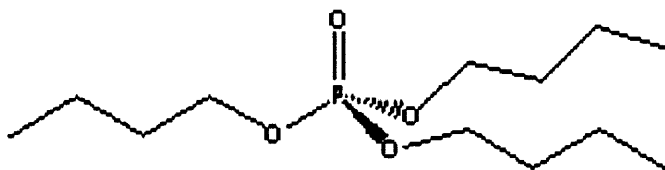


Figure 3-32 Tri-butyl Phosphate

3.5.1.2 TBEP

Tri (2-butoxyethyl) phosphate ($C_{18}H_{39}O_7P$) is displayed in Figure 3-33. At room temperatures it is a light colored, viscous fluid with butyl odor (something akin to lighter fluid) (van Esch, 2000). Like TBP it is used for its plasticizing and fire retarding capabilities. While it is not used in hydraulic fluids it is much more prevalent than TBP in rubber and plastics and is an ingredient of many household floor polishes (National Library of Medicine, 2003). Data shows that approximately 6000 metric tons are

produced yearly (van Esch, 2000). This is reflected in the results of the 1999 survey where it was detected in almost all samples at an average concentration of 3 µg/L in treated wastewater (Frick and Zaugg, 2003). Similarly to TBP no studies regarding the long-term effects of chronic exposure to TBEP have been conducted.

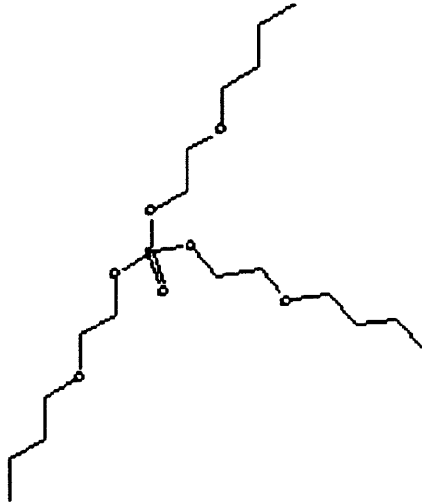


Figure 3-33 Tri (2-butoxyethyl) Phosphate

3.5.1.3 TCEP

The chemical structure of tri (2-chloroethyl) phosphate ($C_6H_{12}Cl_3O_4P$) is displayed in Figure 3-34. At room temperature it is a colorless liquid with a slight odor. Its use as a fire retardant coating in fabrics and polyurethane foams has declined since its peak in 1980 (WHO, 1998). However at its peak production, in 1980, it was being made at a rate of 9000 metric tons per year (WHO, 1998). It is still present in the environment and although detected at smaller concentrations than TBP and TBEP, its consistent presence has been documented by the 1999 and 2004 studies. Unfortunately as with TBP and TBEP no information is available regarding the effects of chronic exposure.

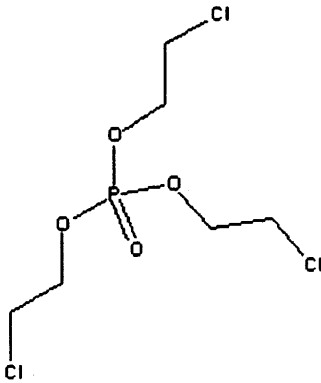


Figure 3-34 Tri (2-chloroethyl) Phosphate

3.5.2 Estimate of Loads

Seven municipal wastewater treatment plants (WWTPs) discharge, either directly or through tributaries, into the Chattahoochee River in the reach between Buford Dam and the GA 280 highway crossing in Atlanta. The CDC study conducted in 1999 (See Chapter 1) tested at four of these WWTPs and consistently detected TBP, TBEP, and TCEP in the treated wastewater entering the Chattahoochee. The four WWTPs, their permitted daily discharge and the average concentration of the three compounds detected in their effluent are listed in Table 3-11, (for the purposes of averaging concentrations that were reported below the detection limit were taken to be half the detection limit). The locations of the plants can be found by consulting Figure 2-4.

**Table 3-11 Phosphate Ester Concentrations Found at WWTPs
(GNR, 1997 & Frick and Zaugg, 2003)**

WWTP	Permitted Discharge (MGD)	Concentration (µg/L)		
		TBP	TBEP	TCEP
Crooked Creek	36	0.19	0.35	0.07
Johns Creek	7	0.26	9.57	0.35
City of Cumming	2	0.17	0.12	0.40
Big Creek	24	0.79	0.45	0.34

The three plants that were not tested are listed in Table 3-12. The locations of the plants can be found in Figure 2-4. In addition to these point source loads, in-stream concentrations were detected at the headwaters of the Big Creek and in Lake Sydney

Lanier, the reservoir impounded by Buford Dam. The method of compiling this information and estimating the phosphate ester loads on the system are discussed in the following sub sections.

**Table 3-12 WWTPs That Were Not Screened for Phosphate Esters
(GNR, 1997)**

WWTP	Permitted Discharge (MGD)
Buford Southside	2
R. M. Clayton	100
R. L. Sutton	40

3.5.2.1 Point Source Loads

The WWTPs discharging directly into the Chattahoochee in the modeled reach are all considered point source loads. Out of the seven discussed above Crooked Creek, John’s Creek, Big Creek, R.M. Clayton, and R.L. Sutton discharge directly into the Chattahoochee. The method for determining the loads over the modeled period (January 12, 2004 – January 16, 2004) was to determine the discharge on the particular day and then multiply that by an estimated average concentration at the plant.

3.5.2.1.1 Estimation of Daily Discharge

The daily discharges for the entire modeled period were available for the Big Creek, Crooked Creek, and Johns Creek plants. The records for January 14, 2004 – January 16, 2004 were available for the R. L. Sutton plant. No records were available for the R. M. Clayton plant. The plants and the known discharges for the modeled period are listed in Table 3-13.

**Table 3-13 Known Daily Point Source Discharges
(Harburn, 2004 & Chastain, 2004)**

WWTP	Daily Discharge (MGD)					Percent of Permit Limit
	1/12/2004	1/13/2004	1/14/2004	1/15/2004	01/162004	
Crooked Creek	25.3	26.3	26.3	26.7	25.8	72%
Johns Creek	4.66	4.95	4.84	4.49	4.89	68%
Big Creek	19.62	18.72	19.83	18.55	18.64	79%
R. M. Clayton						
R. L. Sutton			28.17	26.89	27.25	69%

For the case of the R.L. Sutton Plant, the average discharge over the known days was used as the discharge for the January 12, 2004 and January 13, 2004. The discharge of the R. M. Clayton plant was estimated by first observing that the known discharges were on average 72% of their permitted discharge. The assumption was made that the R. M. Clayton facility was also operating at 72% of its permitted discharge. It has a permitted discharge of 378,500 m³/day and therefore was assigned a daily discharge of 273,100 m³/day for this simulation.

3.5.2.1.2 Determination of Time Variable Discharge

The base case model assumes that the plant discharge is constant through out the day and only varies from day to day as expressed in Table 3-13. The treated wastewater is not discharged from the plants at a constant rate but varies throughout the day. Hourly discharge patterns were available for only one plant, R. L. Sutton. A sensitivity test (discussed in Section 5.3) was conducted by normalizing the discharge curve for a single day at R. L. Sutton by the daily discharge for that day. This normalized curve was applied to the discharges of all five point source loads. The effects of this change were insignificant. For this reason and simplicity, all remaining simulations were run using daily average discharges.

3.5.2.1.3 Determination of Point Source Discharge Concentration

The average concentrations listed in Table 3-11 were applied to the discharges of the corresponding three point source plants (City of Cumming WWTP is not considered a point source since it does not discharge directly to the Chattahoochee, its treatment is discussed in Section 3.5.2.2). Effluent concentrations for the two plants not sampled by

the 1999 study had to be estimated. Since the R. L. Sutton plant is comparable in size to the Crooked Creek plant the average concentration of the Crooked Creek plant was applied to the effluent of the R. L. Sutton Plant. There were no plants of comparable size to the R. M. Clayton plant and therefore a combined average concentration for each compound over all three plants was determined and was applied to the R. M. Clayton effluent.

3.5.2.1.4 Determination of Mass Loadings

Once the daily discharges and the concentrations of the three phosphates in the discharged effluent were determined specification of the mass loadings was a fairly simple task. The daily mass discharged was determined using Equation 3-22.

$$m = Q_{Daily} * \bar{c}$$

Equation 3-22

Where:

- m = mass loading rate [M/T]
- Q_{Daily} = daily discharge from the plant [L³/T]
- \bar{c} = average concentration of either TBP, TBEP, or TCEP at the plant [M/L³]

3.5.2.2 Estimate of Boundary Condition Concentrations

Three model boundaries were identified as having concentrations of TBP, TBEP and TCEP. These are the upstream boundary at Buford Dam, the inflow from the Suwanee Creek at tank 11 and the inflow from the Big Creek at tank 44. Although other tributaries may be carrying concentrations of the three phosphates it was assumed that their concentrations were negligible since they do not receive treated municipal sewage from WWTP outfalls.

3.5.2.2.1 Upstream Boundary at Buford Dam

During the study conducted by Andrews et al. in January of 2004 three samples were taken from Lake Sydney Lanier in the area just upstream of the Buford Dam. These samples were analyzed for concentrations of TBP, TBEP and TCEP. The results of this testing are displayed in Table 3-14. The site where the samples were taken can be located on the map in Figure 3-24 at label 1.

Table 3-14 Concentrations of Phosphate Esters Detected in Lake Sydney Lanier (January 16, 2004) (Andrews, 2004)

Sample	Concentration (ng/L)		
	TBP	TBEP	TCEP
1	4.60	106.0	20.1
2	2.00	80.0	9.12
3	3.70	161.0	4.71
Average	3.44	116.0	11.3

The average concentration of each water quality constituent listed in Table 3-14 was used as a constant concentration boundary condition for the upstream boundary.

3.5.2.2.2 Boundary Concentration at Suwanee Creek

The Buford Southside WWTP discharges into the Suwanee Creek. Its location can be found on Figure 3-9. The Suwanee Creek enters the model at tank 11. It is an ungauged tributary and its flow was estimated to be 1.4 m³/s according to the method outlined in Section 3.2.5.2. The daily discharge during the modeled period for the Buford Southside treatment plant was unknown and was estimated using the same method detailed in Section 3.5.2.1.3. The City of Cumming plant has the same permitted discharge and therefore the Buford Southside plant was assigned the same daily discharge as City of Cumming (Section 3.5.2.2.3). Effluent concentrations of the three phosphate esters were taken to be the same as those reported by the CDC for the effluent of the City of Cumming plant. Daily mass loadings were determined using Equation 3-22.

Concentrations at the boundary entering at tank 11 were determined according to Equation 3-23.

$$C_B = \frac{m}{Q_T}$$

Equation 3-23

Where:

- C_B = concentration at the boundary [M/L³]
- Q_T = tributary inflow [L³/T]

The boundary condition at tank 11 for each day is displayed in

Table 3-15 Concentration Boundary Condition for Suwanee Creek (Tank 11)

Day	C _B (ng/L)		
	TBP	TBEP	TCEP
1/12/2004	7.01	5.80	16.2
1/13/2004	7.01	5.80	16.2
1/14/2004	6.91	5.71	15.9
1/15/2004	6.82	5.64	15.7
1/16/2004	6.65	5.50	15.9

In these estimates the travel time between the Buford Southside outfall and the confluence of the Suwanee Creek and the Chattahoochee is neglected. The processes being modeled here for the Chattahoochee would certainly affect the concentrations of the phosphate esters as they traveled through the reach of the Suwanee between the Buford Southside outfall and its mouth at the Chattahoochee. These assumptions make the concentration estimates high and they should be treated as an upper bound.

3.5.2.2.3 Boundary Condition at Big Creek

The City of Cumming WWTP discharges into the Big Creek as indicated on Figure 2.4. In addition, a poultry processing plant discharges into the Kelly Mill Branch, a small tributary to the headwaters of the Big Creek (Frick and Zaugg, 2003). In-stream

concentrations of all three phosphate esters were reported downstream of the processing plant at the outlet of the Kelly Mill Branch watershed, shown in Figure 3-35 (Frick and Zaugg, 2003). Boundary concentrations at the mouth of Big Creek (tank 44) were assumed to be due to the City of Cumming plant and the in-stream concentrations at the Kelly Mill Branch.

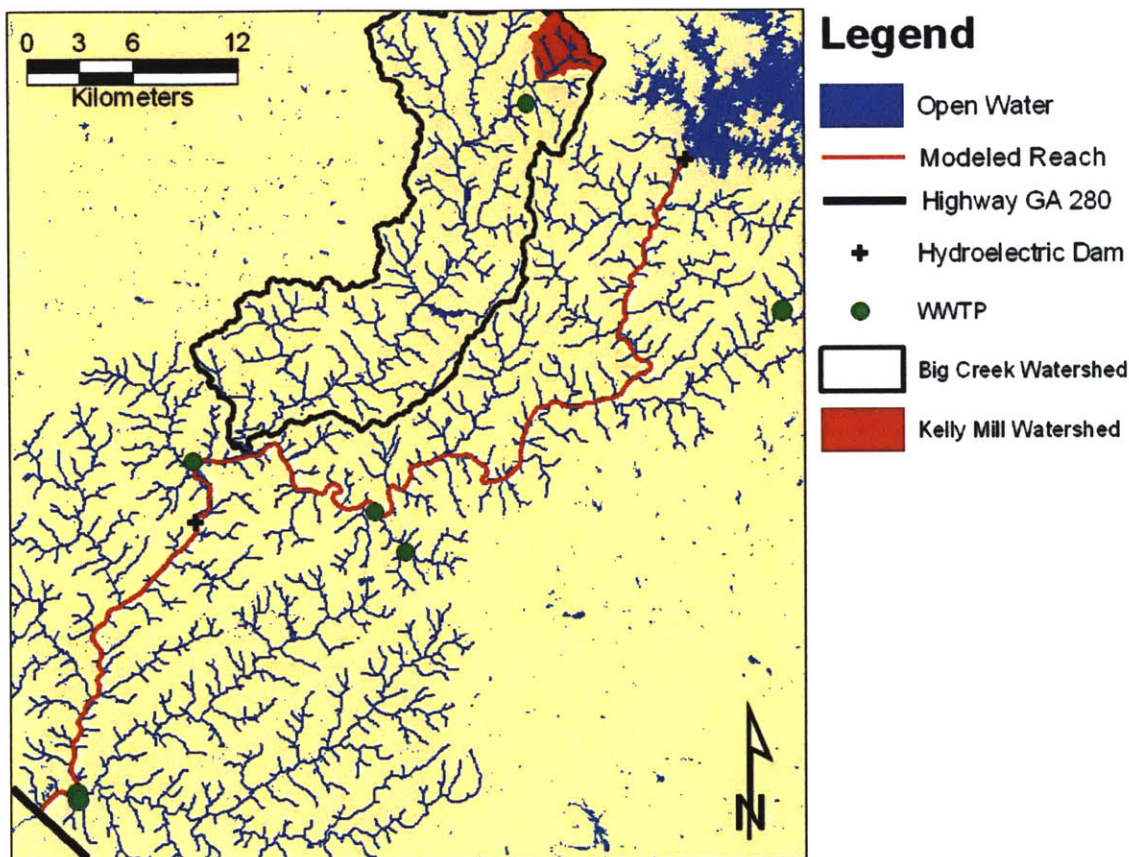


Figure 3-35 Location of Kelly Mill Watershed (Frick and Zaugg, 2003)

Daily discharges for the City of Cumming WWTP were available for January 13 – 14, 2004 and are listed in Table 3-16. The discharge for January 12, 2004 was assumed to be the same as the discharge on January 13, 2004.

**Table 3-16 Daily Discharge for City of Cumming WWTP
(January 13, 2004 – January 16, 2004) (Chastain, 2004)**

Day	Discharge (m ³ /day)
1/13/2004	5054
1/14/2004	4978
1/15/2004	4917
1/16/2004	4792

Using the average concentrations in Table 3-11 and Equation 3-22 daily mass loadings for each of the three phosphates were determined.

Flow for Kelly Mill Branch was estimated method outlined in Section 3.2.5, and was determined to be 0.096 m³/s. Concentrations of the three phosphate esters were taken to be the averages of the concentrations reported in the 1999 study, reproduced here in Table 3-17.

**Table 3-17 Kelly Mill Branch In-Stream Concentrations
(Frick and Zaugg, 2003)**

Sample	Concentration (µg/L)		
	TBP	TBEP	TCEP
1	0.03*	0.45	0.14
2	0.03*	11.80	0.02*
3	0.03*	1.10	0.15
Average	0.03	4.45	0.10

*Concentration below detection limit. Taken to be one half detection limit.

Equation 3-22 was used to calculate a mass loading using the concentrations in Table 3-17 and the estimated flow leaving the Kelly Mill Branch watershed for Q_{Daily} .

The mass loadings from the City of Cumming WWTP and the Kelly Mill Branch Watershed were summed and, using the method outlined in Section 3.2.5, the flow at the mouth of the Big Creek was estimated to be 2.9 m³/s. These values and Equation 3-23 were used to determine the boundary condition at the mouth of the Big Creek (tank 44) for each day in the modeled period. The results of this calculation are displayed in Table 3-18.

Table 3-18 Concentration Boundary Condition for Big Creek (Tank 44)

Day	C _B (ng/L)		
	TBP	TBEP	TCEP
1/12/2004	4.46	149.3	11.4
1/13/2004	4.46	149.3	11.4
1/14/2004	4.40	149.3	11.3
1/15/2004	4.36	149.3	11.2
1/16/2004	4.28	149.2	11.3

As discussed in Section 3.5.2.2.2 we are assuming that there is no reduction in concentration within the reach from the outfalls to the confluence with the Chattahoochee. Because of this assumption, these are upper bounds on the concentration entering at Big Creek.

3.5.2.3 Comparisons of Load Magnitude

Table 3-19 contains the names of the loads cross referenced with the tanks in which they enter the model. This is accompanied by the histogram in Figure 3-36 that shows the comparative orders of magnitudes of each of the phosphate ester loads.

Table 3-19 Point Sources and Corresponding Tanks

Load Name	Tank
Suwanee Creek	11
Crooked Creek WWTP	26
John's Creek WWTP	27
Big Creek	44
Big Creek WWTP	51
R.L. Sutton WWTP	101
R.M. Clayton WWTP	102

From Figure 3-36 it can be easily seen where in the model to expect jumps in concentration. For example TBEP will not show significant increases in concentration between tank 27 and tank 102 because the source at John's Creek is orders –of magnitude larger than any subsequent source before R. M. Clayton. This information will be used in Chapter 4 where we analyze the results of the model.

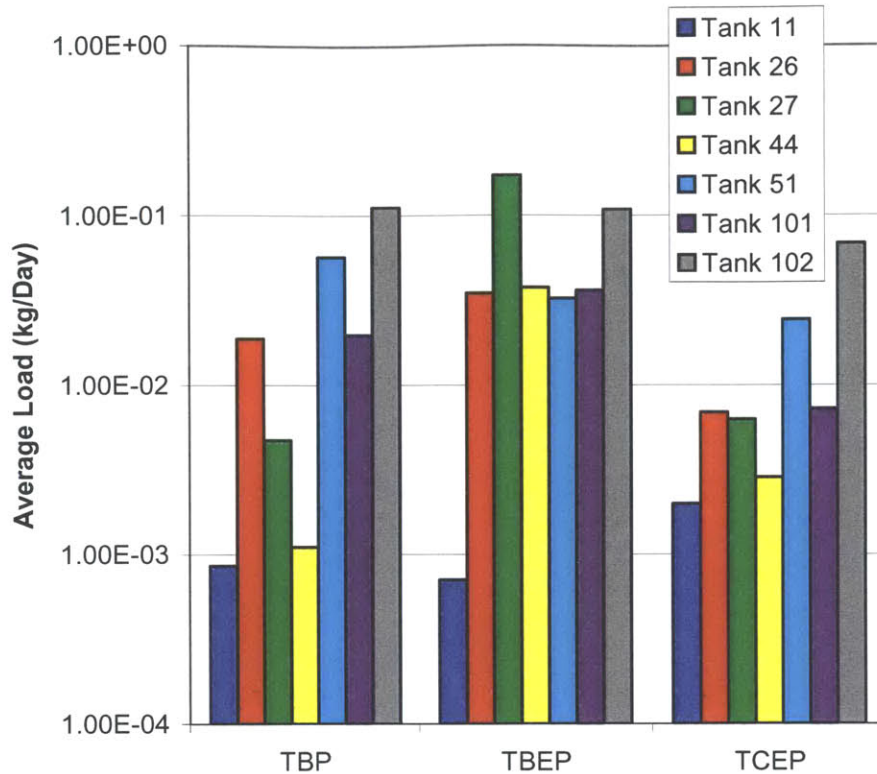


Figure 3-36 Average Daily Phosphate Ester Loads

3.5.3 Generation of Initial Conditions

In order to accurately model conditions in the river during the five days being simulated (January 12, 2004 – January 16, 2004) an initial concentration distribution had to be determined for each phosphate ester. The model begins simulating at midnight January 12. Because midnight January 12 was a Sunday night, the river had been at low flow since the previous day. Therefore in order to achieve a reasonable concentration distribution for the start of the model, conditions in the river at the end of a weekend should be calculated.

To produce this initial concentration distribution the model was run with a simplified flow regime for a forty-two-day cycle. For the first five days of the cycle flows leaving Buford Dam were set to a steady 77.6 m³/s, the average flow during the simulated five days. This is followed by two days of a steady low flow of 19.9 m³/s. All other parameters were kept the same as the base five-day case. The purpose was to simulate

four typical weeks in an effort to achieve the initial concentration distribution described above.

3.5.4 Physical Processes Model

The previous discussion on the phosphate esters model deals with the calculations involved in approximating the amount of phosphate esters being added to the river system. The next sections will discuss the model that simulates the physical and chemical processes at work in the river that reduce the phosphate ester concentrations.

3.5.5 Sorption

3.5.5.1 Overview of Sorption

Sorption is a process in which chemicals dissolved in water bind onto solid surfaces. A chemical specific partition coefficient, K_p , is a constant which describes the ratio at equilibrium of sorbed phase to dissolved phase so that:

$$C_{sorb} = K_p * C_w$$

Equation 3-24

Where:

- C_{sorb} = concentration sorbed to solid phase [M/M]
- K_p = partition coefficient [L^3/M]
- C_w = concentration in water [M/L^3]

A reliable method exists for approximating K_p values for neutral organic chemicals (Hemond and Fechner-Levy, 1994). The method assumes that absorption into organic matter is the primary method of sorption for these compounds. The parameter K_{oc} is the partition coefficient for a particular chemical with organic carbon and is used to determine sorbed concentration as in Equation 3-24. Where a K_{oc} has not been measured one is often approximated using the K_{ow} , the octanol-water partition

coefficient. The K_{ow} describes how hydrophobic a particular compound is and methods are available for converting a K_{ow} into a K_{oc} value. Section 3.5.5.2.1 goes into further details on this calculation.

In the case of the Chattahoochee River, sorption may act as a sink for phosphate esters. Phosphate esters dissolved in the water column may sorb to organic matter in the suspended solids being transported downstream. Once sorbed to the organic carbon the phosphate ester may be removed from the water column through settling.

3.5.5.2 WASP Implementation of Sorption

WASP assumes that the time for the sorption reaction to come to equilibrium is much shorter than the time step and therefore Equation 3-24 can be used. WASP uses the compounds K_{oc} and the fact that the total concentration must be equal to the sorbed concentration plus the dissolved concentration to determine the partition between dissolved and sorbed phases (Ambrose et al., 1993)

$$C = C_w + C_s M_s f_{oc}$$

Equation 3-25

Where:

- C = total concentration of chemical [M/L³]
- C_w = concentration of chemical dissolved in water [M/L³]
- C_s = concentration of chemical sorbed to suspended solids [M/M]
- M_s = concentration of suspended solids in model tank [M/L³]
- f_{oc} = fraction of suspended solids that is organic carbon [dimensionless]

Using Equation 3-24 with Equation 3-25 to determine the fraction of total mass that is dissolved, f_d :

$$f_d = \frac{C_w}{C} = \frac{1}{1 + K_{oc} f_{oc} M_s}$$

Equation 3-26

And similarly the fraction sorbed:

$$f_s = \frac{C_s M_s}{C} = \frac{K_{oc} f_{oc} M_s}{1 + K_{oc} f_{oc} M_s}$$

Equation 3-27

These fractions are determined throughout the model at each model time step. Therefore after first calculating the total concentrations through the mass balance the dissolved and sorbed concentrations can be determined at each tank.

3.5.5.2.1 Determining K_{oc}

WASP offers four options for entering partition coefficients for organic compounds. Only two were used here and only those will be discussed. For more information see the WASP user's manual (Ambrose et al., 1993).

The first option, used for only TBEP, is to enter the K_{oc} directly. For cases where measured K_{oc} values are available this is the simplest option.

For TCEP and TBP no K_{oc} value was available and the value had to be calculated using K_{ow} . The correlation in Equation 3-28 has been shown to hold provided values of a_0 and a_1 are available for the particular compounds.

$$\text{Log}K_{oc} = a_0 + a_1 \text{Log}K_{ow}$$

Equation 3-28

Setting a_1 equal to 0.544 and a_0 equal to 1.377 has been shown to hold for a wide variety of chemicals (Hemond and Fechner-Levy, 2002), and these values were used to calculate the K_{oc} for TBP and TCEP.

3.5.5.3 Sorption Constants Used For Phosphate Esters

Only for TBEP was a calculated K_{oc} value available. This was a $\text{Log}K_{oc}$ of 4.38 (van Esch, 2000)

K_{ow} values were available for TCEP and TBP. These along with the correlation in Equation 3-28 were used to determine K_{oc} . The K_{ow} values used were

- $\text{Log}K_{ow} = 3.99$ for TBP (Nakamura, 1991)
- $\text{Log}K_{ow} = 1.7$ for TCEP (WHO, 1998)

3.5.6 Biodegradation

3.5.6.1 Overview of Biodegradation

Biodegradation is the process by which organic chemicals are broken down by bacterial enzymes. Bacteria in the water column can utilize the energy stored in the bonds of organic compounds and break them down for sustenance. Biodegradation is a complicated process and may depend strongly on both the concentration of the chemical and the size of the bacterial population.

3.5.6.2 WASP Implementation of Biodegradation

WASP provides for different levels of complexity when modeling biodegradation. Models can involve several parameters such as tank- and time-variable bacterial populations or be as simple as a first-order degradation constant applied consistently in each tank. In the current case the only data available were observed first-order rates that were assumed to be due to biodegradation. This data is discussed in the following section.

3.5.6.3 Biodegradation First Order Rates

The study conducted in January of 2004 had as one of its aims the estimation of first-order biodegradation rates for the phosphate esters within the modeled reach (Andrews, 2004). The study reported first-order rate constants for each sample taken. These were

averaged to come up with unique first-order biodegradation rate constants for TBP, TBEP and TCEP. The rate constants used are listed in Table 3-20.

**Table 3-20 First Order Biodegradation Rate Constants
(Andrews, 2004)**

Compound	Biodegradation Rate (day ⁻¹)
TBP	1.99E-02
TBEP	3.72E-02
TCEP	7.60E-03

3.5.7 Volatilization

3.5.7.1 Overview of Volatilization

Volatilization is the process by which chemicals dissolved in water partition across the air-water interface. As in sorption a partition coefficient, the Henry's Law constant, is defined which describes the equilibrium ratio between the dissolved phase of a chemical and the gas phase. However chemical concentrations in the atmosphere above the water surface are assumed to be zero and therefore equilibrium is never reached. It is assumed that the rate of transfer across the air-water interface is proportional to the Henry's Law constant as well as the concentration gradient across the interface. Furthermore it is assumed that only the water at the surface is involved in this transfer. Therefore the rate at which water is renewed to the surface is also taken into account when calculating the transfer rate.

A transfer coefficient, K_v , is a constant that describes the rate at which a chemical can transfer across the air-water interface. K_v is in the form of a velocity and this velocity divided by the depth of the river segment can be used as a decay rate.

Much work has been done on the transfer of oxygen across the air-water interface and therefore many empirical formulae exist to calculate the K_v for oxygen, known as the re-aeration rate, K_a . Taking 32 to be the molecular weight of oxygen, Equation 3-29 is

used to convert the calculated K_a for a particular river to a K_v for a particular chemical other than oxygen in that river.

$$K_v = K_a \sqrt{32/M_w}$$

Equation 3-29

Where:

- K_v = volatilization rate [L/T]
- K_a = oxygen re-aeration rate [L/T]
- M_w = molecular weight of chemical [M]

3.5.7.2 WASP Implementation of Volatilization

WASP uses the Covar (1976) method for calculating K_a (Ambrose et al., 1993). The Covar method considers the velocity and depth of the river segment and uses one of three empirical formulae depending on the velocity and depth conditions (Covar, 1976).

WASP implements the Covar method by using the Owens formula if the depth is less than 0.61 m (Ambrose et al., 1993).

$$K_a = 5.349 \frac{u^{0.67}}{D^{0.85}}$$

Equation 3-30

Where:

- u = velocity of water [L/T]
- D = tank depth [L]

For tanks where velocity is less than 0.518 m/s or depth is greater than $13.584u^{2.9135}$ the O'Connor-Dobbins formula is used (Ambrose et al., 1993).

$$K_L = \left(\frac{D_w u}{D} \right)^{0.5} 0.64 \cdot 10^4$$

Equation 3-31

Where:

- D_w = diffusivity of the chemical in water calculated with Equation 3-32 [L²/T]

$$D_w = \frac{22 \cdot 10^{-9}}{M_w^{2/3}}$$

Equation 3-32

Finally if the velocity or depth does not meet any of the above criteria the Churchill formula is used (Ambrose et al., 1993).

$$K_a = 5.049 \frac{u^{0.969}}{D^{0.673}}$$

Equation 3-33

3.5.7.3 Volatilization Constants Used

Since the Covar method was used, only a Henry's Law Constant and a molecular weight were required for each phosphate ester. The velocity and depth at each model tank were calculated using Equation 3-16 and Equation 3-17.

Molecular weights were calculated from the molecular formula given in Section 3.5.1. The Henry's Law Constants used are listed below.

- $H_{TBP} = 1.41\text{E-}6 \text{ atm}\cdot\text{m}^3/\text{mole}$ (SRC, 2004)
- $H_{TBEP} = 1.2\text{E-}11 \text{ atm}\cdot\text{m}^3/\text{mole}$ (SRC, 2004)

- $H_{TCEP} = 3.29E-6 \text{ atm}\cdot\text{m}^3/\text{mole}$ (WHO, 1998)

3.5.8 Oxidation

3.5.8.1 Overview of Oxidation

Oxidation occurs when free radicals such a hydroxyl radical, $OH\cdot$, encounter organic chemicals and attack the C-H bonds. Radicals are formed in the water column through photochemical reactions.

3.5.8.2 WASP Implementation of Oxidation

WASP models oxidation as a second-order reaction whose rate depends on both the concentration of the chemical and the concentration of free radicals in the water column. The first-order rate for degradation of the chemical due to oxidation by free radicals is determined using Equation 3-34 (Ambrose et al., 1993).

$$K_o = [OH\cdot]k_o$$

Equation 3-34

Where:

- K_o = pseudo-first-order rate constant [T^{-1}]
- $[OH\cdot]$ = concentration of oxidation radicals [M/L^3]
- k_o = second-order oxidation rate [L/MT]

The user specifies tank variable oxidant concentrations and the second-order oxidation rates for the chemicals being modeled.

3.5.8.3 Oxidation Model

The second-order oxidation rate constants used in this model are listed in Table 3-21.

**Table 3-21 Second-Order Oxidation Rate Constants
(Machairas, 2004)**

Compound	Oxidation Rate (L/mole*day)
TBP	8.64E+14
TBEP	1.73E+15
TCEP	1.73E+14

No data was available regarding the concentration of oxidation radicals in the modeled reach of the Chattahoochee. Illuminated surface waters contain hydroxyl radical at concentrations of about 10^{-17} moles/L (Hemond and Fechner-Levy, 1994) and this value was used as the concentration of oxidation radicals in each tank in the model. This is a simplifying assumption and it is recognized that radicals other than hydroxyl may be present and that deeper and more turbid waters will have lower concentration of oxidation radicals. It is assumed that 10^{-17} moles/L is the average concentration of oxidation radicals in the modeled reach.

3.5.9 Neglected Reactions

3.5.9.1.1 Hydrolysis

Hydrolysis is a reaction in which both a chemical molecule and a molecule of water are split and recombined to form two new compounds. Depending on the compound hydrolysis may be catalyzed by basic, acidic or neutral environment. For the three phosphate esters hydrolysis is a base-catalyzed reaction and will only occur significantly in waters with pH of 12 or higher (Schwarzenbach et al., 2003). The pH in the Chattahoochee rarely is less than 6.9 or greater than 7.5 (USGS, 2004) and therefore it is assumed that hydrolysis is not an important reaction for phosphate esters in the Chattahoochee River.

3.5.9.2 Photolysis

Photolysis is the process by which chemical molecules are broken up by sunlight. Every chemical absorbs light within a spectrum specific to that chemical. If the ambient light waves fall with the absorption spectrum of the chemical then enough light energy may be absorbed by the molecule to break it apart. No absorption spectra for the phosphate esters were available for this study. In addition, as discussed in Section 3.5.1, the

phosphate esters are either clear or very lightly colored. A clear compound allows light to pass directly through it and therefore does not absorb light energy. TBEP being lightly colored has some possible potential for photolysis but since this is simply conjecture it will be assumed that photolysis is not an important reaction for any of the phosphate esters being studied.

4 Model Results

In this chapter the results of the model described in Chapter 3 will be discussed. We will first discuss the spatial and temporal concentration distribution, then examine the effect of each of the modeled reactions, and finally we will compare the results of this model with the observations made between January 14, 2004 and January 16, 2004.

4.1 Flow Pattern vs. Concentration

The model predicts that diurnal flow variations imposed by Buford Dam and the regulation of flow at Morgan Falls Dam have an effect on the daily and weekly concentration patterns of the phosphate esters. Due to the position of phosphate ester point sources and depending on the position relative to Morgan Falls Dam these patterns are manifested differently at different locations on the river.

4.1.1 Initial Conditions Model Results

As discussed in Section 3.5.3 the model was run for a forty-two day cycle in order to generate an initial concentration distribution. The results of this model make some predictions as to what the pattern of concentration variance is within the Chattahoochee over a two-month period. This model averages out the flow variation occurring during the five-day workweek when power is generated at the hydroelectric dams. The model uses an average weekly flow and average weekend flow and alternates between them.

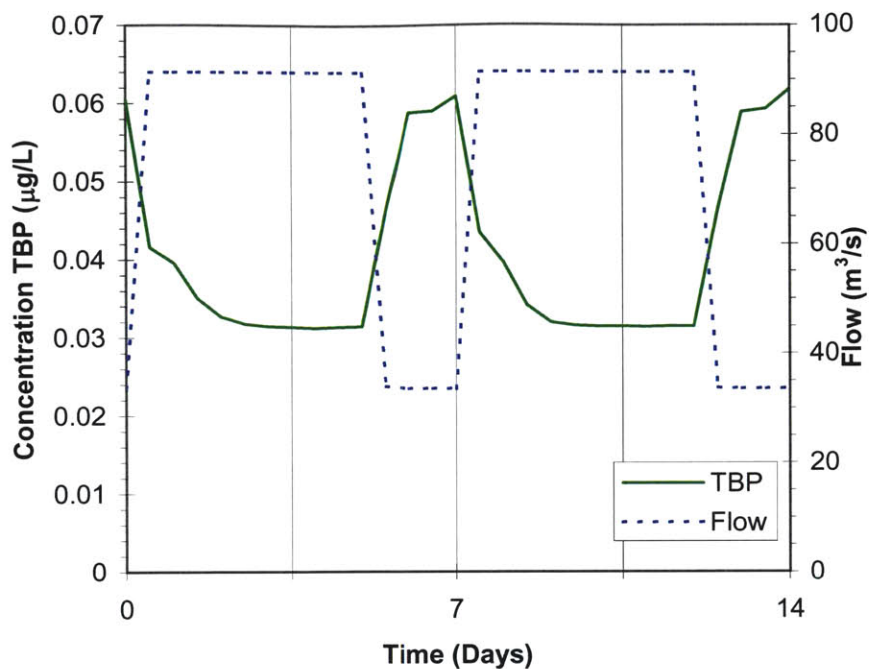


Figure 4-1 Flow and TBP Concentration at Highway GA 280 Crossing (Tank 103) Forty-Two Day Model

Figure 4-1 shows the concentration of TBP in water at the downstream end of the initial conditions model for a two-week period. Flow is also shown on the plot and it is easy to see that TBP concentration varies inversely with flow. During the week when flow is high TBP concentration at tank 103 is approximately 0.032 µg/L. When the weekly low flow period arrives concentration increases by almost a factor of two and then drops back down at the start of the week. Note that the five-day model begins at the end of day 14 shown above. The cycle of concentrations is similar for TBEP and TCEP with TBEP fluctuating between 0.15 µg/L and 0.17 µg/L and TCEP between 0.04 µg/L and 0.025 µg/L.

4.1.1.1 Five Day Simulation and Initial Conditions Model

While the initial conditions model assumes a steady average weekly flow, the five-day simulation resolves the individual flow fluctuations caused by the operation of the hydroelectric dams during the weekdays January 12, 2004 – January 16, 2004 (Section 3.2). While the initial conditions model reveals something about the way concentrations

may vary from week to weekend the five-day simulation zooms in on the fluctuations of flow and concentration that are experienced during the week. Figure 4-2 displays the fluctuations predicted at the Highway GA 280 crossing for a typical week and can be thought of as the details of what happens in between low flow periods in Figure 4-1. The remainder of Section 4.1 will investigate the patterns predicted by the five-day simulation.

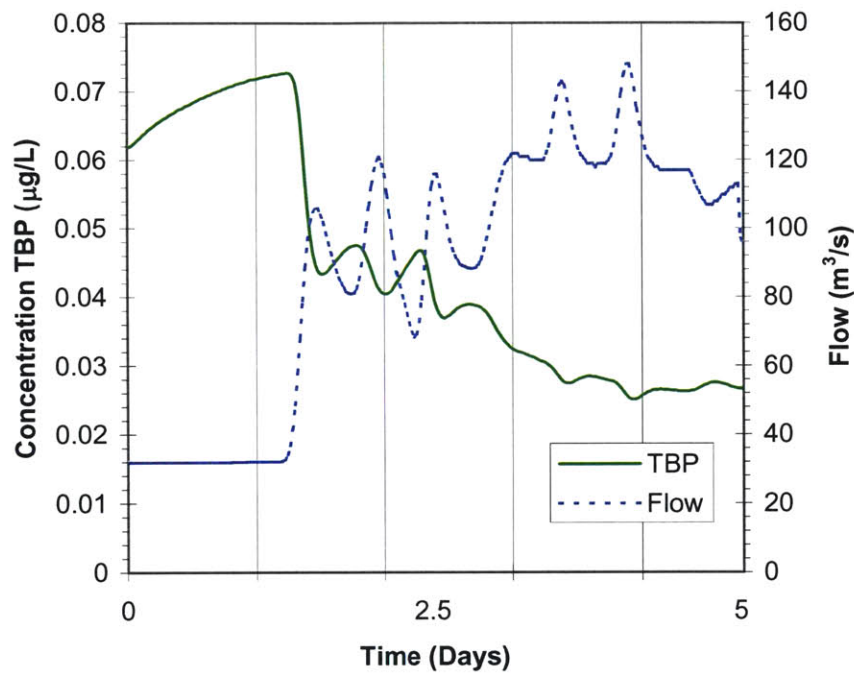


Figure 4-2 Flow and TBP Concentration at Highway GA 280 Crossing (Tank 103) Five-Day Model

4.1.2 Concentration Patterns above Morgan Falls

4.1.2.1 Above Suwanee Creek

Between the Buford Dam release and the mouth of the Suwanee Creek (Tank 11) concentrations remain almost constant and there is very little decline from the initial concentrations listed in Table 3-14. The distance from Buford Dam to tank 10 is approximately 17 kilometers and either the travel time is too short or the concentrations too low for degradation of any kind to have taken much effect. At this point flow also

does not effect the concentration because all water released at Buford Dam has the same initial concentration.

4.1.2.2 Suwanee Creek to Crooked Creek

The inflow at Suwanee Creek is less than $2 \text{ m}^3/\text{s}$ and has a concentration comparable to that leaving Buford Dam except in the case of TBEP where the inflow at Suwanee Creek actually serves to slightly dilute concentrations (for details see Section 3.5.2.2.2). One interesting insight can be made by studying Figure 4-3 and Figure 4-4. Directly below the mouth of Suwanee Creek (Figure 4-3) concentrations are higher during low flow periods due to the greater effect of the Suwanee Creek inflow. Concentrations of TBP entering at Suwanee Creek are two times as large as the background in the Chattahoochee before the confluence. During low flow periods the Suwanee Creek flow is 10% of the Chattahoochee and causes the increase in concentration.

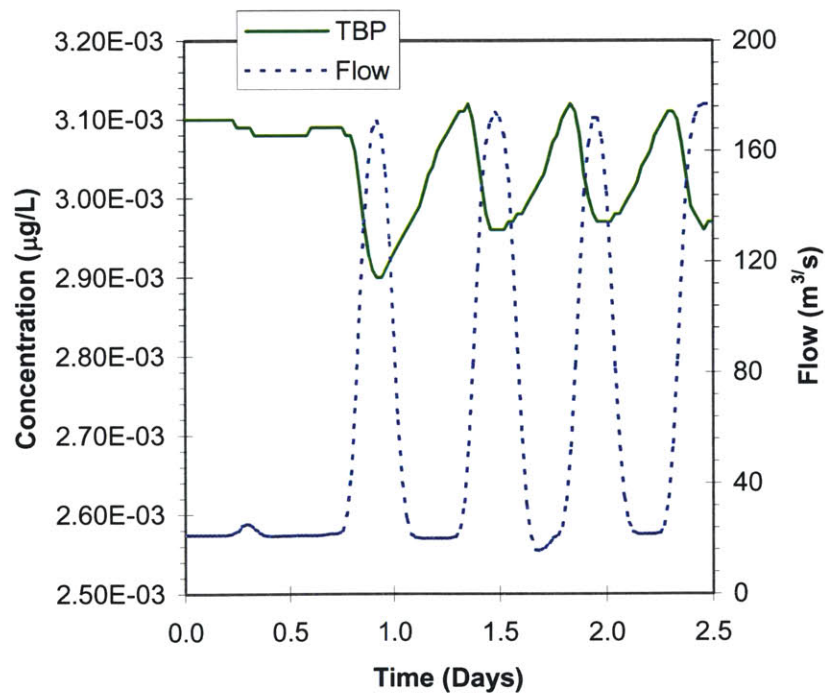


Figure 4-3 Flow and TBP Concentration Directly Below The Mouth of the Suwanee Creek (Tank 12)

In comparison, TBP concentrations decrease during low flow periods 21 kilometers downstream at tank 25 (Figure 4-4). Here lateral inflow in the reach between Suwanee Creek

and tank 26 dilutes the ambient concentrations at low flow and has less effect at high flow resulting in increasing concentrations during the passage of the flood wave. This pattern is less pronounced for TBEP and TCEP and even for TBP the variation is less than a nanogram but nonetheless is a pattern worth noting.

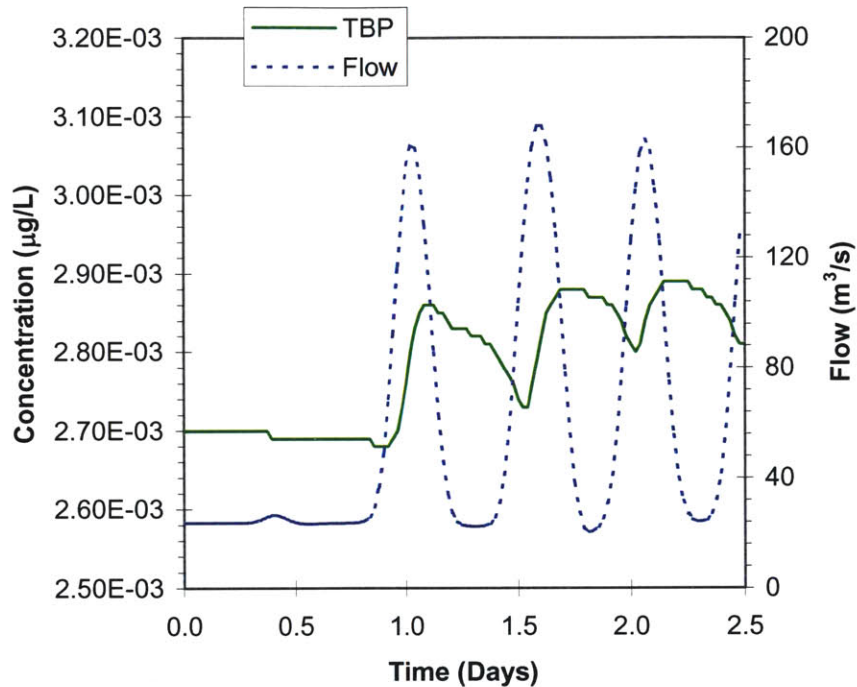


Figure 4-4 Flow and TBP Concentration Directly above the Crooked Creek WWTP Outfall (Tank 25)

4.1.2.3 Crooked Creek to the Mouth of the Big Creek

Two outfalls exist in the beginning of this reach, Crooked Creek WWTP in tank 26 and John’s Creek in tank 27. Crooked Creek is a relatively large source of TBP while John’s Creek is the largest source of TBEP in the modeled reach. Directly downstream of the outfalls, concentrations of TBP rise by 6 ng/L, TBEP rise by 64 ng/L and TCEP rise by 4 ng/L. The pattern of concentration in this reach is similar for all three compounds and is illustrated in Figure 4-5 which shows the first half of the simulation for TBEP in tank 36. Studying Figure 4-5 reveals that concentrations steadily rise during low flow periods and drop off during the passage of the flood wave. In general concentrations of all three phosphate esters follow a similar pattern in this reach.

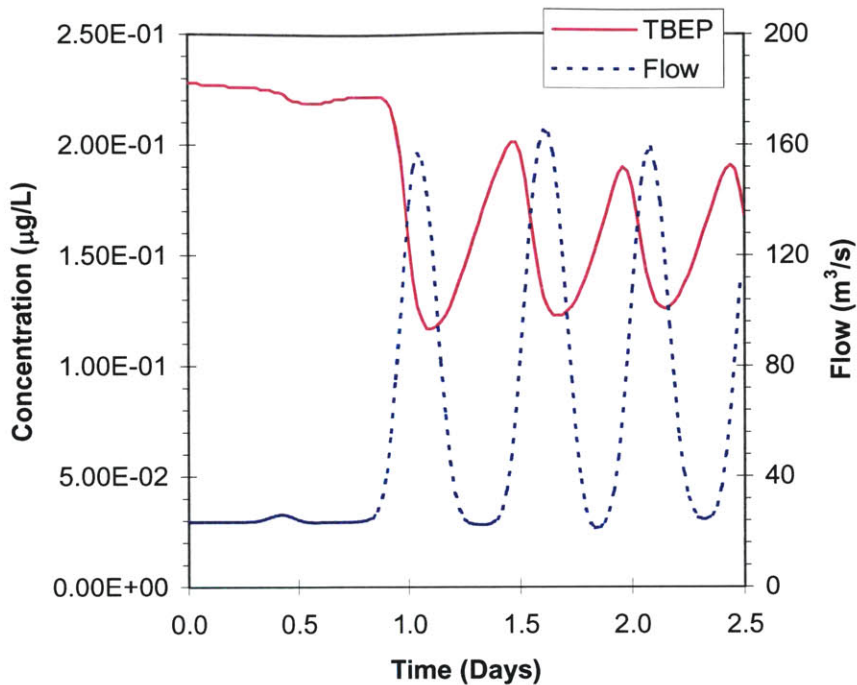


Figure 4-5 Flow and TBEP Concentration in the Center of the Reach between the Crooked Creek Outfall and the Mouth of the Big Creek (Tank 36)

4.1.2.4 Mouth of Big Creek to Bull Sluice Lake

Within this reach the river begins to become wider and slower as it approaches Bull Sluice Lake. Figure 4-6 shows the concentration of TCEP and flow at tank 51 between the confluence of the Big Creek and the Big Creek WWTP outfall. This plot begins at day one of the simulation since before then at this model tank the river is at low flow. One can plainly see that the range of fluctuation in concentration is not as pronounced as upstream. This can be explained by the fact that the tanks in this region have higher volume and therefore do not get fully flushed by the flood waves. It is interesting to note that the concentration does not immediately drop when the first flood wave passes through. This is again a consequence of the tanks in this reach being much larger and therefore do not immediately become diluted by the lower concentration waters arriving on the flood wave.

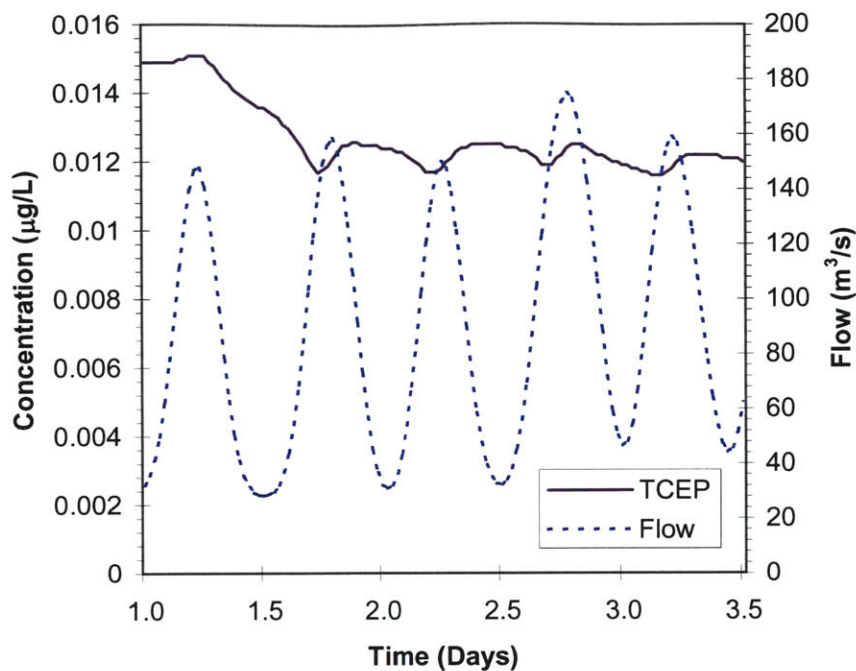


Figure 4-6 Flow and TCEP Concentration between the Mouth of Big Creek and the Big Creek WWTP Outfall (Tank 50)

The behavior of TCEP in the region is representative of the other phosphates as well. Concentrations for the TCEP and TBEP will rise after tank 51 were the Big Creek WWTP outfall discharges. TBEP will not exhibit a marked increase since the TBEP load at Big Creek WWTP and the Big Creek confluence is orders of magnitude lower than the load at John's Creek 15 kilometers upstream (Figure 3-36).

4.1.3 Concentration in Bull Sluice Lake

Concentrations in Bull Sluice Lake are important to address separately since they represent the boundary between two very different concentration patterns. The large volume of Bull Sluice Lake along with the change in flow patterns at Morgan Falls produces these different patterns.

As we have seen in the Section 4.1.2.4 and Figure 4-6 the oscillation between low and high concentrations becomes less pronounced as we move into the slower moving waters near Bull Sluice Lake. The concentration patterns in Bull Sluice Lake are most easily illustrated by looking at TBEP due to it being at a relatively higher concentration,

however all three compounds exhibit much the same pattern in Bull Sluice Lake. Figure 4-7 displays the TBEP concentration and average flow curves for Bull Sluice Lake.

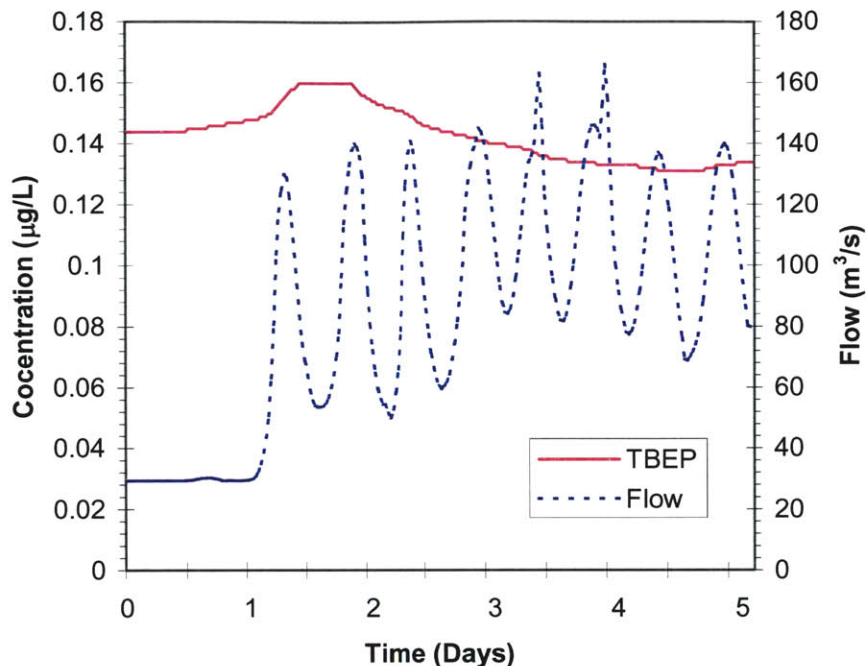


Figure 4-7 Flow and Concentration of TBEP at Bull Sluice Lake (Tank 51)

Studying Figure 4-7 one can see that the concentration of TBEP in Bull Sluice Lake steadily rises coming out of the weekend through Monday (Day 0). At midnight Tuesday (Day 1) the first flood wave arrives at Bull Sluice Lake and for the next half-day concentration rises more sharply as the high concentration waters from upstream are flushed through the system and mix into Bull Sluice Lake. This volume is small though compared to Bull Sluice Lake and after leveling out between noon Tuesday and midnight Wednesday (Day 2) the concentration begins to drop off hitting its minimum in the afternoon Friday (Day 4) when it begins to rise again. It is our conjecture that the concentrations will rise through the weekend repeating a similar pattern again at the start of following week.

4.1.4 Concentration Downstream of Morgan Falls

Concentration downstream of Morgan Falls can be broken down into two different patterns. Patterns in this area are of considerable interest since it is here at tank 99 that the Atlanta Water Works withdraws water for the city of Atlanta. Immediately after the Atlanta Water Works the outfalls of the R.L. Sutton WWTP and the R. M. Clayton WWTP increase the concentration in the final tanks in the model.

4.1.4.1 Concentration between Morgan Falls Dam and Atlanta

The concentrations upstream of the R. M. Clayton and the R. L. Sutton plant outfalls follow a similar pattern as that in Bull Sluice Lake discussed in Section 4.1.3. Bull Sluice Lake can be thought of as a large mixing tank that averages out the concentration fluctuations caused by the diurnal flow cycle. The mean residence time of a water body can be estimated with

$$t_{res} = \frac{V}{Q}$$

Equation 4-1

Where:

- t_{res} = mean residence time of a parcel of fluid [T]
- V = volume of water body [L^3]
- Q = average flow rate through water body [L^3/T]

The water released over Morgan Falls Dam at time t has the average concentration of the waters that have entered since $t - t_{res}$. Only dilution and degradation processes affect the concentration in this reach. Fluctuations in flow caused by the operation of Morgan Falls Dam have no effect, which can be seen in Figure 4-8.

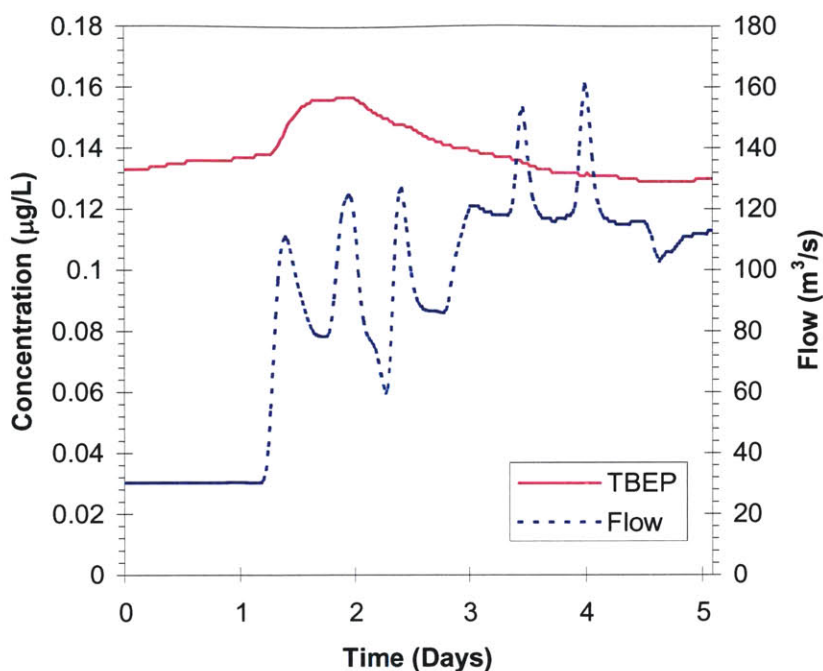


Figure 4-8 Flow and TBEP Concentration in the Reach between Morgan Falls and Atlanta (Tank 79)

It is interesting to note that a slug of relatively high concentration water is flushed from Bull Sluice Lake and travels downstream passing this point between noon on Tuesday (Day 1) and Wednesday (Day 2) morning. This may have implications for drinking water treatment plants drawing water from the Chattahoochee in this reach; this will be discussed further in Chapter 6. It should also be noted that the specific shape of the concentration curves for TBP and TCEP are not exactly the same as that displayed here for TBEP and have subtle differences. Still the general patterns are the same and the above analysis applies for all three phosphate esters.

4.1.4.2 Downstream of the Atlanta Treatment Plants

Discharges from R.M. Clayton and R.L. Sutton WWTPs dominate the concentration characteristics of this portion of the model. R. L. Sutton discharges into tank 101 and is estimated to be the second largest source of TCEP, and is an average size source of both TBEP and TBP. The R. M. Clayton facility is the largest in the modeled reach and discharges into tank 102. This is estimated to be the largest load of TCEP and TBP and

the second largest of TBEP in the reach. Concentrations of all phosphate esters are expected to increase in these final tanks. The model predicts that between tank 100 and 103 TBP exhibits an increase of 16%, TBEP increases by 106%, and TCEP increases by 70%. The differences in percentage of increase can be understood by viewing Figure 3-36 where a relative comparison of load magnitude is made.

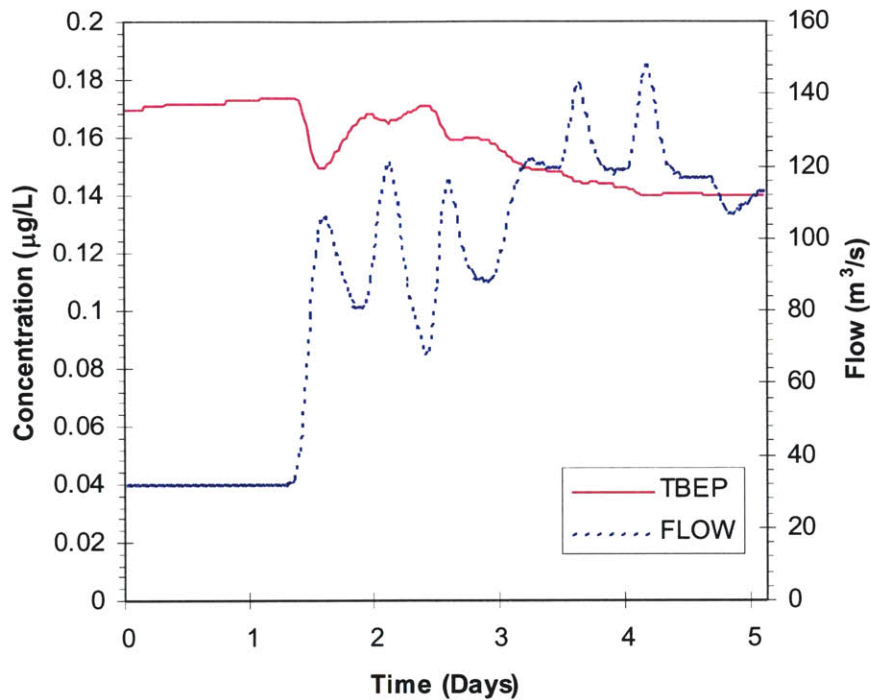


Figure 4-9 Flow and TBEP Concentration at Highway GA 280 Crossing (Tank 103)

The pattern that the concentration vs. time curve takes can be seen in Figure 4-9. The concentration is rising slowly coming out of the weekend at the beginning of the simulation. This is due to the rising concentration of the waters released at Morgan Falls Dam (Section 4.1.4.1) as well as the loads from R.L. Sutton and R.M. Clayton WWTPs being discharged to the weekend low flow. When the first flood wave arrives after midnight on Tuesday (Day 1) a sudden decrease in concentration occurs which rebounds in between the following two flood waves but trails off as the week goes on and high flows flush the high concentrations downstream. Again the pattern of the concentration curves is similar for TBP and TCEP although, as can be seen in Figure 4-2, the rebounds

after the first flood wave are hardly as pronounced and concentration stays relatively low during the week.

4.1.5 Longitudinal Concentration Distribution

As we have seen the concentrations are dependent on flow and source placement. However it may be helpful to have a general idea of how the concentrations increase on average in the downstream direction. Table 4-1 lists the downstream concentration distribution for each phosphate ester.

Table 4-1 Average Concentration Longitudinal Distribution

Tank	Concentration (µg/L)		
	TBP	TBEP	TCEP
10	0.003	0.112	0.011
15	0.003	0.108	0.011
30	0.008	0.159	0.014
45	0.007	0.148	0.013
60	0.022	0.142	0.019
75	0.022	0.139	0.019
90	0.022	0.137	0.019
103	0.044	0.158	0.032

4.2 Sorption Model Results

The sorption model discussed in Section 3.5.5 did not have a significant effect on the concentrations of any of the phosphate esters. TBEP is the compound most likely to sorb to organic matter suspended in the water column and less than 1% of the TBEP concentration in any model tank is transported as sorbed to the solid phase. In this case settling of suspended solids will not be a significant sink of the phosphate esters.

The fraction of organic carbon (f_{oc}) in the base case model is 1% and this was raised to 10% to quickly assess the sensitivity of the model to f_{oc} values. The results of this test showed as much as 4.3% of TBEP being transported as sorbed in the final tank in the model. While this sorbed percentage is still not a substantial fraction of the total TBEP concentration, it represents an increase of a factor of 20 over the previous case. The percentages of each phosphate ester being transported as sorbed to the solid phase for the two cases are displayed in Table 4-2.

Table 4-2 Average Percentage of Phosphate Ester Sorbed to Suspended Solids (Tank 103)

Phosphate	f_{oc}	
	1%	10%
TBP	0.0%	0.4%
TBEP	0.3%	2.8%
TCEP	0.0%	0.0%

Figure 4-10 shows the relationship between concentration of suspended solids and of TBEP transported as sorbed to the solid phase. From studying this figure it is apparent that the percentage of total TBEP concentration sorbed to suspended solids is proportional to the concentration of solids. Therefore one can expect that during turbid conditions such as those discussed in Section 3.4 that sorption could be a much more important process for TBEP and even possibly TBP. Highly turbid conditions were simulated and will be discussed in Chapter 5.

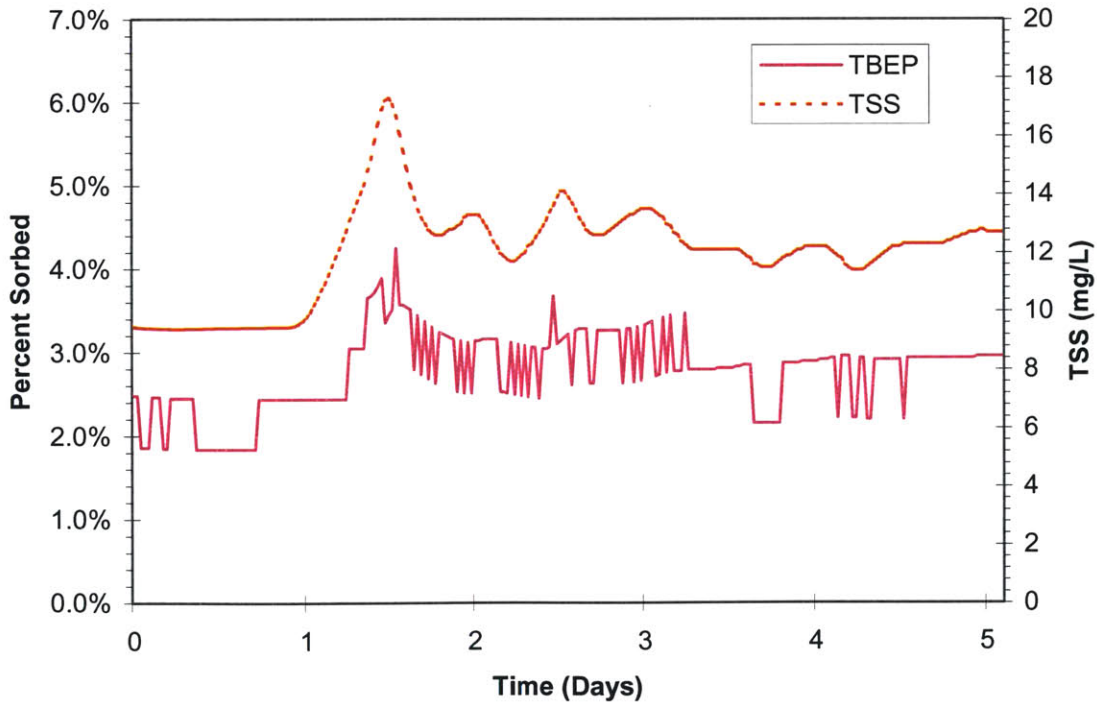


Figure 4-10 TSS and Percentage TBEP Sorbed at Highway GA 280 Crossing (Tank 103) (Note that fluctuations in sorbed percentage are due to numerical imprecision in the output file)

TBEP has been shown to be the most likely to sorb to organic matter and it is interesting to compare the average concentration of TBEP leaving the model at the Highway GA 280 crossing in both cases discussed above. The concentration in tank 103 for the f_{oc} equal to 10% case is 95.5% of the concentration in the f_{oc} equal to 1% case. Although not a significant loss some degradation can be attributed to suspended solid settling. In Section 3.4 we discussed the potential for Bull Sluice Lake to be a site of significant loss of phosphate esters due to settling. It is interesting to note that in both cases the percent of TBEP sorbed to suspended solids in Bull Sluice Lake was less than 1%. Although substantial suspended solids settling may occur here the concentrations of phosphate esters and suspended solids are such that there is not much sorption. The 4.5% is probably distributed throughout the river reach.

4.3 Biodegradation Model Results

The magnitude of the sink due to biodegradation was evaluated by observing concentrations just upstream of the R. L. Sutton WWTP for both the base case model and a case without biodegradation. Phosphate esters that enter the system at R.L Sutton and R. M. Clayton WWTPs do not have a long enough residence time for biodegradation to become a large factor and for this reason were left out of this comparison.

TBEP concentrations were the most affected by biodegradation and were an average of 11% lower than in the model without biodegradation at the observation point (tank 100). TBP was an average of 5% lower and TCEP an average of 2% lower.

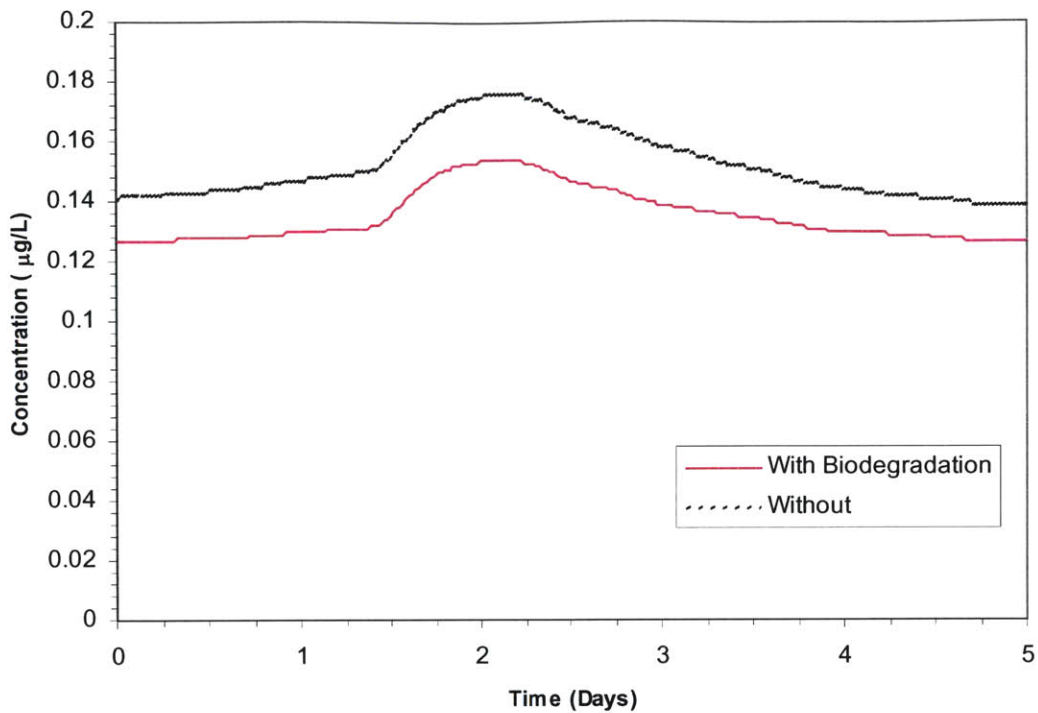


Figure 4-11 Concentration of TBEP Upstream of R.L. Sutton WWTP with Biodegradation and without Biodegradation

Figure 4-11 shows the concentration curves at tank 100 for both the case with biodegradation and the case without biodegradation. It is apparent that the concentration in the simulation with biodegradation is consistently lower. Examination of Figure 4-12 shows how the percentage of loss due to biodegradation changes during the simulation. It reaches a maximum on noon on the second day of the simulation corresponding to the end of the weekend low flow period. This increase in loss to biodegradation is due to the increased travel times during low flow periods between the WWTP outfalls upstream of Morgan Falls Dam and tank 100. As the high flows typical of weekdays begin after noon on the second day, the travel times decrease and biodegradation does not have as much time to take effect.

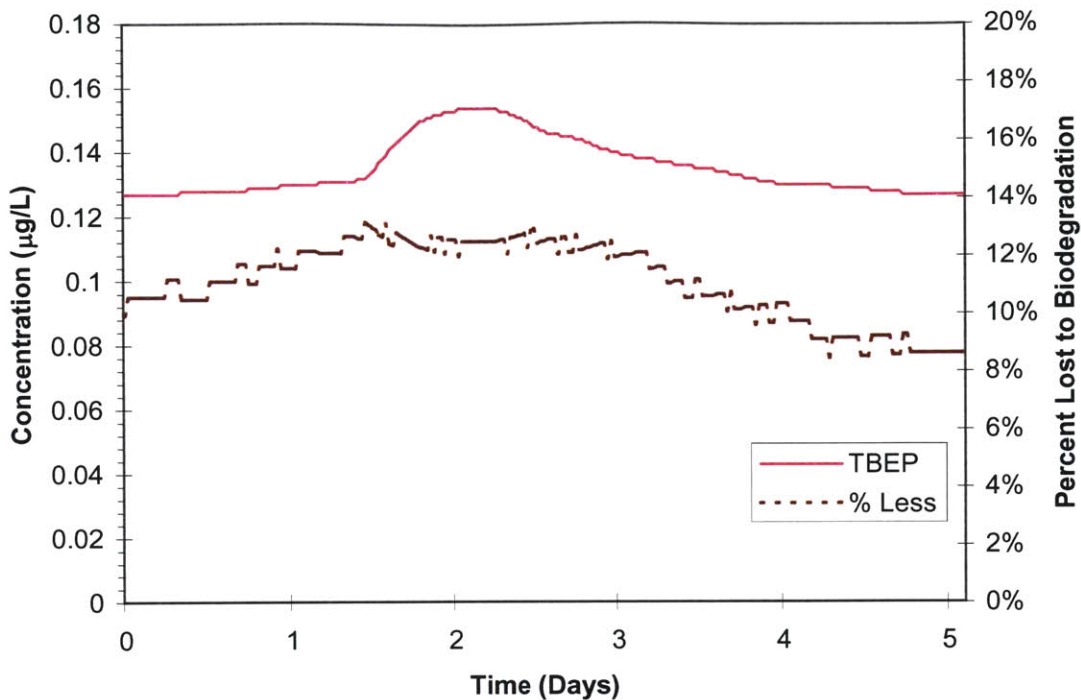


Figure 4-12 TBEP Concentration and Percent Loss Due to Biodegradation Upstream of the R.L. Sutton WWTP

Figure 4-13 shows the average percentage by which the simulation with biodegradation is less than the simulation without biodegradation at five locations along the river. The difference in height of the columns in the graph in Figure 4-13 reveals where in the modeled reach there is the maximum potential for loss to biodegradation. As can be seen from the large increase in the percent lost between tank 45 and tank 60 the biggest potential for loss to biodegradation is in this region. The slower waters in this region, especially in Bull Sluice Lake, result in long travel times through the reach. The percentage lost decreases downstream of the R.L. Sutton and R.M. Clayton outfalls since phosphate esters added by these WWTPs do not remain in the system long enough for an appreciable difference to develop between the two models.

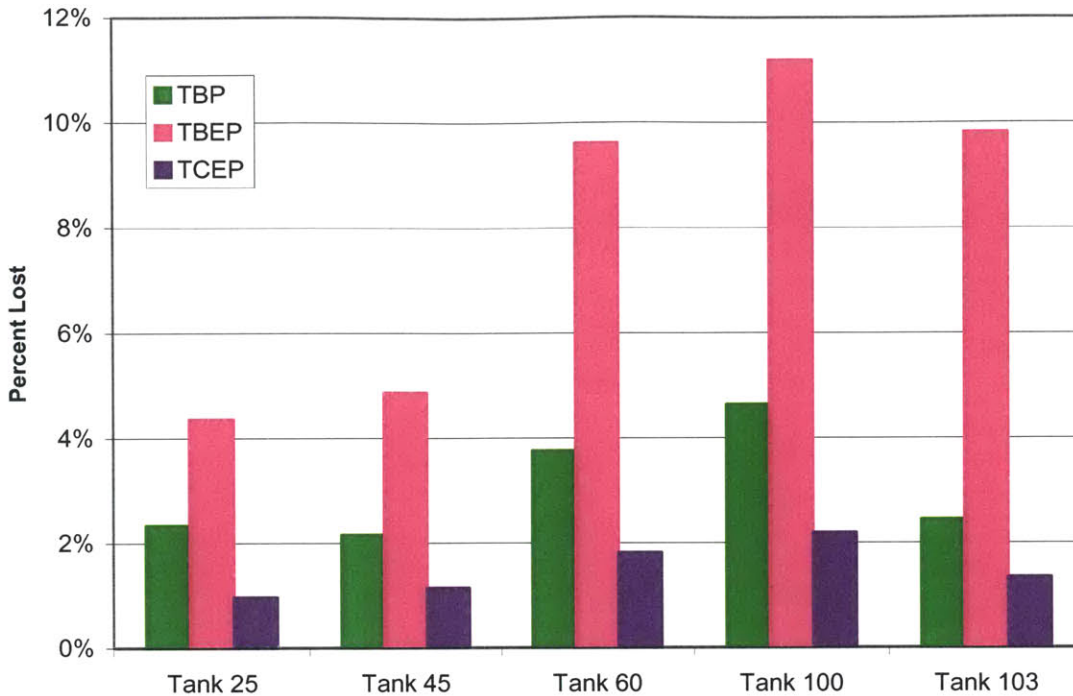


Figure 4-13 Percentage of Cumulative Phosphate Loss to Biodegradation at Locations along the Modeled Reach

4.4 Volatilization Model Results

The magnitude of the sink attributed to volatilization was evaluated by comparing the results of the base case model with the results from a simulation run with volatilization turned off. As in Section 4.3 the comparison is made upstream of the R.L. Sutton WWTP outfall in order to avoid the concentrations added by this plant.

Volatilization was most significant for TCEP though it did not account for much loss and resulted in the TCEP concentration in the base case being only 3% less than that in the case without volatilization. Volatilization was not significant for TBP or TBEP and reduced TBP by 1% of the case without volatilization and did not reduce TBEP at all.

Volatilization rates in rivers are affected by water velocity and channel depth and therefore it is expected that the rate of volatilization for TCEP is affected by the river flow. Figure 4-14 shows TCEP volatilization rates and flows in the modeled reach at the beginning of the third day of the simulation.

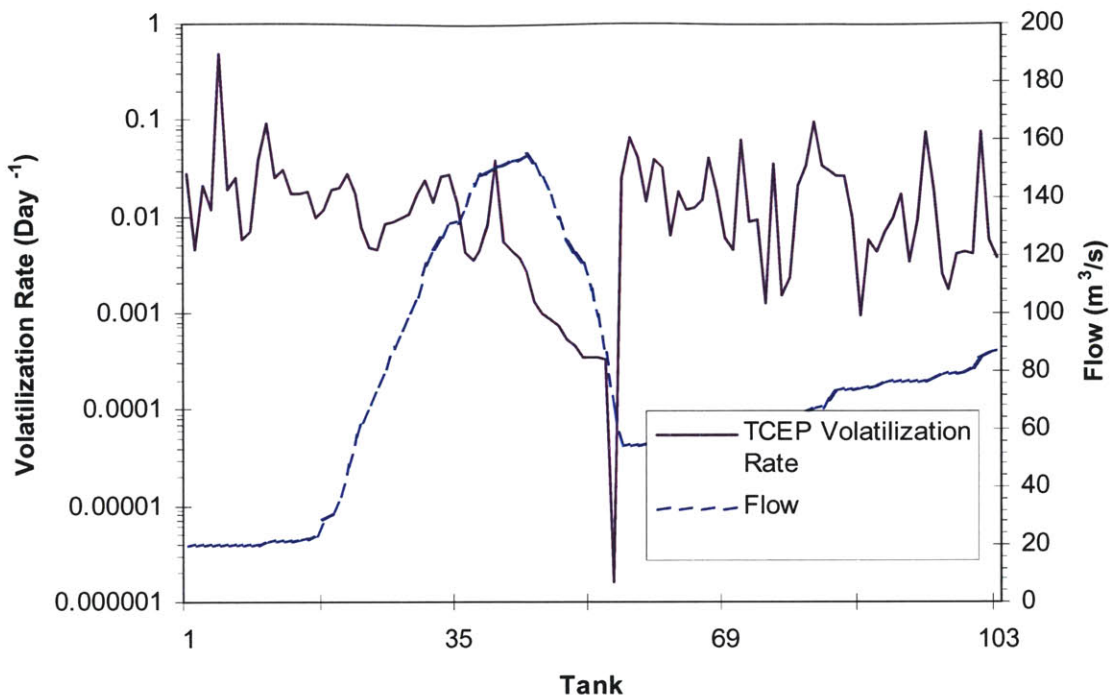


Figure 4-14 Profile of TCEP Volatilization Rate and Flow at Beginning of Third Day

Figure 4-15 shows the volatilization rates and flows six hours after the snapshot in Figure 4-14. A few tanks show marked change in volatilization rate, tank 5 and tank 11 showing the most sensitivity to flow. These are tanks in which the velocity changes dramatically with flow, the tanks having discharge coefficients for velocity of 1.1 and 3.4 respectively. These tanks are at the upstream end where concentrations are low so the rapid volatilization in these tanks does not serve to affect the downstream concentration of TCEP dramatically. Volatilization is most significant for TCEP during low flow periods, however this significance is tempered by the fact that the river reaches where it is most effective carry low concentrations.

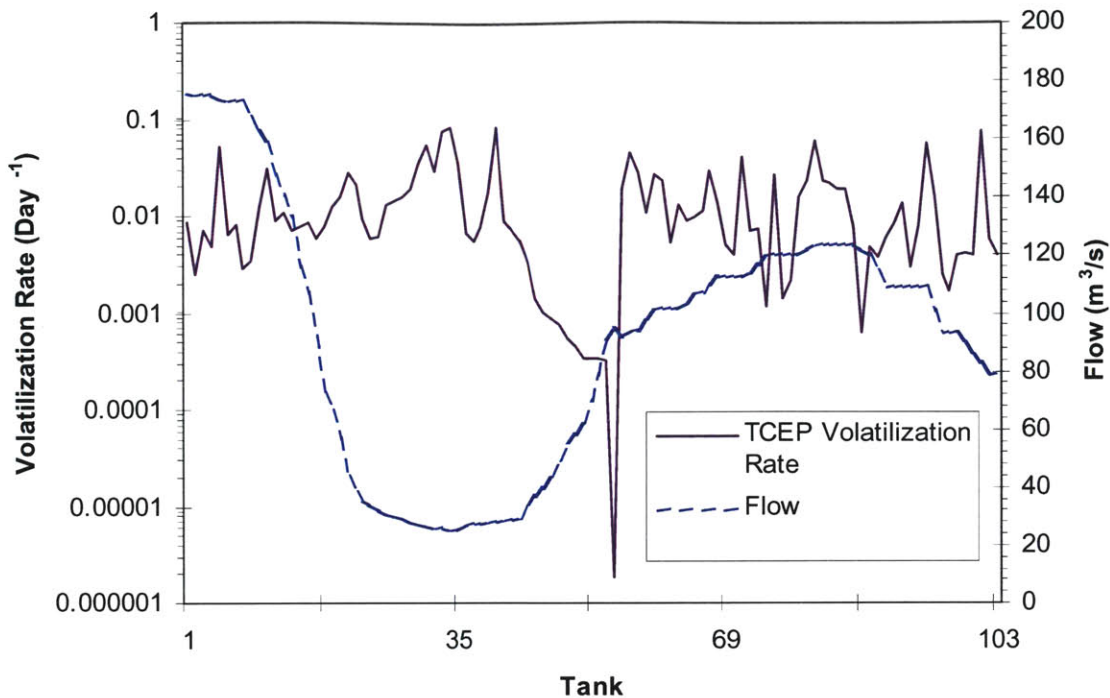


Figure 4-15 Profile of TCEP Volatilization Rate and Flow Six Hours into the Third Day

4.5 Oxidation Model Results

As in the evaluation of the other processes we compared the base case model results with a simulation that did not include oxidation by free radicals. As in the previous analysis we first investigate the concentration at tank 100. TBEP is the most susceptible to oxidation by free radicals and has an average concentration 5% less at tank 100 than the model with oxidation turned off. The concentration of TBP is less affected and has an average concentration in tank 100 2% less than the model without oxidation. TCEP was barely affected by free radical oxidation and was only reduced by 0.5%

Since the model held the concentration of free radicals constant throughout the model (Section 3.5.8.3), the oxidation reaction reduces to a first-order decay. Biodegradation is also modeled as first-order decay and therefore the two reactions will have similar pattern with the exception of the magnitude of the sink. The reader is referred to Section 4.3 for discussion on how oxidation will vary spatially and temporally in the model.

4.6 Comparison to Field Studies

The base case model results were compared to the results of two field studies that sampled for in-stream concentrations of TBP, TBEP, and TCEP. Andrews (2004) took samples at three locations in the modeled reach and Lin (2004) took samples of untreated water drawn from the Chattahoochee at the Atlanta Water Works drinking water treatment plant. The simulated period was chosen so as to cover the days when these samples were taken. Table 4-3 lists the average modeled concentration for the day that the sample was taken along with the observed data. The locations of the sample sites are the same as those taken for turbidity (Figure 3-24) plus the Atlanta Water Works DWTP (Figure 2-4)

**Table 4-3 Sample Sites & Corresponding Model Tank
(Andrews, 2004 and Lin, 2004)**

Tank	TBP		TBEP		TCEP	
	Modeled (µg/L)	Observed (µg/L)	Modeled (µg/L)	Observed (µg/L)	Modeled (µg/L)	Observed (µg/L)
Roswell	0.005	0.010	0.131	0.173	0.012	0.067
Bull Sluice Lake	0.014	0.010	0.132	0.307	0.016	0.024
Atlanta Water Works	0.024	0.027	0.148	0.119	0.020	0.020
GA 280	0.030	0.034	0.147	0.442	0.024	0.132

Figure 4-16 Field Sample Sites

Inspection of Table 4-3 shows good agreement between the model and observations made by Lin (2004) at the Atlanta Water Works sample site (Tanks 99). As has been discussed in Section 4.1.4 the concentrations in this region do not fluctuate with flow but represent the well-mixed concentrations leaving Morgan Falls Dam, and the agreement with observation here supports the analysis. In most other cases the model results are within a factor of two of the observations. Still discrepancies exist.

The observations of TCEP at the Highway GA 280 crossing and to a lesser extent TBEP are significantly greater than the model predictions. This can be explained by observing that the sample site is only 1.6 kilometers downstream from the R.M. Clayton WWTP outfall and 1.9 kilometers downstream of the R.L. Sutton outfall. Phosphate esters released in the outfall will be concentrated on the outfall side of the river and it will take

some time for the lateral mixing processes to spread the phosphate esters uniformly across the channel. A turbulent diffusion coefficient, E_T , describes the speed at which lateral mixing takes place and can be estimated using Equation 4-2 (Fischer et al., 1979).

$$E_T = 0.15du^*$$

Equation 4-2

Where:

- E_T = transverse turbulent mixing coefficient [L^2/T]
- d = average depth of the channel [L]
- u^* = shear velocity given by Equation 3-9 [L/T]

The distance from the outfall that water must travel in the river to be considered laterally well mixed is given by Equation 4-3 (Fischer et al., 1979)

$$X_{mix} = \frac{\overline{u}(2W)^2}{10E_T}$$

Equation 4-3

Where:

- X_{mix} = distance from outfall water must travel to become mixed laterally [L]
- \overline{u} = width and depth averaged channel velocity [L/T]
- W = average width of channel [L]

The velocities, widths and depths between the R.M. Clayton and R.L. Sutton outfalls and the GA 280 sample site estimated using the HEC-RAS model (Section 3.2.3) and Equation 4-2 and Equation 4-3 were used to estimate the distance for the river to become well mixed. This calculation gave an estimate of approximately 30 kilometers. The

concentrations within this 30-kilometer reach can be expected to vary laterally across the channel and pockets of relatively low or high concentration may be encountered in the lateral direction. Our model does not resolve lateral concentration gradients and assumes well-mixed conditions within each model tank. Therefore the model predications made downstream of the R.L. Sutton and R. M. Clayton WWTP discharges may not agree with the observations due to the fact that the samples may have been taken in pockets of high concentration and may not reflect the concentration if mass were well mixed across the channel.

5 Model Sensitivity

As discussed in Section 3.5 there were many places where adequate data was not available and best estimates were made of conditions within the modeled reach. In Chapter 5 we will examine the sensitivity of our model to the value of some of the most important estimates. The categories we will consider deal with characteristics of the suspended solids model, biodegradation model, and the loadings model. Each will be discussed in its own section.

5.1 Suspended Solids Sensitivity

Section 3.5.4 discusses the suspended solids model. A particular suspended solids concentration distribution was hypothesized based on observations made in the field. In addition, the average size and settling velocity of the particles was estimated. The degree to which these estimates may have impacted the results shown in Section 4.2 can be investigated by studying the results of the model when the parameters are varied.

A change was made to the base case model that increased the size of the suspended solids loads by two orders of magnitude. This resulted in an increase in the suspended sediment concentration distribution. Figure 5-1 can be compared to Figure 3-28 to visualize the magnitude of the suspended solids distribution.

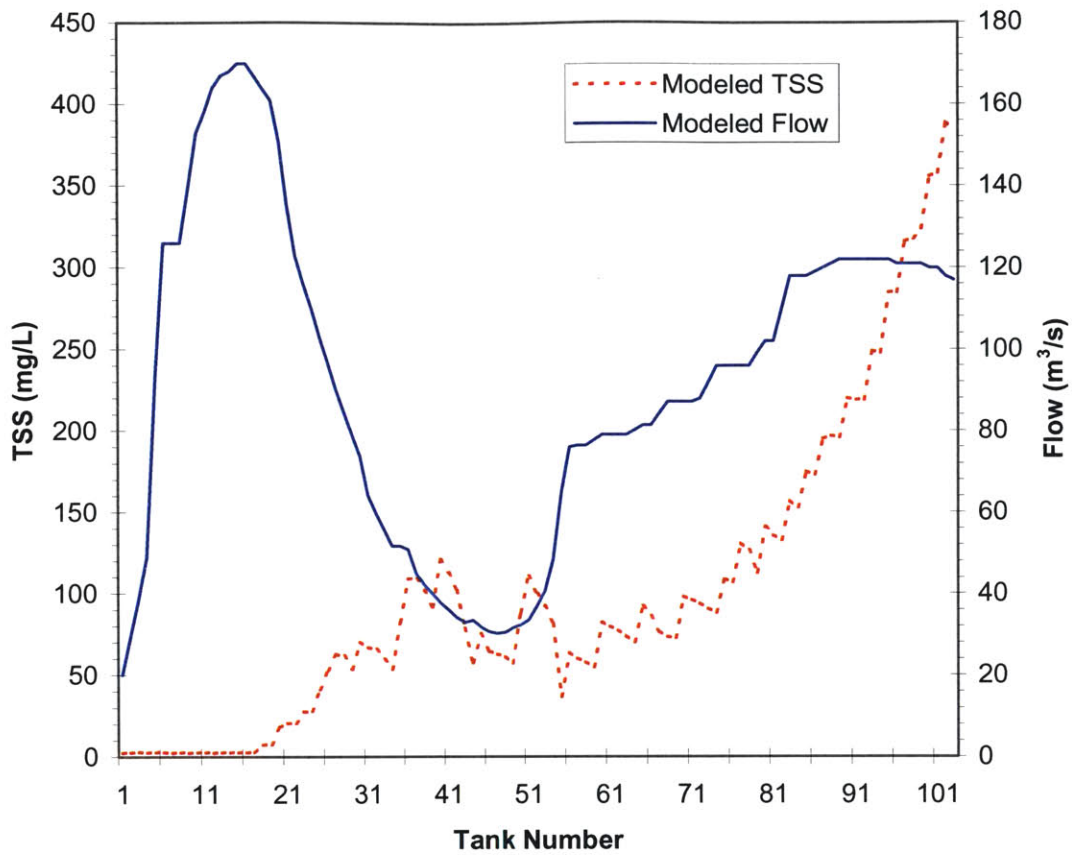


Figure 5-1 TSS and Flow Distribution at Model Time Step 2.0 (High TSS Case)

As in Section 4.2 we will begin the analysis of sorption by determining the average percentage of each phosphate ester transported as sorbed. Results in tank 103 for both the 1% f_{oc} and the 10% f_{oc} cases are listed in Table 5-1.

Table 5-1 Average Percentage of Phosphate Ester Sorbed to Suspended Solids (Tank 103)

Phosphate	Elevated TSS Case		Base Case	
	f_{oc}		f_{oc}	
	1%	10%	1%	10%
TBP	1%	10%	0%	0%
TBEP	7%	43%	0%	3%
TCEP	0%	1%	0%	0%

The increase in sorption in the 1% f_{oc} case is not significant and substantial phosphate ester decay due to settling is not expected during elevated TSS events. However the results of the 10% f_{oc} case show considerable increase in the percentage of sorbed phosphate esters.

As in Chapter 4 the concentration of TBEP in the 10% f_{oc} case will be compared to the base case to evaluate the amount of degradation due to increased sorption. The average concentration in tank 100 for the 10% f_{oc} case is 75% of the concentration in the base case discussed in Chapter 4. There is potential for still greater loss during a more elevated TSS event.

Since the average settling velocity was also assumed we investigated the effect of varying the settling velocity. The 10% f_{oc} case discussed above was altered and two separate cases were produced: the first by assuming an average particle diameter 0.005 mm and the second by assuming an average particle diameter of 0.02 mm. This altered the settling velocity as per Table 3-10. Table 5-2 lists the results of the settling velocity sensitivity tests. Variability in average particle diameter has the effect of altering the TBEP loss to settling by an approximate factor of two.

Table 5-2 Percentage of TBEP lost to Settling for Different Average Particle Diameters

Particle Diameter (mm)	% Lost To Settling
0.005	9%
0.01	25%
0.02	48%

The model predicts the potential for significant loss of TBEP due to particle settling during an elevated turbidity event. The magnitude of the sink depends highly on particle size and fraction of organic carbon. Field observations of these variables should be made to increase the accuracy of predictions made by the model.

It should be noted that this analysis assumed that elevated TSS events occurred without a corresponding increase in flow. It is logical that many of the elevated TSS events would occur during storms and thus would also be accompanied by an increase in flow. This may have an impact on our estimates as it could dilute concentrations of TBEP.

5.2 Phosphate Load Sensitivity

Section 3.5.2.1.2 discusses the assumption in the base case that the discharge from the WWTP is constant throughout the day. This assumption neglects the fact that discharge from municipal WWTPs is not constant but varies throughout the day. Hourly discharge records were available for the R. L. Sutton WWTP for January 15, 2004. For this sensitivity test it was assumed that this represents the typical discharge pattern for all WWTPs in the modeled reach.

The discharge versus time curve for January 15, 2004 at the R. L. Sutton WWTP was normalized by the total discharge for that day. The resulting curve is displayed in Figure 5-2.

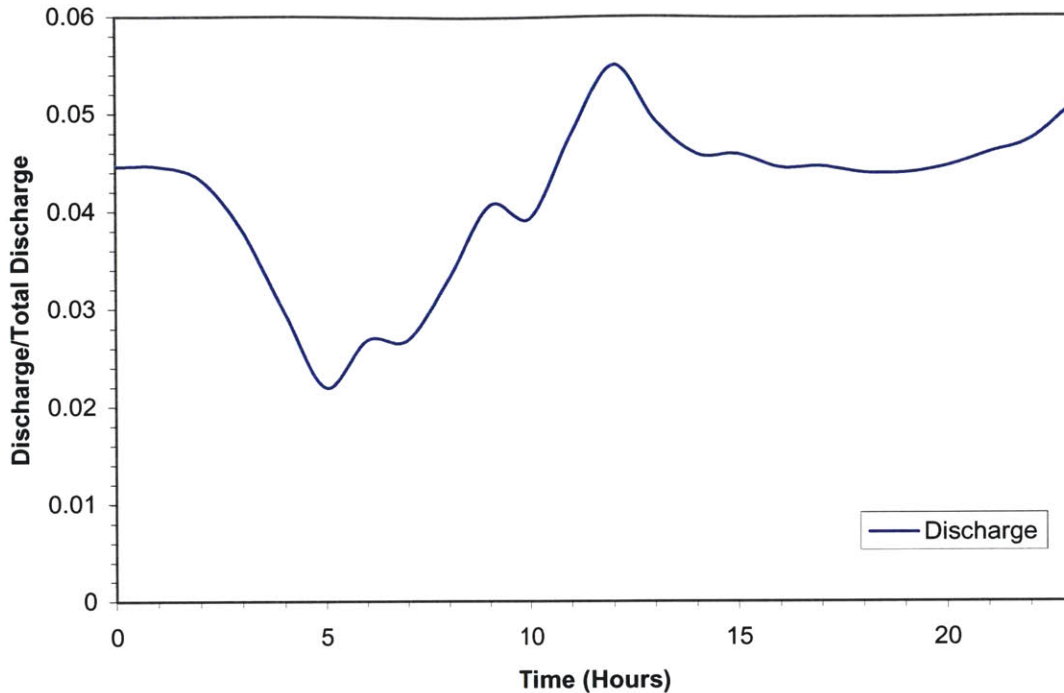


Figure 5-2 Normalized Discharge from R. L. Sutton WWTP (January 15, 2004) (Harburn, 2004)

Applying the curve to the daily discharge for each plant approximated the hourly discharge patterns for each WWTP discharging to directly to the Chattahoochee River. A sensitivity case was run with the new discharge functions and the results are studied below.

The concentration versus time curves directly below the WWTP discharges were compared to the curves at the same locations for the base case model. For simplicity only the results from TBEP are discussed here and can be generalized to describe the behavior of the other phosphate esters.

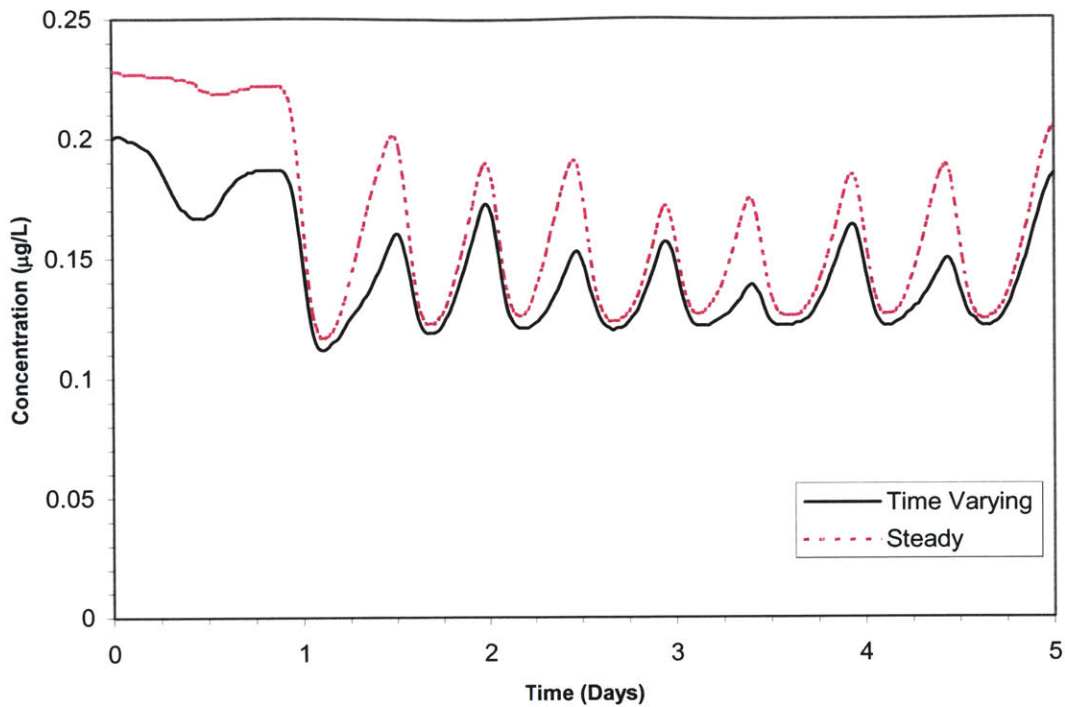


Figure 5-3 TBEP Concentrations at Tank 28 for the Base Case and Time Varying Load Case

Figure 5-3 shows the TBEP concentration versus time curve for both the base case and the load sensitivity case at tank 28, directly downstream of the Crooked Creek and John’s Creek WWTP outfalls. Concentrations in the time varying load case at tank 28 are an average of 10% lower than in the base case. This deficit is carried throughout the model and the average concentrations in tank 103 are still 10% lower in the time varying load case.

John’s Creek is the largest source of TBEP in the model (See Figure 3-37); thus it follows that concentration variations resulting from this discharge have the largest effect on the discrepancies between the sensitivity and the base case. Figure 5-4 shows the discharge in the time varying case and river flow at the Johns Creek outfall. Inspection of the figure shows that the minimum WWTP discharge occurs at river low flow. As shown in Section 4.1, discharge during low flow periods result in the greatest concentration increases. Therefore the low discharge corresponding to low flow reduces peak

concentration. When the peak discharge arrives high flows quickly follow and the concentration is not able to reach the level it does in the base case.

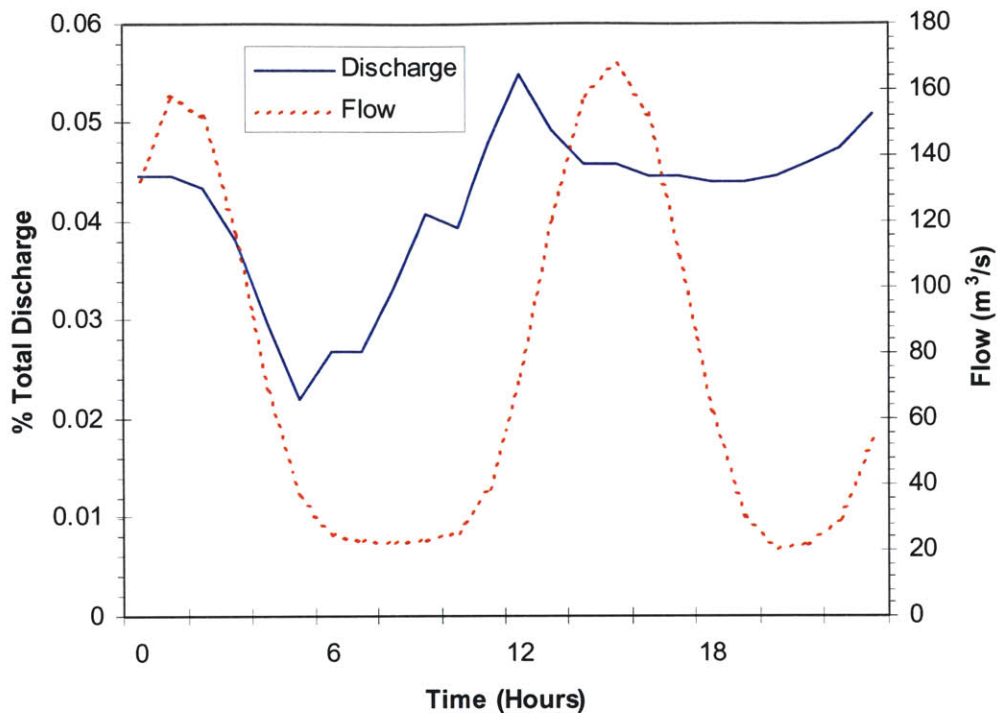


Figure 5-4 Assumed Discharge Pattern and Flow at John's Creek Outfall for January 13, 2004

Model sensitivity is greatest for TBP, which had an average concentration 15% lower than that in the base case. In general concentration predictions made by the base case model may be as much as 18% too high if the discharge patterns of the plants are similar to that assumed in the time varying case. Further work on the model should obtain accurate discharge records for the days being modeled as a peak discharge during the low flow periods may have the opposite affect as described above.

5.3 Biodegradation Sensitivity

The biodegradation rates used in the model were experimentally derived yet there is still considerable uncertainty in their exact values (Andrews, 2004). Confidence intervals were provided with the rate constants. It is important to apply the confidence intervals to the rate constants and investigate the results of the model sensitivity to the uncertainty.

The sensitivity analysis on the biodegradation rate constants was conducted by varying the biodegradation constants within the 50% confidence interval provided by Andrews, 2004. Table 5-3 lists the biodegradation rate constants used in the high, low, and base cases.

Table 5-3 Biodegradation Rate Constants For the Sensitivity Analysis Comparison

Sensitivity Case	Rate Constants (Day ⁻¹)		
	TBP	TBEP	TCEP
High	0.051	0.066	0.047
Base	0.020	0.037	0.008
Low	0.000	0.009	0.000

The results of both sensitivity cases were compared to the base case in tank 100 of the model (See Section 4.3). To make the comparison, the average concentration for each sensitivity case was divided by the base case average concentration. The results are listed in Table 5-4.

Table 5-4 Results of Biodegradation Sensitivity Test

Phosphate Ester	Sensitivity Case	
	Low	High
TBP	105%	92%
TBEP	105%	89%
TCEP	103%	87%

Inspection of the results of the sensitivity test reveals that the low case only increases the average concentration by 5% (only 3% in the case of TCEP). The results of the high biodegradation case show approximately a 10% drop in average concentration for each of the compounds. This is especially important for TCEP, which showed the least response to any degradation process in the base case results. Nonetheless the results show that uncertainty in the biodegradation constants may effect the predicted concentrations by a maximum of 10%.

6 Conclusions

6.1 General Conclusions

This study developed a water quality model of phosphate esters in the Chattahoochee River using the U.S. EPA WASP model (Ambrose et al., 1993). The model predictions were reasonably close to observations of phosphate ester concentrations made during the modeled period. These results show that predictions of phosphate ester concentration distributions in the Chattahoochee River are feasible through a numerical modeling approach. Furthermore the results show that the diurnal flow pattern imposed by the operation of the hydroelectric dams affects the concentration distribution in time and space. Any future attempt to model water quality in this reach of the Chattahoochee River must account for the time varying river flow.

The predictions of the model allow the phosphate esters to be rated on a scale of resistance to the natural attenuation processes. TCEP is the most resistant followed by TBP. TBEP is the most susceptible to degradation. TBEP was predicted to be most susceptible to biodegradation and loss due to sorption to settling particles. TBEP concentrations in the base case scenario were an average of 11% lower than the model run without biodegradation. However, even after increasing the biodegradation rate for TBEP by a factor of 2 concentrations remained reasonably close to the base case concentration. This indicates that travel times between the WWTP outfalls above Morgan Falls Dam and downstream DWTP intakes are insufficient for biodegradation to substantially reduce TBEP concentrations.

Loss due to sorption to settling solids may also be a significant mechanism for removing TBEP from the water column under certain conditions. Gaps in data forced the approximation of many of the parameters in the suspended solids model and the magnitude of predicted TBEP loss due to sorption to settling solids proved to be highly sensitive to variations in organic carbon content and average particle size. Observations of the suspended solids characteristics in the Chattahoochee River are necessary to further evaluate the magnitude of this sink. It must also be kept in mind that TBEP

sorbed to settling particles deposits on the riverbed where concentrations build up over time and may be re-released to the water column.

The above conclusions suggest that from the standpoint of keeping Chattahoochee River water concentrations low, TBEP is the preferred phosphate ester to use when practicable. Further studies must be conducted to evaluate the potential for TBEP buildup in the riverbed.

.The discussion in Section 4.1.3 explains the pattern of concentration downstream of Bull Sluice Lake and upstream of the R.L. Sutton and R.M. Clayton WWTPs. Two municipal drinking water treatment plants servicing the greater Atlanta area draw raw drinking water from the Chattahoochee River in this reach. Results discussed in Section 4.6 indicate that the model predictions reasonably agree with observations made at the most downstream of these DWTPs, The Atlanta Water Works DWTP. The patterns suggest that a pulse of relatively high phosphate ester concentration travels through this reach on the second day of the week and that concentrations in the drinking water may be higher during this time.

Data is not available concerning the long term effects of chronic exposure to phosphate esters at the concentrations detected in the Atlanta drinking water. In the absence of such information it must be assumed that phosphate ester contamination of public drinking water may pose potential health hazards. The predictions made by the model can be used to effectively predict phosphate ester concentrations at the drinking water intakes between Morgan Falls Dam and the downstream WWTP outfalls. These predictions could be useful in scheduling additional drinking water treatment measures to reduce phosphate ester concentration should those concentrations be deemed health hazards.

6.2 Suggestions for Further Study

There are several places where our knowledge of conditions within the river was lacking and required us to make estimates that affected the predictions made by the model. The following is a list of areas where more information is necessary to increase the accuracy of the model.

6.2.1 Free Radical Distribution

Gaps in data regarding the distribution of free radicals within the modeled reach required that the free radical distribution be hypothesized (Section 3.5.7). The phosphate esters are highly reactive with hydroxyl radicals as shown by their second-order oxidation rate constants (Machairas, 2004). A study of the distribution of free radicals in the Chattahoochee River would allow us to better evaluate the potential for phosphate ester oxidation by free radicals.

6.2.2 Suspended Solids and Organic Carbon Content

It was shown in both Sections 4.2 and 5.1 that the organic carbon content of the suspended solids has a large effect on the degree to which the phosphate esters sorb to settling suspended sediments. Observations of the average organic carbon content of suspended solid material in the modeled reach will greatly enhance the accuracy of the suspended solids model. In addition, information on the solid particle size distribution would more firmly establish a settling velocity and therefore the rate at which sorbed phosphate esters are removed from the water column..

The discussion of the elevated TSS conditions (Section 5.1) indicates that elevated TSS events may be caused by storms and therefore be accompanied with high flows. Flow and TSS data collected during these events could help construct a version of the model that accounted for more of the parameters contributing to the concentration changes in these situations.

6.2.3 Biodegradation Rates

There is still considerable uncertainty in the biodegradation model. Further experiments to reduce the range of possible biodegradation rate values will help to evaluate the magnitude of the sink attributed to biodegradation.

6.2.4 Varying Loads

It was shown in Section 5.2 that concentration predictions could be affected by loads varying in time due to cycles in treated wastewater discharge. Cycles may also exist in effluent concentrations and it may effect the predictions if these cycles were resolved.

Works Cited

- Admas, Eric. Water Quality Control.
Cambridge, MA: Printed class notes Massachusetts Institute of Technology, 2004.
- Ambrose, Robert B. Jr., Tim A. Wool, and James L. Martin. The Water Quality Analysis Simulation Program, WASP5. Athens, GA: Environmental Research Laboratory U.S. Environmental Protection Agency, 1993.
- Andrews, Mathew B.. “Natural Attenuation of Organophosphates in River Systems: Case Study Chattahoochee River”. Master of Engineering Thesis Massachusetts Institute of Technology, 2004.
- Andrews, Mathew B., Samuel F. Haffey, Joseph C. Lin, and Alexandros Machairas. “Phosphate Ester Pollutants in the Chattahoochee River”. Masters of Engineering Project Report Massachusetts Institute of Technology, 2004.
- ArcGIS Version 8.1, Computer Program.
Redlands, CA, ESRI, 2003.
- Brunner, Gary W. HEC-RAS River Analysis System User Manual Version 3.1.
Davis CA: U.S. Army Corps of Engineers Hydrologic Engineering Center, 2002.
- Chastain, Eddie. “Inquiry for discharge rates”.
E-mail to Samuel Haffey, 23 Feb 2004.
- Cherry, R.N., R.E. Faye, J.K. Stamer, and R.L. Kleckner. “Summary of the River-Quality Assessment of the Upper Chattahoochee River Basin, Georgia”. U.S. Geological Survey Circular 811, 1980
- Covar, A.P..”Selecting the Proper Reaeration Coefficient for Use in Water Quality Models”. Proceedings of the U.S. EPA Conference of Environmental Simulation Modeling, April 19-22, 1976.
- Environmental Protection Agency, U.S. (EPA). Water Discharge Permits.
<http://www.epa.gov/enviro/html/pcs/pcs_query_java.html>
(24 Nov 2003)
- Evett, Jack B. and Cheng Liu. Fundamentals of Fluid Mechanics.
New York: McGraw-Hill Book Company, 1987.
- Fischer, Hugo B., E. John List, Robert C.Y. Koh, Jorg Imberger, and Norman H. Brooks. Mixing in Inland and Coastal Waters. San Diego: Academic Press, 1979.

Frick, Elizabeth A., Daniel J. Hippe, Gary R. Buell, Carol A. Couch, Evelyn H. Hopkins, David J. Wangsness, and Jerry W. Garrett. "Water Quality in the Apalachicola-Chattahoochee-Flint River Basin, Georgia, Alabama, and Florida, 1992-1995" U.S. Geological Survey Circular 1164,. 1998.

Frick, Elizabeth A., and Steven D. Zaugg. "Organic Wastewater Contaminants in the Upper Chatthoochee River Basin, Georgia, 1999-2002." Proceedings of the 2003 Georgia Water Resources Conference, April 23-24, 2003.

Georgia Department of Natural Resources (GNR) Environmental Protection Division. Chattahoochee River Basin Management Plan 1997. Atlanta, GA. Georgia: Department of Natural Resources, 1997.

Harburn, James. "discharge rates Sutton & South Cobb".
E-mail to Samuel Haffey, 3 Mar 2004.

Hemond, Harold F. and Elizabeth J. Fechner-Levy. Chemical Fate and Transport in the Environment. San Diego: Academic Press, 1994.

Hydrologic Engineering Center (HEC). HEC-2 Water Surface Profiles User's Manual. Davis, CA: U.S. Army Corps of Engineers Hydrologic Engineering Center, 1990.

Kopanski, Thomas. "RE: inquiry for discharge rates".
E-mail to Samuel Haffey, 19 Feb 2004.

Lin, Joseph C.. "Determining the Removal Effectiveness of Flame Retardants from Drinking Water Treatment Processes". Master of Engineering Thesis Massachusetts Institute of Technology, 2004.

Machairas, Alexandros. "The UV/H₂O₂ Advanced Oxidation Process in UV Disinfection Units: Removal of Selected Phosphate Esters by Hydroxyl Radical". Master of Engineering Thesis Massachusetts Institute of Technology, 2004.

Microsoft Excel 2000. Computer Program.
Microsoft Corporation, 1999.

Nakamura, A., "Environmental Health Criteria 112 Tri-n-Butyl Phosphate".
Environmental Health Criteria, World Health Organization, 1991.

National Library of Medicine. Household Products Database.
<<http://householdproducts.nlm.nih.gov/>>
(12 May 2003)

NSTATE, Georgia, The Geography of Georgia.
<http://www.netstate.com/states/geography/ga_geography.htm>
(8 May 2004)

- Olson, Robert. "Re: request for Chattahoochee cross sections".
E-mail to Samuel Haffey. 17 Feb. 2004.
- Schwarzenbach, Rene P., Philip M. Gschwend, and Dieter M. Imboden. Environmental Organic Chemistry. Hoboken, NJ: Wiley, 2003.
- Shanahan, Peter and Sharron C. Gaudet. "Mixing and Transport of Pollutants in Surface Water". New York: Standard Handbook of Environmental, Science, Health and Technology, McGraw Hill, 2000.
- Shanahan, Peter and Donald R. F. Harleman. "Transport in Lake Water Quality Modeling". Journal of Environmental Engineering 110.1 (1984).
- Sheehan, Daniel. Using the Stock Hydrology Tools in ArcGIS.
<<http://web.mit.edu/1.963/www/Lab6/>>
(1 Oct 2003)
- State of New Mexico Environment Department. Total Maximum Daily Load (TMDL) Report for the Jemez River Watershed. Santa Fe, NM: Resource Technology Inc., 2002.
- Stamey, Timothy C.(USGS). "Re: [RE] <http://ga.wayterdata.usgs.gov/nwis/current/>".
E-mail to Samuel Haffey. 7 Mar 2004.
- Syracuse Research Corporation (SRC). PHYSPROP Database.
<<http://www.syrres.com/esc/physdemo.htm>>
(8 May 2004)
- U.S. Geological Survey (USGS). National Elevation Dataset.
<<http://gisdata.usgs.net/NED/default.asp>>
(6 Nov 2002)
- U.S. Geological Survey (USGS), National Land Cover Data, 1992,
<<http://landcover.usgs.gov/nationallandcover.asp>>
(20 Oct. 2003)
- U.S. Geological Survey (USGS). Real-Time Data for Georgia.
<<http://waterdata.usgs.gov/ga/nwis/rt>>
(8 May 2004)
- U.S. Geological Survey (USGS). "Sandy Springs Quadrangle, Georgia".
7.5-Minute Series (Topographic), U.S. Geological Survey, 1997.
- van Esch, G.J.. "Environmental Health Criteria 218 FLAME RETARDANTS: TRIS(2-BUTOXYETHYL) PHOSPHATE, TRIS(2-ETHYLHEXYL) PHOSPHATE

AND TETRAKIS(HYDROXYMETHYL) PHOSPHONIUM SALTS”.
Environmental Health Criteria. World Health Organization, 2000.

Viessman, Warren Jr., and Gary L. Lewis. Introduction to Hydrology.
Upper SaddleRiver, NJ: Pearson Education, 2003.

Willey, R.G., and Denis Huff. Chattahoochee River Water Quality Analysis, Final Report
to the Waterways Experiment Station and Savannah District. Davis CA: U.S.
Army Corps of Engineers Hydrologic Engineering Center, 1978

World Health Organization (WHO). “Environmental Health Criteria 209 FLAME
RETARDANTS: TRIS(CHLOROPROPYL) PHOSPHATE AND TRIS(2-
CHLOROETHYL) PHOSPHATE”. Environmental Health Criteria, World Health
Organization, 1998.

Appendix: Model Segmentation

